MODELING ADOPTION OF CARINATA PRODUCTION AND DESIGNING THE SUPPLY CHAIN OF CARINATA-BASED SUSTAINABLE AVIATION FUEL PRODUCTION IN THE SOUTHERN UNITED STATES

by

KAZI MASEL ULLAH

(Under the Direction of Puneet Dwivedi)

ABSTRACT

Carinata (*Brassica Carinata*) is a promising crop for producing sustainable aviation fuel (SAF) in the Southern United States. However, a lot of information on the adoption of carinata as a feedstock for SAF production is missing. Similarly, information about the cost-effectiveness and environmental feasibility of carinata-based SAF across the supply chain is still unknown. In this context, this study explored the adoption challenges of carinata as a newly introduced bioenergy crop using a spatially explicit agent-based model (ABM), and then estimated the production cost and intensity of greenhouse gas emission of carinata-based SAF production with deterministic and 12 multiperiod stochastic supply chain models. The ABM assumed the principles of profit maximization, neighborhood influences, risk aversion behavior of farmers, followed by three estimation procedures - a) the profitability difference between traditional crop rotations (with and without carinata at different contract prices), b) the adoption rate of neighboring farmers, and c) their land allocation decisions from managing a risky portfolio of enterprises. The deterministic supply chain model was developed with a Mixed-Integer Linear Programming approach integrated with the Geographical Information System and Life Cycle Analysis for a 20 years simulation

period along with four annual seasons for continuous seed supply purposes. The stochastic models were the extension of the supply chain configuration of the deterministic model, where models were run for four different simulation periods (5, 10, 15, 20-years) with three probabilistic scenarios (99%, 95%, and 90% confidence interval). The supply chain models determined the locations of farms and facilities (e.g., storage units, crushing mills, biorefineries) by minimizing the overall cost of the systems. The ABM results showed that the proportion of land allocated to carinata to the total farmland under field crops were 38% and 85% after 33 years under the low (2.5%) and high (5%) initial neighborhood adoption rates, respectively, with a contract price of $13/bushel. The minimum price of SAF, estimated from supply chain models, ranged between $1.14-1.86 L^{-1} while achieving 63-65% carbon saving in any scenarios compared with conventional aviation fuel. The multi-scale spatial and temporal modeling frameworks developed as a part of this dissertation could aid the development of the bioenergy landscape in Georgia and beyond.

INDEX WORDS: Agent-based Modelling, *Brassica Carinata*, Bioenergy, Greenhouse Gas, Life Cycle Assessment, Mixed-Integer Programming, Stochastic Programming, Sustainable Aviation Fuel, Little River Watershed, Georgia.

MODELING ADOPTION OF CARINATA PRODUCTION AND DESIGNING THE SUPPLY CHAIN OF CARINATA-BASED SUSTAINABLE AVIATION FUEL PRODUCTION IN THE SOUTHERN UNITED STATES

by

KAZI MASEL ULLAH

BS, Urban and Regional Planning, Bangladesh, 2008

MS, Urban and Regional Planning, Bangladesh, 2012

MS, Geographical Information Science, Sweden, 2014

A Dissertation Submitted to the Graduate Faculty of The University of Georgia in Partial Fulfillment of the Requirements for the Degree

DOCTOR OF PHILOSOPHY

ATHENS, GEORGIA

2022

MODELING ADOPTION OF CARINATA PRODUCTION AND DESIGNING THE SUPPLY CHAIN OF CARINATA-BASED SUSTAINABLE AVIATION FUEL PRODUCTION IN THE SOUTHERN UNITED STATES

by

KAZI MASEL ULLAH

Major Professor:	Puneet Dwivedi
Committee:	Lan Mu
	Ke (Luke) Li
	Daniel Geller

Electronic Version Approved:

Ron Walcott
Vice Provost for Graduate Education and Dean of the Graduate School
The University of Georgia
May 2022

DEDICATION

I would like to dedicate this research to my parents, Late Mr. Kazi Asad Ullah and Mrs. Hosne Ara Asad.

ACKNOWLEDGEMENTS

First, I would like to show my deep gratitude to my Major Professor, Dr. Puneet Dwivedi, for his mentorship and guidance since the beginning of my Ph.D. program at the University of Georgia. Without his help and wholehearted support at the different stages of my Ph.D. journey, I could have lost my way. He not only supervised my dissertation works but also supported me a lot during many challenging situations; becoming a dad in the midway of my Ph.D. study is one of the best examples.

I am thankful to my Ph.D. committee members, Drs. Lan Mu, Ke Li, and Daniel Geller, who agreed to be part of my Ph.D. program. I will be thankful to them for their routinely supports and feedback to enrich my research work, set my program of study, and finally, for accepting my limitations within the scope of my Ph.D. research.

I will never forget the support from all my fellow lab members in Dwivedi's Forest Sustainability Lab, who always responded to me for any kind of help. Especially, I should mention the names of Dr. Farhad Hossain Masum, Mr. Syed Mohammad Asiful Alam, and Dr. Suraj Upadhaya. Their prior experiences in UGA graduate studies helped my study easier for many unnoticeable situations.

I would like to be grateful to the SPARC program (https://sparc-cap.org/). I thank the members of the SPARC program and its associated partner organizations for their kind support. Especially, I appreciate Dr. John Field, Scientist at Oak Ridge National Laboratory, who shared carinata yield and soil organic carbon data.

I am thankful to different United States organizations, such as USDA, USDOT, EPA, GDOT, and others for making the valuable datasets openly accessible. Special thanks to Mr. Justin R. Thift, Rural Development Specialist, GDOT, who helped me configure the railway dataset through personal communication. My sincere thanks are also to the University of Georgia Information Technology Outreach Services and the University of Georgia Weather Network for their landownership and weather data support.

I am grateful to the faculty and staff members of Warnell School of Forestry and Natural Resources, as well as the University of Georgia, for their administrative and academic support. I always found Kate deDufour at the Warnell School as a great student welfare staff, who never feels tired of supporting students.

Finally, I am thankful to my family and relatives for their encouragement and support throughout my all academic attainments. I thank my wife for taking care of our child during my Ph.D. journey and be a source of encouragement throughout my academic journey at the Warnell School. I will always remain grateful to my elder brother, Kazi Abu Hena Rasel, for becoming our family guardian from an early age.

TABLE OF CONTENTS

LIST OF TABLES

LIST OF FIGURES

CHAPTER 1

INTRODUCTION & LITERATURE REVIEW

Currently, commercial aviation is responsible for 2.6% of annual global carbon dioxide (CO_2) emissions [1]. This proportion of carbon emissions by the aviation sector is expected to grow at 4.6 % by mid-century [2]. The aviation sector in the United States contributes 12% of transportation emissions of the country, which account for three percent of total greenhouse gas (GHG) produced across all the national economic sectors [3]. Using sustainable aviation fuel (SAF) is the best remaining option to combat GHG emissions from the aviation sector in the United States for several reasons. First, for the last 60 years, the United States reduced the energy intensity of air travel by 75% by using advanced engine technologies as well as improving air traffic operations [4]. However, the per capita aviation fuel use in the United States is around 284 liters, which is six times higher than the world average and is highly dependent on petroleum-based conventional aviation fuel (CAF) [4]. Second, SAF can reduce GHG emissions by up to 80% [5]. Therefore, the federal government announced a new 'Sustainable Aviation Fuel Grand Challenge' that targeted to produce at least 11.4 billion liters of sustainable aviation fuel (SAF) production per year to reduce greenhouse gas (GHG) emissions to 20% by 2030 and produce 132.5 billion liters of SAF per year in the long term to meet 100% of aviation fuel demand by 2050 [6].

SAF can be produced from different plants or oil seeds, such as Camelina, Corn Stover, Switchgrasses [7], Jatropha, Soybean, Palm [8], Willow, Sugarcane [9]; from other renewable sources, such as residual woody biomass [10] and Algae [11]; and even from municipal wastes among other residues [2]. Among all these possible sources, dedicated oil seed crops are preferred to other

feedstock sources for having rich oil content and no food value [12]. However, oilseed for SAF production needs a balanced distribution of supply with a larger yield to meet the demand, in addition, to maintaining environmental sustainability, such as no competition with food crops, compatibility with current crop rotations to avoid deforestation, as well as no direct or indirect impact on land use changes [13]. Considering these prerequisites, carinata can be an appropriate alternative for producing SAF in the Southern United States [14].

Brassica carinata, sometimes called Ethiopian mustard, Abyssinian mustard, or simply carinata, is a promising annual oilseed crop for the commercial production of SAF [14,15]. Carinata is rich in oil content (42%-52%); has high frost and drought tolerance; therefore, it can be cultivated with other row cops without competition with food crops [14,16]. As a cover crop, carinata can provide several ecosystem services by reducing soil erosion, nutrient leaching, increasing soil organic matter, and retaining moisture [17]. In the Southeast (SE) United States, carinata can be grown with a potential yield of 0.55 t/ha [18]. In Alabama, Georgia, and Florida, carinata can be potentially cultivated on about 1.4 million ha of fallow agricultural land during the winter season [19]. On the other hand, thirteen southern states of the United States consume about one-third of the nation's total aviation fuel consumption [20]. Therefore, the large supply of carinata feedstock can meet the immediate demand of SAF regionwide.

However, several economic, behavioral, and environmental factors affect the adoption of bioenergy crops. The lack of an established market [21], price and yield risks [22], inexperience with new management practices, and cost of new crop-specific equipment [23] are some significant factors that deter farmers from adopting bioenergy crops. Farmers' attitudes towards adopting bioenergy crops are also affected by behavioral factors, such as the influence of neighboring farmers [24] and individual risk preferences [25]. Addressing these challenges is required as the first step to building

farmers' positive attitude toward adopting energy crops and ensuring feedstock availability. However, two primary factors pose challenges for producing and distributing advanced transportation biofuels, including SAF, besides feedstock availability, i.e., conversion technology and biomass supply chain (BSC) [26]. The biochemical composition of carinata has been proven suitable for many conversion technologies, while the supply chain of carinata-based aviation fuel in the Southern United States needs to be examined [27]. Moreover, the feedstock availability might have uncertainty in addition to farmers' attitudes, such as yield risks associated with soil moisture quality [26,28] and local weather conditions [29]. Therefore, BSC needs to be examined under a considerable number of risks and uncertainties.

Considering the above backdrop, this dissertation fulfilled three objectives about the adoption of carinata as a potential bioenergy crop and utilizing it as a feedstock for producing and distributing SAF in the Southern United States. The first objective is to ascertain the land allocation decisions of farmers regarding the adoption of carinata. The second objective is to design a carinata-based SAF supply chain. Finally, the third objective is to design a carinata-based SAF chain under uncertainty. To fulfill these three objectives, the dissertation applied an agent-based bioenergy adoption modeling technique, a deterministic supply chain model, and a stochastic supply chain model.

1.1. The Agent-based model

A typical agent-based model has three elements – (i) a set of agents; (ii) a set of agent relationships and methods of interactions; and (iii) the agents' environment [30]. Agents can be characterized as autonomous, social, adaptive, and heterogeneous in their attributes and behaviors. From modelers' perspective, a set of rules and estimation procedures are required to observe

agents' interaction, e.g., how farmers behave in response to an unestablished energy crop market. Agents' environment is location-based and sensitive to environmental parameters over the landscape. Therefore, the limitation of traditional econometric-based or theoretical microeconomic models to incorporate heterogeneous behavioral constraints and spatial interactions can be easily avoided in ABMs [31]. However, the existing ABM literature on bioenergy crop adoption is not truly spatially explicit [24,32]. Then, none of the studies, to the best of my knowledge, has jointly analyzed the three basic principles of farmers' agent, i.e., farmers are 1) profit maximizers [22,24,25]; 2) influenced by their neighboring; and 3) risk-averse [22,25]. In this dissertation, we offer a novel utility-based economic model that fulfills the gaps in existing literature at least in two ways - a) ensure the spatial explicitness of the model so that the interaction with the physical environment is captured in the most realistic manner; b) incorporating three essential elements (namely, profitability, neighborhood influences, individual risk perceptions) so that farmers' economic, social, and behavioral aspects are tightly embodied along with biophysical conditions.

1.2. The supply chain models

BSC consists of a discrete process that usually comprises harvesting feedstock, preprocessing and storing of biomass, arriving biomass at conversion facilities (e.g., biorefinery), and reaching refined fuels to the consumer to meet the demand [26] (Figure 1.1). This discrete process is dependent on several spatial and temporal factors [12]. The spatial factors, such as feedstock's yields and locations, capacity and locations of facilities (e.g., storage units, crushing mills, biorefineries), and existing transportation modes and network infrastructures affect the supply chain decisions of a biofuel. The seasonality and availability of feedstocks as well as variability of demands, are the temporal factors that have an impact on the short-term and long-term viability of

biofuel production. Besides, the environmental sustainability of BSC can be questionable if the net-GHG emission offset is not feasible [33]. Optimizing the capacity and locations of feedstocks and facilities by connecting with appropriate transportation routes and simulating steady flows of seeds and materials in accordance with SAF demand is a complex job [12,26,28]. However, the development of such a modeling tool is pivotal to building a cost-effective supply chain for biofuel and estimating the net-GHG emission [33–35].

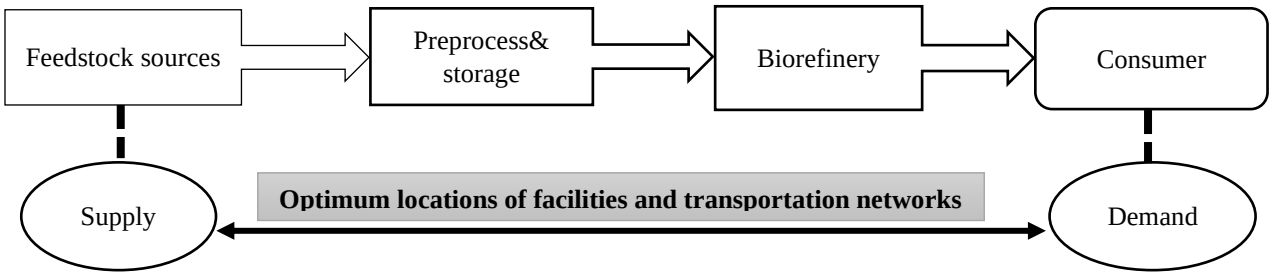

Figure 1.1: Typical diagram of a biofuel supply chain.

Mixed-integer linear programming (MILP) is the most widely used technique for modeling BSC [26]. Several contemporary BSC modeling studies plugged Geographical Information System (GIS) into the MILP models to configure supply chains with actual transportation modes and networks [35–41]. However, to the best of our knowledge, none of the GIS-based BSC literature jointly incorporated the spatial, temporal, and emission issues to develop a sustainable BSC policy. As a result, the GIS-based supply chain literature largely missed showing the environmental feasibility of producing and distributing SAF and the utility of the supply chain models for operationalizing at the longer period scheduling. To fulfill these vital research gaps, we built a deterministic supply chain model using the MILP technique integrated with GIS and LCA for 20 years period with four seasonal supply and demand conditions for each year.

Several studies endeavored to capture the potential uncertainties in BSC [33,42–46]. Among the literature, the most prominent approach is the use of stochastic programming [33,42–44]. However, to the best of our knowledge, none of the stochastic programming approaches were integrated with a GIS-based supply chain model. The GIS-based BSC approaches, which apply accurate and precise transportation networks and modes, can be directly utilized in MILP models to optimize the numbers, capacities, and locations of feedstock's farms and facilities to satisfy a certain level of demand at a minimum cost [35,47]. However, none of those studies incorporated the uncertainty in BSC design and two major aspects were missing – 1) the planning decisions affected by simulation periods; 2) the carbon footprint generated by the proposed BSCs. To fulfill this shortcoming in existing literature, we extended our deterministic supply chain model with a stochastic technique by applying multi-period simulations under several scenarios of uncertainty in carinata seed supply. We run the simulations for 5, 10, 15, and 20-years periods with three probabilities scenarios of seed supplies (99%, 95%, and 99% confidence intervals).

1.3. Policy implications

One of the major strategies to reduce GHG emissions and thereby mitigate climate change impacts is the use of biofuels [48]. However, the success of biofuel use is largely dependent on the tradeoff between the economics and carbon footprint of biofuel production. Determining appropriate carbon abatement cost is one of the useful techniques to understand this tradeoff and feed into policy measures to promote sustainable biofuels [49]. After understanding the adoption challenges, we determined the carbon abatement costs from our supply chain modelings at several multiperiod probabilistic scenarios. Thus, our study would be helpful for setting appropriate policies to promote the adoption of carinata in general, as well as taking specific policy measures, such as

imposing a rational amount of tax burden on CAF so that investors get a fair price for producing carinata-based sustainable aviation fuel (CSAF) regardless of different uncertainty conditions.

CHAPTER 2

ASCERTAINING LAND ALLOCATION DECISIONS OF FARMERS ABOUT THE ADOPTION OF CARINATA AS A POTENTIAL CROP FOR SUSTAINABLE AVIATION FUEL PRODUCTION IN THE SOUTHERN UNITED STATES [1]

[1] Ullah K.M., & Dwivedi, P. Submitted to [GCB Bioenergy], [07-Jan-2022].

Abstract

The adoption of a bioenergy crop is affected by various factors, including but not limited to the characteristics of farmers, farm economics, market forces, and physical environment. This study develops a spatially explicit agent-based model for ascertaining the adoption rate of carinata (*Brassica carinata*) among the farmers in the Little River Experimental Watershed located in the southern state of Georgia in the United States. Each farmer's adoption behavior is modeled using a) the profitability difference between traditional crop rotations (with and without carinata at different contract prices), b) the adoption rate of neighboring farmers, and c) their land allocation decisions from managing a risky portfolio of enterprises. Carinata production in the winter season once every three years has no conflict with the most profitable and popular traditional row crop rotations, such as cotton-cotton-cotton and cotton-cotton-peanut, to a larger extent. The results show that 28% and 85% of farmers in the watershed will adopt carinata after 33 years at a contract price of $13/bushel (bu) under two different assumptions of low (2.5%) and high (5%) initial neighborhood adoption rates. The proportions of land allocated to carinata to the total farmland under field crops are 38% and 85% after 33 years under the same low and high neighborhood adoption rates, respectively. Our results suggest that fixing the appropriate contract price of carinata will bring additional profits to farmers without any major foreseeable agronomic risks, thereby increasing the adoption rate of carinata at a regional level.

Keywords

Agent-based Modelling, Aviation Sector, Diffusion Theory, Economic Modeling, Energy Crop, Farm Economics, Risk Portfolio, Sustainability.

2.1. Background

Currently, commercial aviation is responsible for 2.6% of annual global carbon dioxide (CO_2) emissions [1]. This proportion of carbon emissions by the aviation sector is expected to grow to 4.6% by mid-century [2]. In 2016, the International Civil Aviation Organization (ICAO) commenced Carbon Offsetting and Reduction Scheme for International Aviation (CORSIA) to achieve carbon-neutral growth from 2020 [50]. Several efforts have also been made to optimize air traffic management to minimize carbon emission [51,52]. However, the success of those policies and mechanisms is dependent on how actively the aviation industry can operationalize them [53,54]. A direct way for reducing carbon emissions and lowering the dependency on fossil fuels is by utilizing sustainable aviation fuel (SAF) [13]. However, feedstock for SAF production should have a larger yield, cover a wider distribution, must not compete with food crops, and should be compatible with current crop rotations to avoid deforestation and other potential direct and indirect land use changes.

Brassica carinata, sometimes called Ethiopian mustard, Abyssinian mustard, or simply carinata, is a promising annual oilseed crop for the commercial production of SAF [14,15]. Carinata is not only rich in oil content (42%-52%), but it also has high heat and drought tolerance; therefore, it can be cultivated without competing with food crops [14,16]. As a cover crop, carinata can provide several ecosystem services by reducing soil erosion, nutrient leaching, increasing soil organic matter, and retaining moisture [17]. In the Southeast (SE) United States, carinata can be grown with a potential yield of 40-60 bushels/acre [18]. In Alabama, Georgia, and Florida, carinata can be potentially cultivated on about 3.5 million acres of fallow agricultural land during the winter season [19]. By using this full potential of carinata feedstock production, carinata-based SAF could replace up to 2.3% of conventional aviation fuel consumption in the United States. It has been

reported that the carinata-based SAF could reduce up to 68% of greenhouse gas emissions relative to conventional aviation fuel in the Southern United States [55].

However, the adoption of bioenergy crops is affected by a number of economic, behavioral, and environmental factors. The lack of an established market [21], price and yield risks [22], inexperience with new management practices, and cost of new crop-specific equipment [23] are some significant factors that deter farmers from adopting bioenergy crops. Farmers' attitudes towards adopting bioenergy crops are also affected by behavioral factors, such as the influence of neighboring farmers [24] and individual risk preferences [25]. Environmental concerns, such as the effects of local climate, can be a determinant factor for farmers' decisions on cultivating energy crops [29].

Several models have been developed to capture farmers' behavioral responses towards the adoption of bioenergy crops [21,23,24,56–58] and for adopting other crops in general [59–62]. Approaches embedded within the agent-based modeling (ABM) framework have appeared as an elegant tool for farm-scale modeling, where heterogeneous farmers' behaviors and their interactions with the biophysical environment and others are not oversimplified [63]. Specifically, the limitation of traditional econometric-based or theoretical microeconomic models to incorporate heterogeneous behavioral constraints and spatial interactions can be easily avoided in ABMs [31].

The ABMs represent a system's individual components and their behavior [64]. Instead of modeling the whole system based on characteristics or variables, ABMs model individual agents and interactions among them as well as with the local environment. In a typical ABM, the agents are autonomous, social, adaptive, and heterogeneous in their attributes and behavior [30]. In the context of agriculture, farmer agents in ABM are adaptive to dynamic market conditions. Agents' interaction with the environment is location-based; therefore, ABMs are simulated typically within

a spatial framework [25]. Thus, ABM can be an effective tool to capture complex relationships among farmers' behavior, market forces, and physical environment over time [63], especially in light of the adoption of emerging bioenergy crops such as carinata. However, only a handful of studies have used ABMs in the context of bioenergy crop adoption (Table 2.1). Huang et al. [24] used a linear programming (LP) model to represent farmers' behaviors, where an individual farmer makes a decision based on maximizing his profit and minimizing the environmental impacts of neighbors' influence. Alexander et al. [25] revealed interactions of supply chain between biomass power plant investors and farmers through a mathematical programing-based estimation procedure. The use of mathematical programming is also found in several other studies [65–69]. Among other techniques, Schulze et al. [32] and Shastri et al. [70] applied the general economic equilibrium model, and Brown et al. [56] used multivariate statistical models. A closer look at existing studies suggests that so far, no study, to the best of our understanding, has jointly analyzed the role of utility preferences, the influence of neighbors' adoption rates, and risk perceptions of farmers on the overall adoption of bioenergy crops at the landscape level.

Additionally, existing studies have only partially accounted for the interactions of farmers with their local environment. First, the models are not truly spatially explicit (except Malawska & Topping [71]). For instance, the spatial environment of the model developed by Schulze et al. [32] is based on hypothetical grid-based cells, where the size of land parcels is uniform for all the farmers. Thus, their model missed the heterogeneity in farm sizes and distribution of traditional crops that affect the decision of bioenergy crop adoption. Ding et al. [65] created spatially explicit farm-scale modeling to identify each agent's crop cultivation history and acreage of crop covers. They used Zonal Operator in ArcGIS 10.0 to aggregate 30 x 30 m resolution crop raster into each parcel owned by an individual agent. However, their aggregation with the majority zonal operator cannot

detect the area of different crop types under a given parcel. Second, like any other crop, the production of bioenergy crops is affected by climatic conditions [29]. For traditional crops, such uncertainty is manageable with the experiences of farmers, but for bioenergy crops, farmers are often inexperienced. To the best of our knowledge, none of the ABM-based studies have considered the sensitivity of bioenergy crop production relative to changes in climate.

Table 2.1: Selected studies using agent-based models for bioenergy crop adoption. *ANOVA, cluster analysis, logistic regression. MP = Mathematical Programming, GE = General Equilibrium.

Author (Year)	**Geography**	**Estimation Procedure**	**Name of the bioenergy crops**
Alexander et al. (2013) [25]	United Kingdom	MP (non-linear)	Miscanthus, Willow
Brown et al. (2016) [56]	Scotland	Multivariate Statistics*	Oilseed rape, Willow, Forestry
Ding et al. (2015) [65]	Iowa, United States	MP (linear)	Perennial grasses, Corn Stover
Guillem et al. (2015) [66]	Scotland	MP (non-linear)	Willow, Miscanthus
Huang et al. [24]	Iowa, United States	MP (linear)	Switchgrass
Jin et al. (2019) [67]	Indiana, United States	MP (linear)	Switchgrass
Malawska and Topping (2018) [68]	Denmark	MP (linear)	Energy maize
Schulze et al. (2017) [32]	Germany	GE	Short rotation forestry
Shastri et al. (2011) [73]	Illinois, United States	GE	Miscanthus
Shu et al. (2020) [69]	Poland	MP (linear)	Sorghum

To fulfill existing shortcomings in the literature, we aimed to build a spatially explicit ABM to understand the land allocation scenarios resulting from the adoption of carinata in the SE United States. We offer a novel utility-based economic model to fulfill the following purposes: a) ensure

the spatial explicitness of the model so that the interaction with the physical environment is captured in the most realistic manner; b) incorporating three essential elements (namely, profitability, neighborhood influences, individual risk perceptions) so that farmers' economic, social, and behavioral aspects are tightly embodied along with biophysical conditions, and c) observing the emerging price scenarios that can indicate various potential levels of adoption of a bioenergy crop within the study area. To obtain our objectives, first, we use the true land parcels of farmers and the historical remote sensing-based crop covers to capture the traditional crop rotations and available land resources for cultivating carinata. We disaggregate crop covers both spatially and temporally within the parcel boundary, thereby contributing towards overcoming the limitation of existing studies which do not incorporate spatially explicit datasets [24,32]. Second, we apply our first stage of the profitability model based on farm-level production economics and weather impacts, thereby offering a novel method to estimate the impacts of climate on the potential loss of bioenergy crops. Then, we use the Diffusion of Innovation Theory [74] to incorporate the neighborhood influences on farmers' decisions to adopt a new crop. With this procedure, we find the future adoption rate of farmers at different initial willingness scenarios in their neighborhoods. Finally, we apply a risk portfolio approach for individual farmers to maximize their final utilities and observe the corresponding land allocation scenarios under different price scenarios throughout the simulation periods.

2.2. Study area

The Little River Watershed (LRW) is located in the Southern Coastal Plain physiographic region of Georgia (Figure 2.1). The LRW is characterized by broad, flat alluvial flood plains with low-gradient, poorly defined channels, sandy soils, and slow-moving streams [75]. Our study area is

located in the northeastern upper basin part of the Little River Watershed, which is cited as the Little River Experimental Watershed (LREW). The LREW contains parts of Tift, Turner, and Worth counties. It is comprised of five sub-basins (at the 12-digit hydrological unit) ranging from 6,000 to 23,500 acres totaling 82,500 acres. Around 32% of the study area is occupied by cropland in 2019 [76]. The estimations from Cropland Data Layers (CDL) between 2009 and 2018 show that the croplands are mainly occupied by row crops, while cotton and peanuts are historically predominant (Figures 2.2 & 2.3). Almost all of these row croplands remain fallow in the winter season. In 2009, around 5% of cropland was utilized for winter crops, which was 0.1% in 2018. On average, only 0.8% of total agricultural land was used for cultivating winter crops annually between 2009 and 2018.

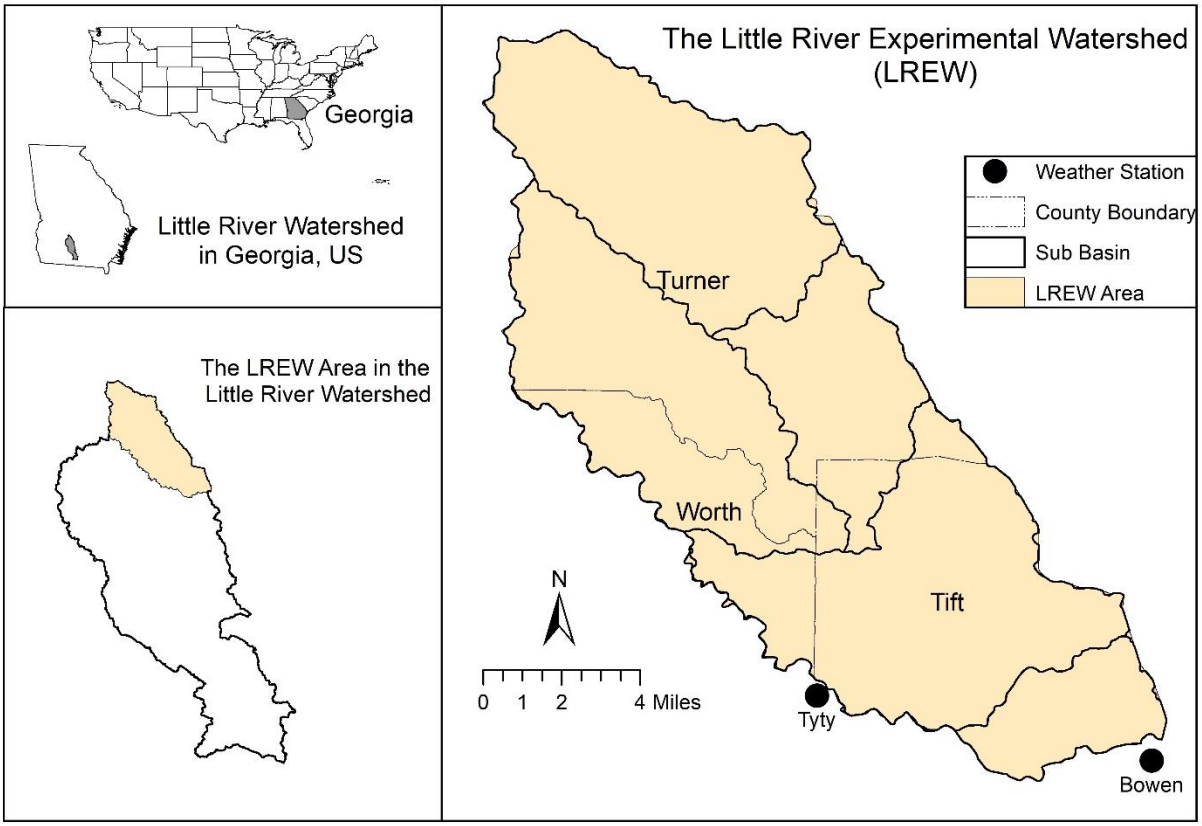

Figure 2.1: Location of the Little River Experimental Watershed (LREW) and surrounding weather stations.

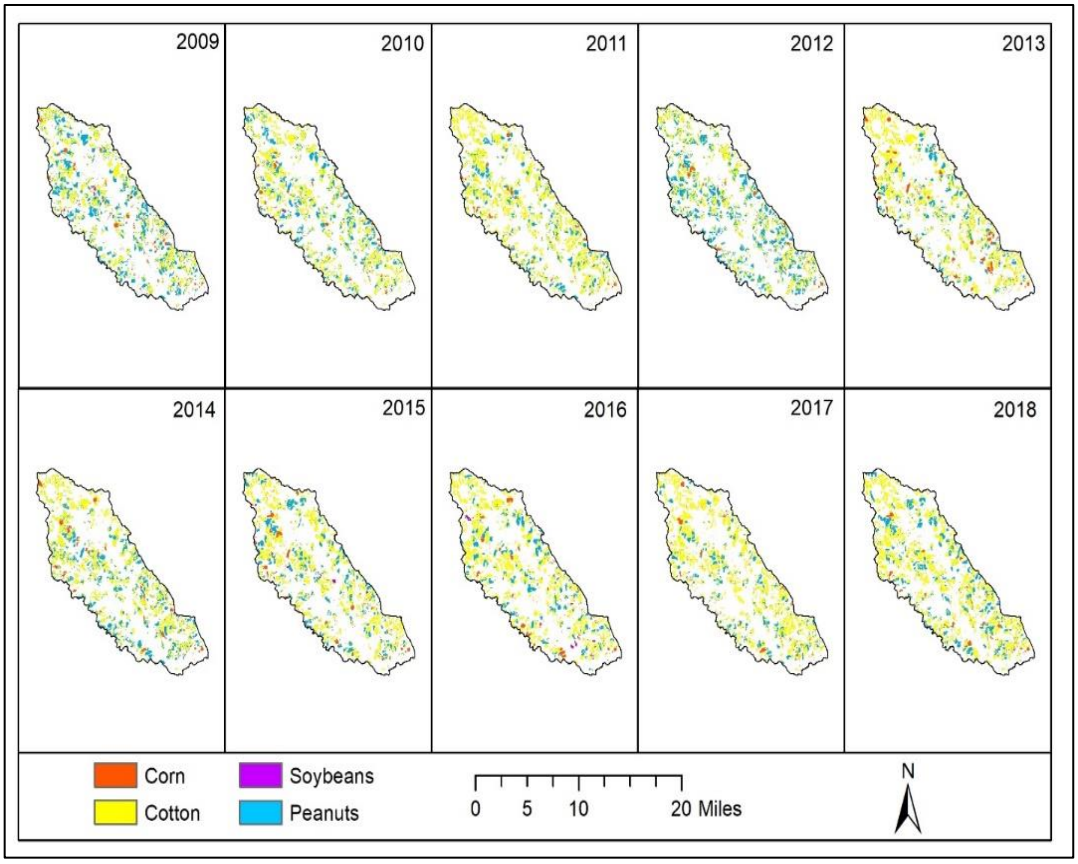

Figure 2.2: Area under major row crops in the study area between 2009 and 2018. Source: USDA, NASS [76].

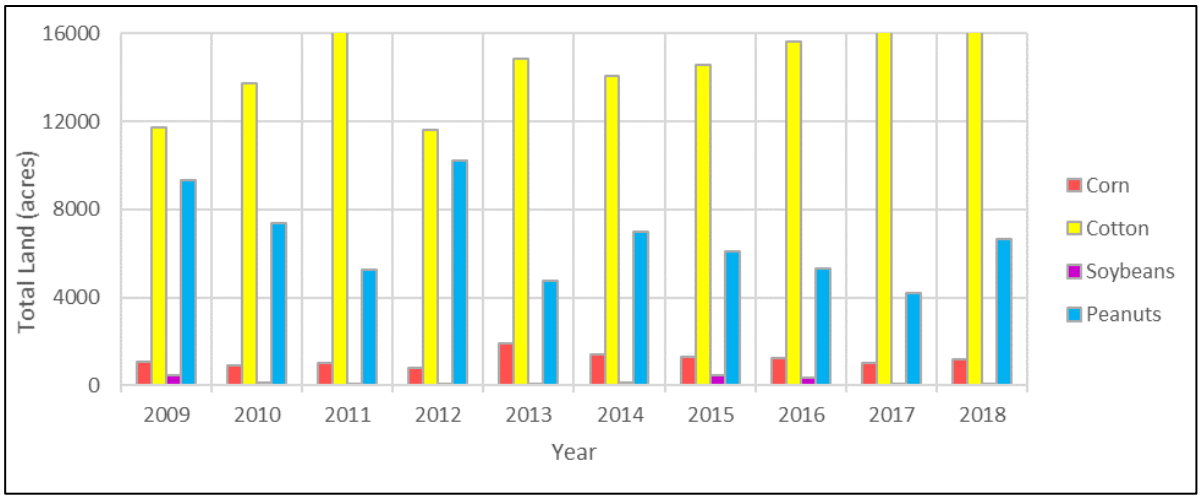

Figure 2.3: History of land cover (major row crops) in the study area. Source: USAD, NASS [76].

2.3. Methodology

2.3.1. Data Description

2.3.1.1. Geospatial data

We used two geospatial datasets in the study to make it spatially explicit, i.e., Crop Data Layer (CDL) and Landownership data, or parcel data. CDL raster data at 30 m resolution was procured from the USDA National Agricultural Statistics Service Cropland Data Layer (2019). We obtained the parcel data in ESRI shapefile format from the University of Georgia Information Technology Outreach Services.

2.3.1.2. Crop production costs and returns

Table 2.2 shows the key variables of annual crop yields, prices, and production costs that determine the profitability of four major crops from 2009 through 2019. The production costs involve operating costs for producing a crop, including seeds, fertilizer, irrigation, fuels, and other similar services. The allotted overhead costs, such as costs of labor, machinery and equipment, taxes, insurance, and other general farming overheads, are not included in net return estimations. The net return of a crop was calculated primarily from these three economic variables. The data were summarized according to USDA Economic Research Service (2020). The recorded yields for all crops are distributed normally at a p-value (≥ 0.05) according to the Shapiro-Wilk normality test. However, the corn price and production cost are not distributed normally over the years.

2.3.1.3. Carinata yield, production costs, and the initial contract price

There was no historical record of carinata yields and production costs in the study area. However, estimates were available from the experimental plots established under the Southeast

Partnership for Advanced Renewables from Carinata (SPARC), a Coordinated Agricultural Project supported by the United States Department of Agriculture National Institute of Food and Agriculture. The estimated yields of carinata can vary from low (40 bu/acre), medium (50 bu/acre), and high (60 bu/acre) yielding scenarios, and the estimated average operating cost to produce carinata is $275/acre [18]. Considering the minimum yield and average operating cost, the price of carinata should be at least around $7/bu to cover variable production costs. Therefore, in our model, we set the initial farmgate contract price of carinata as $7/bu.

Table 2.2: Variables affecting the profitability of major row crops and their normality test between 2009 to 2019. Source: USDA Economic Research Service [77]. (1 bu corn = 56 lb, 1 bu Soybeans = 60 lb). *p-value for Shapiro-Wilk normality test. ** 2012 price for peanut is excluded for an extremely high price ($0.34/lb). The production costs involve operating costs for producing a crop, which include costs of seeds, fertilizer, irrigation, fuels, and other similar services. The allotted overhead costs, such as labor costs, machinery and equipment, taxes, insurance, and other general farming overheads, were not included in net return estimations.

Return variables	**Crop Name**	**Unit**	**Mean**	**Sd**	**p-value***
Yield	Corn	bu/acre	154	17.5	0.74
	Cotton	lb/acre	840.9	98.4	0.73
	Cottonseed	lb/acre	1360.2	159	0.73
	Soybean	bu/acre	35.8	3.7	0.73
	Peanut	lb/acre	4122.5	383.3	0.05
Price	Corn	$/bu	4.82	1.3	0.01
	Cotton	$/lb	0.745	0.1	0.47
	Cottonseed	$/lb	0.083	0.02	0.10
	Soybean	$/bu	10.96	1.8	0.12
	Peanut**	$/lb	0.21	0.03	0.15
Production cost	Corn	$/acre	372.43	38.7	0.02
	Cotton	$/acre	559.61	44.6	0.30
	Soybean	$/acre	184.26	22.9	0.34
	Peanut	$/acre	489.86	36.6	0.34

2.3.1.4. Weather data

One of the challenges of promoting carinata in the SE United States is the susceptibility to frost events [19]. In the SE region, carinata, as a winter crop, can be exposed to the fluctuation of temperature from 50^0 F during the day to below 20^0 F on the same night, giving the crop only a little time to harden off [78]. For our study area, we collected 15-minute temperature data from the University of Georgia Weather Network (www.weather.uga.edu). Data were collected for the two nearest stations of the study area, i.e., Bowen and Tyty (Figure 2.1). We summarized the occurrence of critical daily temperatures, which is below 20^0 F for the day of occurrences (Table 2.3). The temperature fell below 20^0 F in several years. Especially in 2014, when the duration was 7 hours for Bowen, and similar temperatures were recorded two times (8 and 3 hours) in Tyty.

Table 2.3: Duration of temperature recorded below 20^0F in Bowen and Tyty.

Stations (month/year of installation)	Year	Julian day	Duration (hour)
Bowen (07/2003)	2005	24	1
	2014	7	7
	2015	8	1
Tyty (04/2006)	2014	7	8
	2014	8	3
	2015	8	3
	2018	18	1

2.3.2. Assumptions

There are three broad assumptions in our model. We first assumed that farmers are profit maximizers [22,24,25]. Then, we assumed that farmers are influenced by their neighboring farmers when it comes to adopting a new bioenergy crop [24,25]. Finally, we assumed that farmers are risk averse[22,25]. These three assumptions are reflected at different modeling stages in this study. Figure

2.4 explains the steps undertaken for ascertaining farmers' decision-making framework to complete this study.

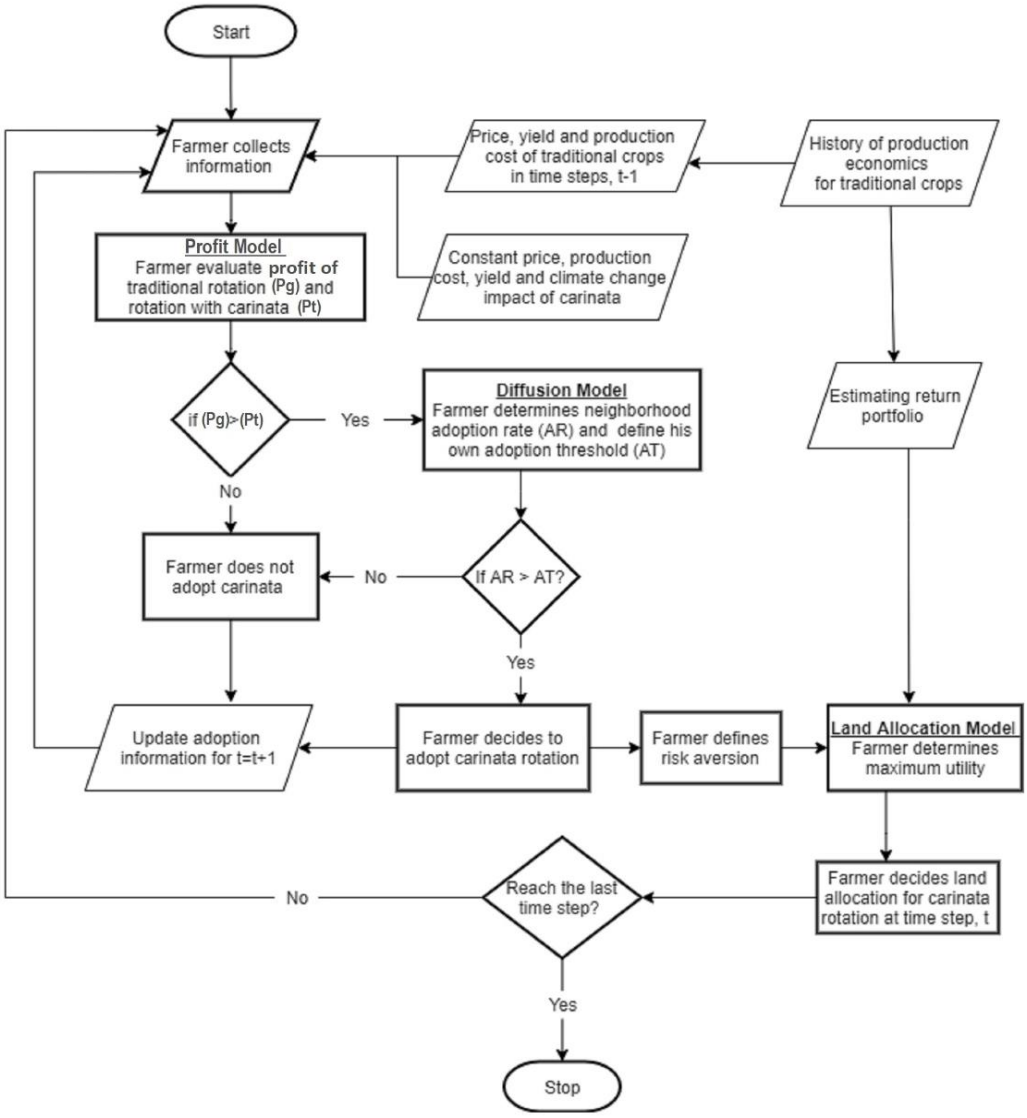

Figure 2.4: Flowchart of farmers' decision-making model

2.3.3. Initializing the model

Each farmer in our model is an agent who owns one or more parcels of farmlands. The minimum size of the parcels is 10 acres, which is also a minimum acreage to represent small agricultural farmland in Georgia [79]. There are 650 farmer agents in the data provided by the

University of Georgia Information Technology and Outreach Services. Before taking a decision on adopting carinata, each agent evaluates several physical conditions of their agricultural landscape, i.e., potential land resources for cultivating carinata, appropriate rotation plan for carinata, and potential impact of climatic events. The land resources and rotation plan were determined by using geospatial tools, where land parcels and historical CDL data were utilized. The potential impact of weather was calculated using Eq. 1. A detailed discussion on the evaluation of physical environmental conditions is provided in the Supplementary Information (Appendix 1).

$$WIP = (1 - H * L)^{d} * 100\ \% \ldots\ldots\ldots\ldots\ldots\ldots\ldots\ldots (1)$$

where, *WIP* = Weather Impact Potential, *H* = probability of one or more frost event frequencies in a year, L = proportion of crop damage potential due to event exposures, and d = number of occurrences in a given season.

2.3.4. Agents' decision-making model

Farmer agents' adoption decisions of carinata are reflected in three sub-models of profit modeling, diffusion modeling, and land allocation modeling. The profit modeling evaluates farmers' profits of row crop rotations with and without carinata. The diffusion modeling determines farmers' attitudes towards adopting carinata under neighborhood influences. The land allocation modeling estimates the proportion of land farmers will allocate for cultivating crops in rotation with carinata according to their risk portfolio. Farmers decide to allocate land for carinata for the current period only when they find their profit with carinata rotation is greater than without carinata rotation in the previous period, and the neighborhood influences from the same previous period build a positive outlook for adoption. For each farmer, the adoption behavior of the current period is updated and feeds into the next time step. Thus, the model works in a recursive manner

until the end of the simulation period. Figure 2.4 shows the flow of farmers' decision-making framework spread across three sub-models.

2.3.4.1. Profit modeling

The profit from the three-year rotation of traditional row crops is subject to expected return in Net Present Value (NPV) for the given land resources in association with yields, market prices, cost of production for the previous period of rotation (Figure 2.4). Thus, the profit from traditional rotations without carinata for period *t* was calculated using Eq. 2.

$$Pt = \sum X_{i,t-1,n,c} * \ (Y_{t-1,n,c} * P_{t-1,n,c} - C_{t-1,n,c}) * \ NP_{t,n} \quad \ldots\ldots\ldots\ldots\ldots\ldots\ldots\ldots\ldots\ldots \quad (2)$$

The first term in Equation (2), $X_{i,t-1,n,c}$, is the acreage of land allocated for crop *c* by farmer *i* at the n^{th} year of rotation period *t – 1*. *n* values are 1, 2, or 3 that represents 1st, 2nd, and 3rd year of period *t*, respectively. *t* = 0, 1, 2, ….11 steps of time with each three-year rotation period, where *t* = 0 is the base period. *c* = 1, 2, 3, 4 of crops, where 1 = corn, 2 = cotton, 3 = soybeans, and 4 = peanuts. The second term is the profit of a crop for a particular year calculated from yield (*Y*), price (*P*), and cost (*C*). The third term, *NP*, is the multiplier to determine the NPV, where $NP_{t,n} = (\frac{1}{1+r})^{(3t+n)}$, and *r* is the real discount rate [80].

The profit from crop rotation with carinata was calculated using Eq. 3, where the contract price, yield, production cost, and climate impact for carinata were constant over the simulation period (Figure 2.4).

$$Pg = X_{i,}(C * NP_{t,n=1} + C * NP_{t,n=2} + Ca * CIP * NP_{t,n=2} + P * (1-k) * NP_{t,n=3}) \quad \ldots\ldots\ldots (3)$$

where,

X_i = Total field crop land area of farmer i

C = profit from cotton, ∀ profit = Y*P-C

Ca = profit from carinata

CIP = Climate Impact Potential

P = profit from peanuts

K = yield loss of peanuts for late cultivating after carinata, $\forall k = 0.1$

$NP_{(t,n=1,2,3)}$ = multiplier of NPV values in the 1st year,2nd year, and 3rd year, respectively, for period t

The profits in Eq. 3 were calculated from a function of yield, price, and production cost, similar to the second term in the parenthesis of Eq. 2. There could be some loss of peanuts yields due to planting after growing carinata between mid-November to end-May. We assigned an average loss of 10% estimated from Drake et al. [81].

2.3.4.2. Diffusion modeling

Adopting carinata is a new experience for farmers in the LREW. The cumulative adoption of carinata is therefore analogous to new technology diffusion, which will empirically follow an S-shaped curve [25,74]. As the study was conducted on a small-scale watershed level, we assumed that farmers are under the same social group and are equally informed about the diffusion of the new technology. Therefore, the neighbors' influences apply consistently to all farmers in the watershed, although they will respond individually (and possibly differently) to these influences, thus affecting the rate of diffusion of the innovation, i.e., the adoption of carinata as a bioenergy crop in the winter months.

A number of approaches have been proposed for modeling technology diffusion processes [82], especially for adopting new agricultural technologies in the ABM framework [83]. In this study, we applied an adoption threshold approach [25]. The approach follows two parameters, i.e., local adoption rate (AR) and individual adoption threshold (AT). The current AR was determined from the net proportion of positive minus negative profit experiences from carinata among the farmers from the previous time step. Each farmer was assigned an adoption threshold (AT) value that

defines his degree of 'resistance' to change. If the AR value for a time step is greater than the AT of an individual farmer, then the famer shows a positive attitude about adopting carinata due to neighborhood influence (Figure 2.4). At the very beginning, there is no farmer, who is experienced in adopting carinata. The innovative farmers (usually risk preferers) will adopt carinata in first time step if only the profit conditions are met. Innovators will create the first net-positive AR. If the initial contract price of carinata is not as high as to get positive return for the innovators, a new price is set for the model. The positive experience of innovators will influence other farmers. When other farmers find the adoption rate due to adopting carinata by the innovators in the community is higher than their own AT, then other farmers cultivate carinata in the second time step. Sequentially, all the farmers including innovators and other farmers will update their experiences over each next time step in the simulation periods.

The AT values of individual farmers were assigned from normal distributions with a mean of 0.2 [25,67]. Two different distributions were used using standard deviations of 0.102 and 0.1216, respectively, to set the innovator category as 2.5% and 5% of total farmers. As the diffusion rate is slow in the earlier stage, only a small portion of farmers are willing to adopt carinata. In the default case, 2.5% of the farmers initially are willing to adopt new technology according to the theory of Diffusion of Innovations [74]. We selected 5% innovators to generate a less restrictive adoption rate and a higher willingness to adopt a new crop in the initial stage. The AR was fixed at 0 for the base year. By using the selected distribution of AT, innovators had negative AT values. Thus, setting an AR value of 0 at the initial stage fulfills the neighborhood requirement mathematically. That is to say, the innovators also adopt carinata if their AT values are less than AR even though there were no experienced farmers in the community at the base year.

2.3.4.3. Land allocation sub-model

It is unrealistic to assume that the farmers interested in adopting carinata will allocate all of their farmland for cultivating carinata [67]. Therefore, we used the land allocation modeling to optimize farmers' profits under individual risk aversion [84] (Figure 2.4). Each farmer's attitude to risk is held constant throughout the simulation period but can vary across the farmers. In this model, each farmer decides the proportion of land utilized for a particular crop rotation based on the portfolio of returns and the volatilities of the selected crop rotations. We applied a portfolio choice rule, initially proposed by Markowitz [85] and Freund [86], for facilitating decision-making about the land allocated to carinata production. The choice rule (here, we call the land allocation decision rule) was set by the expected returns, farmers' individual risk aversion parameters, and the variance-covariance matrix of returns. The variance-covariances represent the volatility, which needs to be compared with the returns to obtain an efficient frontier. The efficient frontier, where an individual farmer would operate, is achieved by maximizing the expected return and minimizing the volatility, where individual risk preference parameter set the degree of volatility that an individual farmer is willing to accept to maximize profit. The decision rule that optimize the profit of a farmer in terms of distribution of land allocation across the selected rotations is shown in Eq. 4 [87–89].

$$Maximize\ P_i = w'R - \frac{1}{2}\lambda_i w'\sigma^2 \mathrm{w} \quad \ldots\ldots\ldots\ldots\ldots\ldots\ldots\ldots\ldots\ldots \quad (4)$$

$$s.t. \sum_k w_k = 1, \qquad w' \geq 0$$

where,

P_i = expected profit of farmer i

R = target expected returns from each three years crop rotations

w = weights of the land assets

λ_i = risk aversion value of farmer i.

σ^2 = variance-covariance matrices of historical returns from crop rotations

We derived the weights of land allocation for each rotation using Equation 4, which we multiplied with total land resources to achieve the final land allocation decisions of individual farmers. Three rotations, such as cotton-cotton-cotton, cotton-cotton-peanut as traditional rotations and cotton-cotton-carinata-peanut as energy crop integrated rotation, were considered to determine the highest possible profit. For simplicity, we only consider cotton-cotton-cotton and cotton-cotton-peanut as traditional rotations. These two rotations were the most popular and profitable in the study area (Appendix 1, Section A.1.2). The net return of each rotation is the average of three years of NPV values calculated from the yield, prices, and production cost histories (between 1997 and 2018) of respective crops. For carinata, there was no price history. Therefore, we assumed the price variations of canola (sd = 2.7) would encapsulate the level of uncertainty for adopting carinata. We used the price history of canola from the USDA National Agricultural Statistics Service (https://quickstats.nass.usda.gov/). The risk aversion parameter was assigned for each farmer from a uniform distribution with a range of 0.5-1.5 [25]. To execute the formula, we used the *PortfolioAnalytics* package in *R* [89]. The software package has an in-built algorithm to determine the weights by maximizing the utility from the historical net-return data. However, we prepared a function to simulate all the individual farmers under a single command with their risk aversion parameter.

2.3.5. Model simulation over the watershed landscape

The landscape of the study area was designed with 25 x 26 cells, where each cell represented the total field crop area of a farmer agent. The model was simulated over 33 years (2018-2050) with a rotation period of three years for each time step (t). The base year ($t=0$) is

2018-2020, and the simulation was started with information on crop production economics from 2015-2017. Table 2.4 shows the values of parameters, which are the inputs to simulate the profit sub-model as well as sensitivity analysis of production economics.

Table 2.4: Utility model parameters and their values to run simulations. One bu corn = 56 lb. One bu Soybean = 60 lb. One bu carinata = 50 lb. N(μ, ס^2) represents the normal distribution, P(μ) represents the Poisson distribution).

Parameters	**Values for simulation**
Corn yield	N (154 bu/acre, 17.5)
Cotton yield	N (840.9 lb/acre, 98.4)
Cottonseed yield	N (1360.2 lb/acre, 159)
Soybean yield	N (35.8 bu/acre, 3.7)
Peanut yield	N (4122.5 lb/acre, 383.3)
Carinata yield	50 bu/acre
Corn price	P ($4.82/bu)
Cotton price	N ($0.745/bu, 0.1)
Cottonseed price	N ($0.083/bu, 0.02)
Soybean price	N ($10.96/bu, 1.8)
Peanut price	N ($0.21/lb, 0.03)
Carinata contract price	$7/bu, $9/bu, $11/bu, $13/bu, $15/bu
Corn production cost	P (372.43/acre)
Cotton production cost	N ($559.61/acre, 44.6)
Soybean production cost	N ($184.26/acre, 22.9)
Peanut production cost	N ($489.86/acre, 36.6)
Carinata production cost	$275/acre
Annual discount rate	6%

In the profit modeling, the mean and standard deviation values of respective traditional crop yields were used (Table 2.4). Similarly, the mean and standard deviation values were used for the price and production cost of traditional crops except for corn. The corn price and production cost were not normally distributed (Table 2.2). Therefore, Poisson distribution with mean price

($4.82/bu) and mean production cost ($372.43/acre) of corn were used as model inputs to capture the skewness in the distribution. In carinata, the average yield (50 bu/acre) and production costs ($275/acre) are fixed [2]. Different levels of the fixed contract price of carinata were applied for undertaking the sensitivity analysis. The effect of time on returns from the various crop rotations was achieved with an annual discount rate of 6% [90].

We captured the possible market, production, environmental, neighborhood, and risk sensitivities by setting the parameter values. To implement the simulation work, we preprocessed the agents' environment first, especially using geospatial techniques for estimating total land resources and the best rotation with carinata. Then, we built our profit and diffusion sub-models in the *NetLogo 6.2.0.* environment (Figure 2.5, detail codes are available in Appendix 2). Then, the full model, including the land allocation decision model, was run in *RStudio, version 4.0.2.*, while the *RNetLogo* package was used to maintain the interface between *NetLogo* and *RStudio.* Figure 2.5 shows the output of a model run by 2050 at a carinata price of $13/bu, a higher initial willingness scenario, i.e., AT = N (0.2, 0.1216), and a risk aversion parameter with uniform (0.5-1.5). For each price and initial willingness scenario, the model was run 30 times. Thus, the model is simulated for 300 runs for five different price scenarios and two willingness scenarios, which gave 3300 land allocation outputs for eleven-time steps over the study area. Then, the average values of 30-runs in each scenario were analyzed to observe the adoption rate and land allocation pattern over the landscape and over time.

[2] Carinata as an energy crop is still under experimental level in the SE United States. At the time we progressed our research, there was not sufficient data on yield variation and production costs. Therefore, we used deterministic production economics for carinata in this study.

2.4. Results

Figure 2.6 shows the number of farmers who will adopt carinata at different contract prices in two initial willingness scenarios. According to Figure 2.6 (a), the adoption rates tend to go high with the higher contract price of carinata. For instance, around 17, 47, 114, 167, and 267 farmers out of 650 would adopt carinata by 2050 with a contract price of $7, $9, $11, $13, and $15, respectively. These trends also suggest that the increase of adoption rates with higher prices is not always linear. Neighborhood influence plays a vital role. Specifically, with a lower adoption rate at the earlier stages, the adoption pattern follows a slightly upper trend even though the prices are higher. For example, only around 9% of farmers would adopt carinata by 2035 with the price of $13/bu and $15/bu.

The influences of the neighborhood are more clearly visible in Figure 2.6(b) besides the impacts of prices. With a higher initial adoption rate (5%), the adoption rates will rise sharply between 2029 to 2038 at the prices of $11, $13, and $15. Even at the price of $9, the adoption number will increase steadily, and around 52% of farmers will adopt carinata by 2050. However, at the earlier stages, those rates are lower compared to long-term adoption rates, which supports Rogers' classical diffusion theory as well [74]. For instance, 85% of the farmers would adopt carinata by 2050 with a contract price of $13, while the adoption rate is around 23% after 12 years from the base year. For the low initial willingness condition, the adoption rate after 12 years is only 5% at the same price. However, the perfect segmentation of farmers' categories according to the classical diffusion theory is not within the scope of this study. Besides, there are also arguments against such perfect segmentations [91].

Figure 2.5: The output of a model run at carinata price $13/bu, Adoption threshold = N (0.2, 0.1216), Risk aversion = Uniform (0.5-1) after the end of the simulation period. The 'true' cells represent the farmers who will cultivate carinata at the end period and 'false' represent the farmers who will not adopt carinata.

It could be challenging to fix an accurate contract price of carinata as the crop is still relatively new in the region. However, our modeling results suggest that $13/bu could be a reasonable initial contract price for both adoption scenarios. Because, at this price, the adoption numbers will remain almost the same as that of $15/bu until 2035 under a low initial willingness scenario (Figure 2.6(a)). For a higher initial willingness scenario, the adoption rates will not be significantly higher with the contract price of $15/bu than $13/bu (Figure 2.6(b)). We also found that about 38% of row cropland in the study area could be utilized for carinata cultivation by 2050 in the low initial willingness scenario at $13/bu. In the high initial willingness scenario, this percentage could be as high as 85% in the study area. Please refer to Table 2.5 for more details.

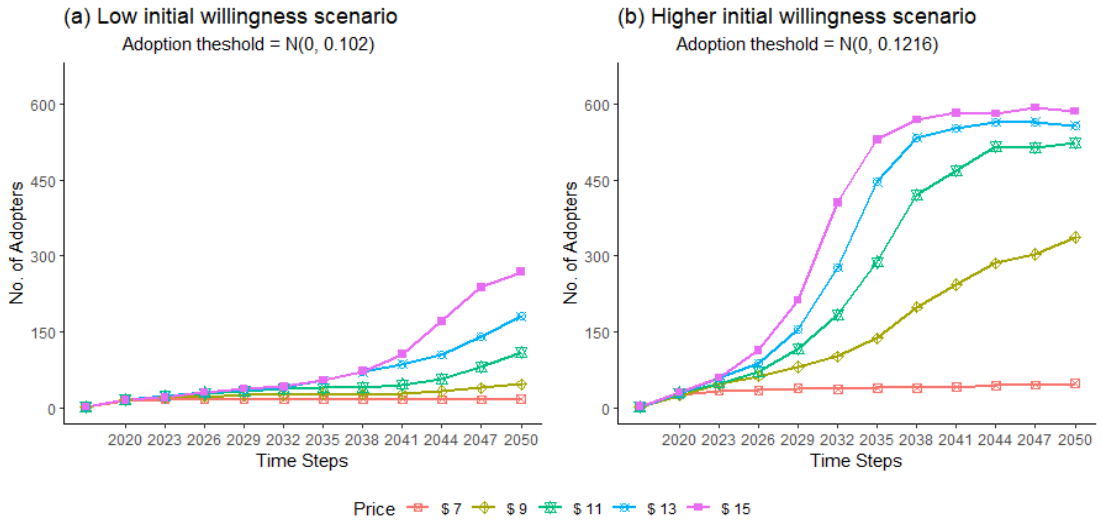

Figure 2.6: Number of agents adopting carinata at different prices under two adoption scenarios.

2.5. Discussions

Alexander et al. [25] reported similar findings to our results, i.e., the adoption behavior of the farmers, determined with AT values, highly influences the adoption of the energy crops over the simulation period. Jin et al. [67] also found a similar result with the same low initial willingness and adoption threshold parameters (2.5% innovator). However, there is a fundamental difference between our study and the other two studies. In those two studies, the number of adopters diminishes in the long run. In our case, the trend never goes downwards. Because, in our study, we assumed farmers decide on adopting energy crops based on most recent profit experiences. In other studies, if farmers experience a negative gain from energy crops, they will never adopt the new crop in the future, even after a long period. But, such an assumption could not be valid, at least in the context of carinata [91]. For instance, Christ et al. [91] found that individual farmer's negative experiences can deter them from adopting carinata; however, positive experiences of neighboring farmers can regain confidence about carinata adoption. Thus, in our model, we assigned the rule so that farmers with negative experiences did not adopt carinata for the next

rotation period but could adopt again afterward (s) when they found the neighborhood adoption rate was higher than their adoption threshold.

Besides, Alexander et al. [25] applied a considerably higher adoption threshold (25% innovator) to observe the higher initial willingness. This rate seems unreasonably high. Therefore, we applied a 5% adoption threshold in case of a high willingness scenario and still found significantly higher adoption rates over time. The positive adoption behavior of the farmers also ensures that a high percentage of land is allocated to the new crop (Table 2.5). However, no study was found to make a valid comparison with these results because of the differences across the study areas, feedstocks, and the information reported in the literature.

Nonetheless, if the higher initial willingness is ensured, there are two underlying reasons that would influence the farmers to allocate a higher portion of land allocation to cultivate carinata. First, in the traditional row crop rotations, almost all of the farmland in the LREW remains fallow in the winter season. Therefore, introducing carinata has no conflict with other crops, and there is no opportunity cost for conventional farming practices. Hence, if the contract price of carinata can add to the profitability by integrating with the traditional agricultural system, farmers will show positive attitudes towards its adoption. Our model reflects upon this positive attitude among farmers and brings our study closer to the field reality. Second, individual risk perceptions of the farmer agents are crucial for making land allocation decisions. In our modeling inputs, carinata appeared as the least risky enterprise. In the LREW, cotton is the most popular crop, possibly, for its consistency in net return. While peanuts are the most profitable crop, the market price is highly volatile. Therefore, in our model, cotton-cotton-cotton rotation was allocated as an average of around 11% of the cultivated land, and cotton-cotton-carinata-peanut rotation was on average allocated to around 89% of the cultivated area. Even though there is variability in net return for

peanuts and carinata (for which canola was used as a proxy in regards to price), the total profits from this proposed rotation trade-off with the risks that can be expected as they are perceived by the farmers, hence, the new crop could be preferred over the traditional rotations.

Table 2.5: Total land allocated for carinata in the study area and their ratios with total cropland with 30 model runs at the contract price, $13/bu, and under risk aversion parameter = U(0.5, 1.5).

	Low initial willingness		**High initial willingness**	
Year	**Land Allocated (acre)***	**Land Allocation Ratio****	**Land Allocated (acre)***	**Land Allocation Ratio****
2020	392	2%	785	4%
2023	589	3%	1374	7%
2026	785	4%	2158	11%
2029	1177	6%	4121	21%
2032	1374	7%	7457	38%
2035	1962	10%	12558	64%
2038	2158	11%	14913	76%
2041	2747	14%	15698	80%
2044	3532	18%	16091	82%
2047	5102	26%	16483	84%
2050	7457	38%	16679	85%

2.6. Conclusion

According to our model simulation results, it is obvious that the adoption of a new energy crop into an integrated agriculture system is influenced by initial willingness to adopt new technology. The willingness to try a new crop is dependent on farmers' individual attitudes as well as the influence of neighboring farmers. However, the willingness to grow the new crop is also determined by the added utility that will be gained by the farmers. Estimates of expected utility were derived from concurrent agricultural production functions and price market conditions as well as the farmers' attitudes to risk. Historical production and market conditions were also

observed to find the possible effects of price volatility on the individual farmer's sensitivity to risk. The results from our model have at least two important policy implications for bioenergy investors, policymakers, and extension people.

Firstly, a risk premium and or subsidy for the farmers may be required to adjust the return with a low fixed contract price to the level required for farmers to adopt carinata. The results of our study reflect the level of carinata prices, at which a considerable portion of farmers can enter the market. But, if the demand for feedstock diminishes, farmers may not find those fixed prices sustainable. The future extension of our current model will integrate the effects from the feedstock supply chain to find the most accurate fixed prices where farmers can sustain production in the presence of short- and long-term volatility in supply and demand conditions. However, with the current state of this model, it is clear that if biorefinery investors cannot offer a desirable fixed contract price, farmers will need a subsidy to adopt carinata. Weather factors may have potential effects on yield. In that case, our model might be helpful to calculate a risk premium from probable net returns under the fixed contract prices. The subsidy and risk premium can maintain a stable price market, which has further implications for increasing the land acreage allocated to carinata.

Secondly, our model suggests a clear relationship between initial willingness among the farmers to adopt this new crop with the expansion of the area of carinata cultivated. Therefore, knowledge campaign programs should be facilitated from the beginning to encourage farmers to adopt carinata. Such programs should continue over time so that the initial rate of growth in energy crop cultivation does not diminish.

We addressed both the social and economic factors of adopting bioenergy crops in our modeling approach. The environmental variable, such as the effect of weather sensitivity on bioenergy crop production, is embedded in our model, though that variable had no effect in the

context of our study area. In our future work, possibly for extending our model to the entire SE region, the weather impact variable will be useful. However, one major limitation arises in our model for studying a small-scale watershed study area. We did not address the supply chains of the feedstock market and potential carbon emissions throughout that supply chain. Our future research will cover this research gap by exploring sustainable supply chain models in association with determining carbon footprint using life cycle assessment.

In summary, we determined the land allocation decisions of farmers for adopting carinata based on three principles that a farmer agent follows – profit maximization, neighborhood influences, and risk aversion. To evaluate the adoption behavior of farmers, we included the agronomic, biophysical, climatic conditions, and crop production economics in a simulation model to obtain a potential solution for carinata adoption at the landscape level. The approach taken in this study significantly extends the existing research frontier on the adoption of bioenergy crops, as we have elegantly combined various existing for capturing the dynamics of a farmer's crop adoption decisions. Besides, existing literature does not have sufficient transparency in discussing modeling framework, spatial explicitness, or sharing of computational codes. Therefore, we built an innovative agent-based modeling tool to address the shortcomings of existing models and solve the land allocation problems in the context of the adoption of carinata as a feedstock for sustainable aviation fuel production in the United States, in general, and the Southern United States, in particular. However, this modeling tool needs to be verified with more sensitivity analysis, field verification, and the possible inclusion of other stochastic decision-making tools (e.g., stochastic dominance analysis). We hope that the modeling tool developed in this study will feed into future research where more advanced versions of the same will be used for forecasting the adoption behavior of farmers regarding new agricultural technologies in the SE United States and beyond.

CHAPTER 3

DESIGNING CARINATA-BASED SUSTAINABLE AVIATION FUEL SUPPLY CHAIN IN GEORGIA USING GIS AND MIXED-INTEGER LINEAR PROGRAMMING [3]

[3] Ullah, K.M., Masum, F.H., Field, J., & Dwivedi, P. To be submitted to [Biofuel, Bioproducts & Biorefining]

Abstract

Carinata is identified as a potential crop for producing sustainable aviation fuel (SAF) in the southern United States. However, much of the cost-effectiveness and environmental feasibility of carinata feedstock remained unknown as the supply chain of carinata-based SAF has not yet been unveiled. Thus, this study aims to design a supply chain model for carinata-based SAF production by optimizing the location of farms and facilities (e.g., storage units, crushing mills, biorefineries) with a minimum transportation cost under a set of supplies and a demand condition. An integrated Mixed Integer Linear Programming (MILP) model associated with the Geographical Information System (GIS) was built to design a spatially explicit supply chain configuration. The GIS-based network analysis preselected the candidate locations of farms and facilities and determined minimum cost and emission routes. The MILP model determined the final selection of the farms and facilities' number and locations over those routes. With this supply chain configuration, the minimum price of SAF was estimated at \$1.14 L^{-1}, which is \$0.64 higher than the conventional aviation fuel (CAF). The carbon emission was 964.82 g CO_2e L^{-1} of carinata-based SAF, which is 63% relative carbon savings compared to the emission from CAF. The study found that a carbon tax of \$387.13 t^{-1} of GHG emissions on CAF would be needed to promote the use of carinata-based SAF in the region.

Keywords

Aviation Sector, *Climate Change*, *Sustainable Development*

3.1. Introduction

The commercial aviation industry in the United States has made a significant improvement in the energy efficiency of an average aircraft by using advanced engine technologies as well as improving air traffic operations [4]. For the last 60 years, the United States has reduced the energy intensity of air travel by 75%. However, the per capita aviation fuel use is around 284 liters, which is six times higher than the world average, and 2.3, 7.5, and 37.5 times that of Europe, China, and India, respectively [4]. The greater use of aviation fuel in the commercial aviation industry of the United States is factored by a high volume of international and domestic air travel. For instance, in 2019, around 927 million passengers traveled within the United States by air, which was 21% of global air flight passengers for the same year [92]. As a result of using conventional petroleum-based aviation fuel for carrying such a high volume of passengers, the aircraft industry contributes 12% of United States transportation emissions, which account for three percent of total greenhouse gas (GHG) produced across all the national economic sectors [3].

In response to combat GHG emissions, the Government of the United States adopted a new 'Sustainable Aviation Fuel Grand Challenge' that targets to produce at least 11.4 billion liters of sustainable aviation fuel (SAF) production per year by 2030 to reduce emissions by 20%, and produce 132.5 billion liters of SAF per year in the long term to meet 100% of aviation fuel demand by 2050 [6,93]. It is expected that the use of SAF could reduce the greenhouse gas emissions of the aviation sector by 80% [1]. Additionally, SAF can be blended into the CAF, the resulting blended fuel is fully certified as Jet A or Jet A-1, and could be supplied using existing airport infrastructure and standard procedures. However, feedstock for SAF production needs a balanced distribution of supply with a larger yield to meet the demand, in addition, to maintaining environmental sustainability, such as no competition with food crops, compatibility with current crop rotations to

avoid deforestation, as well as no direct or indirect impact on land use changes [13]. Considering these prerequisites, carinata can be an appropriate alternative for producing SAF in the southern United States [14].

Brassica carinata, sometimes called Ethiopian mustard, Abyssinian mustard, or simply carinata, is a promising annual oilseed crop for the commercial production of SAF [14,15]. Carinata is rich in oil content (42%-52%); has high frost and drought tolerance; therefore, it can be cultivated with other row cops without competition with food crops [14,16]. As a cover crop, carinata can provide several ecosystem services by reducing soil erosion, nutrient leaching, increasing soil organic matter, and retaining moisture [17]. In the Southeast (SE) United States, carinata can be grown with a potential yield of 0.55 t/ha [18]. In Alabama, Georgia, and Florida, carinata can be potentially cultivated on about 1.4 million ha of fallow agricultural land during the winter season [19]. On the other hand, thirteen southern states of the United States consume about one-third of the nation's total aviation fuel consumption [20]. Therefore, the large supply of carinata feedstock can meet the immediate demand of SAF regionwide.

However, two primary factors that pose challenges for producing and distributing advanced transportation biofuels, including SAF, besides feedstock availability are conversion technology and biomass supply chain (BSC) [26]. The biochemical composition of carinata has been proven suitable for many conversion technologies, while the supply chain of carinata-based aviation fuel in the southern United States needs to be examined [27].

BSC consists of a discrete process that usually comprises harvesting feedstock, preprocessing and storing biomass, arriving biomass at conversion facilities (e.g., biorefinery), and reaching refined fuels to the consumer to meet the demand [26]. This discrete process is dependent on several spatial and temporal factors [12]. The spatial factors, such as feedstock's yields and

locations, capacity and locations of facilities (e.g., storage units, crushing mills, biorefineries), and existing transportation modes and network infrastructures affect the supply chain decisions of a biofuel. The seasonality and availability of feedstocks as well as variability of demands are the temporal factors that have an impact on the short-term and long-term viability of biofuel production. Besides, the environmental sustainability of BSC can be questionable if the net-GHG emission offset is not feasible [33]. Optimizing the capacity and locations of feedstocks and facilities by connecting with appropriate transportation routes and simulating steady flows of seeds and materials in accordance with SAF demand is a complex job [12,26,28]. However, modeling is pivotal to building a cost-effective supply chain for biofuel and estimating the net-GHG emission [33–35].

Mixed-integer linear programming (MILP) is the most widely used technique for modeling BSC [26]. Several contemporary BSC modeling studies plugged Geographical Information System (GIS) into the MILP models to configure distributed supply chain [35–41,94]. In a centralized supply chain configuration, higher economies of scale can be obtained with fewer and larger processing facilities, but it also implies higher upstream transportation costs due to mobilizing biomass from dispersed and distanced feedstock locations [34,95]. A distributed supply chain is, therefore, often suggested for BSC configuration as a trade-off between the economies of scale and transportation costs by establishing smaller facilities closer to the biomass resources [95], which can also be upscaled with a higher number of or larger facilities [34]. In these pursuits, the GIS-based BSC approaches enabled the investigation of the transportation networks and modes, which can be directly utilized in MILP models to optimize the number, capacities, and locations of feedstock's farms and facilities to satisfy a certain level of demand at a minimum cost [35,47].

However, to the best of our knowledge, none of the GIS-based BSC literature jointly incorporated the spatial, temporal, and emission issues to develop a sustainable BSC policy. Then,

demand sites of SAF are targeted to the central airports of the studied regions [96,97]. The major airports in the United States, most of the time, are connected with pipelines (data-usdot.opendata.arcgis.com); and 76.9 % of refined petroleum products are transported by using pipelines [98]. Pipelines are more economical and have less GHG emissions compared to the road and rail transportation modes [99,100]. However, only Jeong et al. [36] included pipelines in their GIS-based supply chain model. As a result, the majority of the GIS-based SAF supply chain studies in the United States might have potentially missed the minimum cost and emission route options to transfer the refined SAF from the distributed biorefineries to the centralized airports.

In light of the above context, our study aims to develop an integrated carinata-based SAF supply chain using GIS in Georgia, a state located in the Southern United States. We built a combination of distributed (by locating facilities) and centralized (by targeting major airports) supply chain models by incorporating spatial and temporal factors. To do that, we set potential candidate locations for farms and facilities; applied the ESRI ArcGIS *Network Analyst* tool to identify the least-cost transportation routes from the existing networks of road, rail, and pipelines; and used the MILP technique to estimate the optimum locations of farms and facilities as well as the flow of biomass for 20 years with four seasonal quarters in each year. In addition, we evaluated the GHG emissions over the supply chain configuration to determine the carbon abatement cost so that the policy supports necessary to analyze the tradeoff between SAF and CAF [49].

3.2. Methodology

3.2.1. Study area

Georgia is a state in the Southeastern region of the United States, having an area of 153,910 km^2. The major land covers of the states are forest (58%), agriculture/pasture (20%), transportation

(6%), and others (16%) such as urban areas, open water, and so on (https://narsal.uga.edu/gap/landcover/). The landscape of Georgia is divided into five physiographic regions –Appalachian Plateau, Valley and Ridge, Blue Ridge, Piedmont, and Coastal Plain [101]. The major agriculture activities occur in the Upper Coastal Plain, which covers the central and southwestern portions of the state. The state's dominant agricultural production, i.e., peanut, cotton, and vegetable industry, are located here. Even though Georgia is located near the Appalachian coalfields and oil and natural gas basins, the state does not have significant fuel reserves (https://www.eia.gov/state/print.php?sid=GA). However, with around two-thirds of the state's forestland and 4.05 million ha of agricultural land (https://narsal.uga.edu/gap/landcover/), Georgia has the availability of abundant biomass to produce renewable biofuels. Especially, the vast majority of agricultural land occupied by cotton and peanuts remains fallow in the winter season [76]. Those fallow lands can be utilized for cultivating carinata to produce SAF.

There is also a high demand for SAF in Georgia, as the world's busiest airport, the Hartsfield-Jackson Atlanta International Airport (shortly, Atlanta airport), is situated in Georgia. Currently, Atlanta airport alone consumes around 3.9 million t of CAF, which is around 5.2% of the total CAF consumption in the United States [102]. Besides, the counties of Georgia are well connected with its 7,360 km of active rail lines (http://www.dot.ga.gov/IS/Rail) and 1,540 km pipelines for transporting refined petroleum-based products (https://data-usdot.opendata.arcgis.com/). Therefore, a cost-effective distributed supply chain could be established in Georgia for carinata-based SAF production.

3.2.2. The system, process, and overview of modeling

The supply chain system of the model included five echelons – 1) farms, 2) storage units, 3) crushing mills, 4) biorefineries, 5) airport(s) (Figure 3.1). Carinata seeds were harvested from the fields and transported to the storage units. However, in the harvesting season (1st quarter) a portion of the seeds went to crushing mills directly from farms depending on the demand to avoid loading and unloading costs at the storage units. The rest of the portion of seeds were stored in storage units for the next quarter of the year and sent to crushing mills sequentially based on seeds' availability and demand. At the crushing mills, the seeds were converted to crude oil, and high-protein animal meal, also called carinata meal, as a co-product. The crude oil was transported to the biorefinery, where it was refined to obtain SAF and other co-products, e.g., propane and naphtha. The Hydro-processed Easter and Fatty Acids (HEFA) technological pathway was utilized to produce SAF. A detailed discussion on used HEFA technology is available in Alam et al. [103]. The distributed supply chain was configured to select the farms' locations, and the number of storage units, crushing mills, and biorefineries according to the interconnection between materials flow and demand. Thereafter, a centralized process was followed to transport the SAF from the biorefineries to the depo, assumed to be located at the Atlanta airport. The materials were carried along the least-cost transportation routes using available modes, stations, and intermodal facilities.

According to the above system process and boundary, the optimization model applied two major techniques, i.e., a GIS-based Network Analysis and a MILP-based supply chain optimization (Figure 3.2).

GIS datasets (feature data) were used to select potential locations (candidate locations) of farms and facilities and build transportation network data using roads, rails, pipelines, and junctions (e.g., stations, intermodal facilities). The candidate locations and transportation networks were used to

estimate the least-cost transportation routes from origins to destinations (O-D cost matrix). The GHG emissions throughout those least-cost routes were also calculated. Including that least-cost route data along with other datasets and parameters, such as farming areas, yields, unit costs of seeds and co-products, operational costs, capital costs, the capacity of facilities and conversion factors, the optimum locations of farms and facilities were selected. The minimum costs were obtained as direct output from the optimum supply chain model. The LCA GHG emission was calculated separately over the supply chain configurations using the unit GHG emissions of facilities along with emissions from transportation. Finally, the carbon abatement cost was determined from the supply chain costs and GHG emissions.

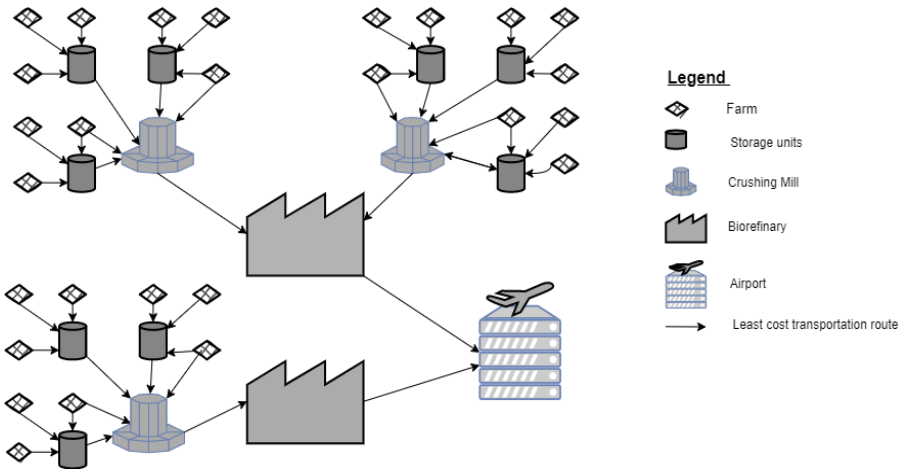

Figure 3.1: The system boundary of the carinata-based SAF

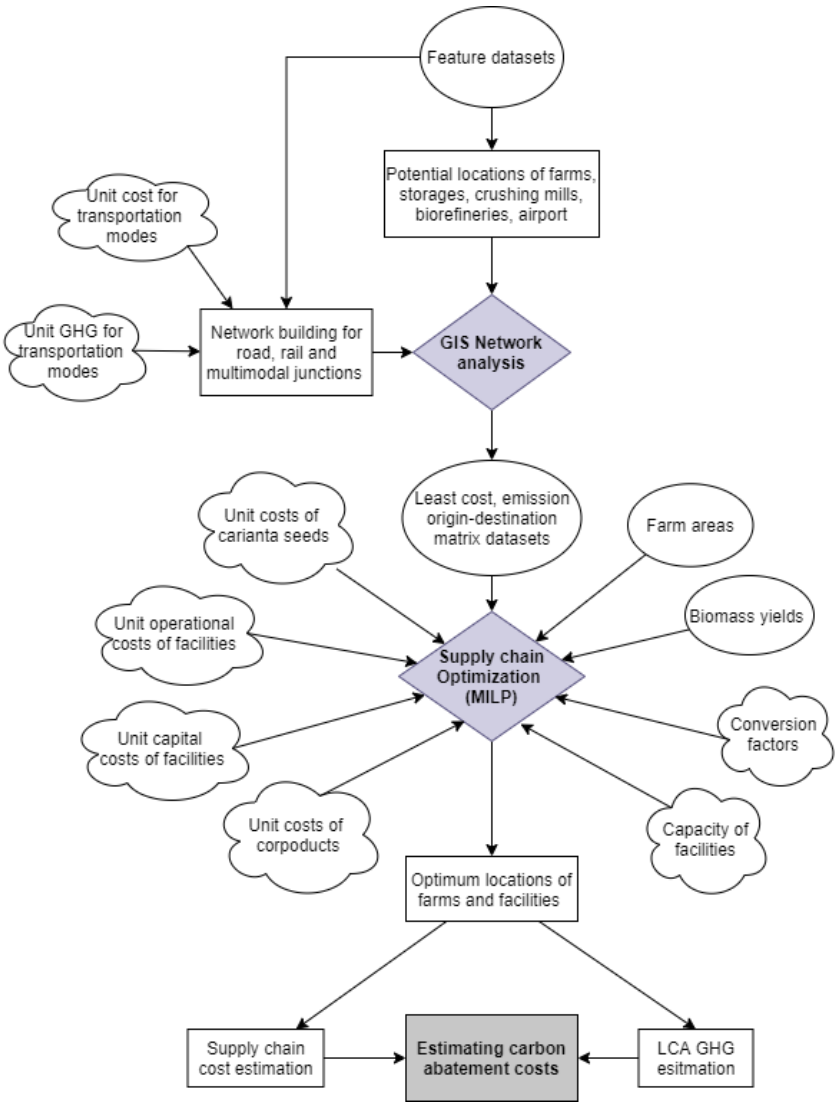

Figure 3.2: GIS-based integrated supply chain modeling framework

3.2.3. Potential locations of farms and facilities

The candidate counties of carinata feedstock were selected from the possible seed production on the available land, a data set generated by the DayCent model [104,105] (Figure 3.3 (a & b)). The spatially explicit DayCent model was previously calibrated to represent carinata grown in the Southeastern United States based on data from Agrisoma Biosciences, Inc (now NuSeed Inc.). The model was simulated on the cultivated annual cropland as per the 2016 National Land

Cover Database. The DayCent simulations were assumed that carinata is grown as a winter cover crop between the two cotton cash crops of a three-year cotton–cotton–peanut rotation, with moderate-intensity field preparation, planting in mid-November, and harvesting in late May. The rotation was suggested to avoid herbicide effects [106]. The centroids of the candidate counties were considered as feedstock supply sites, assuming that the feedstock would be collected near the center of the counties. The centroids of the candidate counties were also selected as the candidate locations of storage units, crushing mills, and biorefineries. From the DayCent model, the potential Soil Organic Carbon (SOC) sequestration was also measured due to the production of per metric ton carinata seeds (Figure 3.3 (c)).

3.2.4. Building network database and network analysis

A geodatabase of Georgia's multimodal transportation network was built by combining the spatial databases of roads, railroads, pipelines, and junctions (e.g., rail stations, intramodal facilities) using ESRI ArcGIS tools (Figure 3.2). The junctions allowed transferring materials from one transportation mode to another economical mode. The GIS database of road and railroad was collected from TIGER (Topology Integrated Geographic Encoding and Referencing) [107]. The rail stations, pipelines, intramodal facilities, and airport database were obtained from the Bureau of Transportation Statistics [108]. Before building the geodatabase, cost and emission attributes were assigned over the network lengths (in km) for each transportation mode. Table 3.1 presents the cost and emissions of transportation modes for transporting each metric ton of materials per km. There were loading and unloading costs associated with seed collection from fields and dispatching at the storage sites. Those costs were included while building the MILP model. The loading-

unloading costs of collecting seeds for the crushing mills, unrefined oil, and SAF were negligible compared to the total transportation costs [35]. Hence, those costs were ignored.

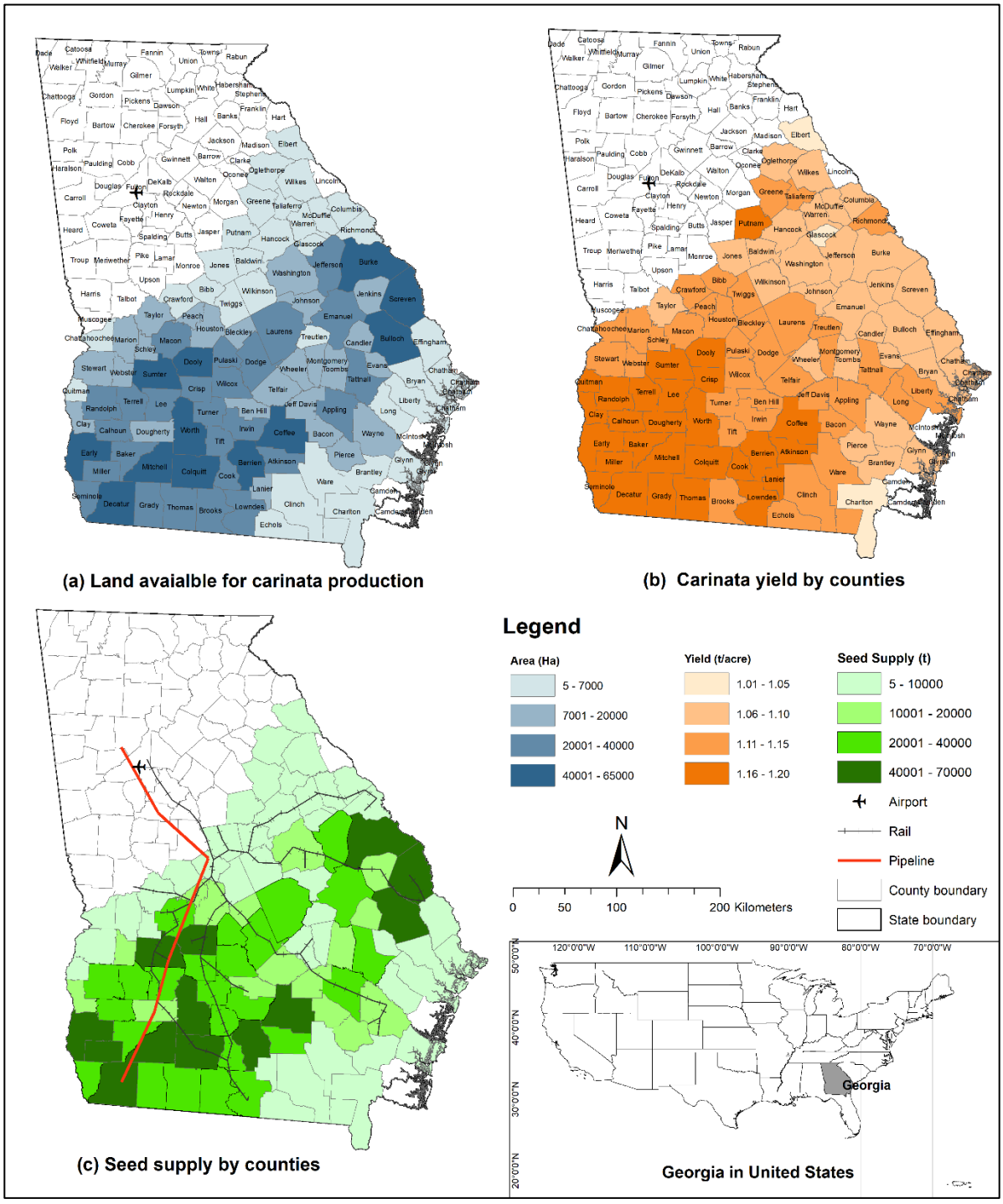

Figure 3.3: County-wise land availability for carinata production, annual seed production, and soil organic carbon sequestration potential in Georgia.

Table 3.1: Transport cost and emission by transportation modes

	Modes			Unit
Item	**Rail**	**Road**	**Pipeline***	
Seed transport	.050016 [99]	0.1027**		$/t-km
Oil/SAF transport	.050016 [99]	0.0959**	0.04736 [100]	$/t-km
GHG emissions	.000101 [109]	0.00011**	0.00009 [110]	CO_2e/t-km

* Pipeline can be only used for refined SAF transportation.
** Butch Cobb, grain accounting supervisor, and hedge manager, AGrowStar, Davisboro, Georgia, United States.

Once the transportation network database was built, the minimum cost routes were determined by applying the O-D cost matrix, a function of the ESRI ArcGIS *Network Analysts* tool. The O-D cost matrix function evaluated the minimum transportation costs for transporting per unit of materials (i.e., tonne) between farms-storages, farms-crushing mills, storages-crushing mills, crushing mills-biorefineries, and biorefineries-airport. The minimum cost routes could be determined from a combination of transportation modes, not necessarily limited to a single mode. The approach can be explained in Figure 3.4, where roadway and railway transportation modes were applied. For example, the least-cost route between County A and County B, and County B and County C are connected by roadway and utilize trucks for material transportation. Railway exists on County A and closes to County B. But, those two counties cannot utilize the rail network option as they are not connected with any close multimodal stations to transfer the materials from truck to rail, even though railway could be a cheaper option. While County A and County C use the longest distance for using the railway as this is the cheapest option and connected with stations. Along the estimated minimum cost routes using the *Network Analysts* tool, the total accumulated GHG emissions were calculated depending on the modes used for transportation.

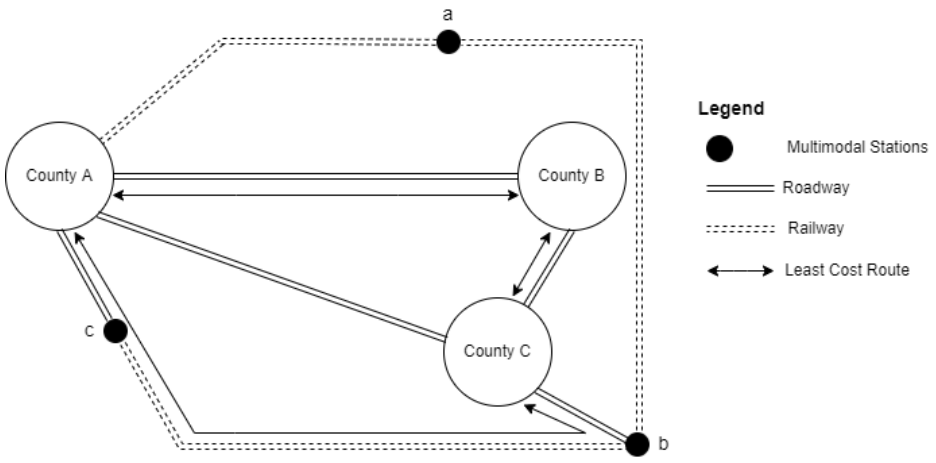

Figure 3.4: The minimum cost route estimation approach using *Network Analyst* tool.

3.2.5. Mixed Integer Linear Programming

The MILP function was built to optimize the location and number of farms and facilities by minimizing the supply chain cost of seeds, the capital cost of facilities, operational cost, transportation cost, and maximizing the coproduct sales. The demand threshold of the supply chain was estimated to be 100% of SAF. The capacities of all the facilities were fixed. However, the number of storage facilities in the estimated locations could vary depending on the flow of materials. Because to meet the large demand for seeds, multiple numbers of small storage units were necessary for the candidate counties. In the case of crushing mills and biorefineries, a maximum of one facility could be availed for a candidate county to maintain the decentralized supply chain. All the unit costs of seeds, capital costs, operational costs, and co-product sales were also fixed. However, except for the capital costs, all the costs were adjusted with inflation and discounted rates. The model was simulated for 20 years. The definition of sets, variables, factors, and constraints used in Eq. (1-16) and associated unit and data sources are presented in Table 3.2.

Table 3.2: Sets, variables, parameters, factors, and constraints used in MILP function.

	Symbols	Definitions
Sets	c, s, o, b	Candidate counties for carinata seeds supply, storage units, oil crushing mills, and biorefineries, respectively.
	D	Demand node, i.e. Atlanta airport
	T	Years of operations, t = 1,2…...20
	Q	Quarters of years, q=1,2…4
Variables	$AC_{c,q}$	Acres harvested to produce carinata seeds in county c at quarter q
	$\Upsilon_{c,q}$	Seed supply limit at county c in quarter q
	S_s	Number of storage facilities created in county s
	O_o	Number of oil crushing mills created in county o
	B_b	Number of biorefineries created in county b
	$FS_{c,s,q}$	Seed transported from fields at county c to storage s at quarter q
	$SS_{s,q}$	Seed stocked in the storage s at quarter q
	$FO_{c,o,q}$	Seed transported from the field at county c to crushing mill o at quarter q
	$SO_{s,o,q}$	Seed transported from storage s to crushing mill o at quarter q
	$OB_{o,b,q}$	Oil produced and transported from crushing mill o to biorefinery b at quarter q
	$BA_{b,d,q}$	SAF produced and transported from biorefineries b to airport d at quarter q
Parameters	$A_{c,t}$	Area available for planting carinata seeds in county c for year t, acre
	β	An adjustment with inflation rate (1.9%) and discounted rate (6%)
	P	Price of carinata seeds at quarter q, $441/t
	Y_c	Yield of carinata seeds in county c, tonne (see SI 1)
	PP_q	Production possibility in quarter q; if q=1, PP_q = 1, else PP_q = 0
	SCAP, OCAP, BCAP	Fixed capital cost of opening storage ($125,000), crushing mill ($16,130,000), biorefinery ($409,220,000), respectively [111]
	LU	Loading or unloading cost of seeds, $4.4/t [112]
	SOP, OOP, BOP	Operational cost for storage ($8.8/t of seeds), crushing mill ($19.54/t of oil), and biorefinery ($941.2/t of fuel), respectively [103]
	$TC_{c,s}$	Transportation cost of seed from farms in county c to storage s, $/t-km (O-D matrix)

	$TC_{c,o}$	Transportation cost of seed from farms in county c to crushing mill o, $/t-km (O-D matrix)
	$TC_{s,o}$	Transportation cost of seed from storage s to crushing mill o, $/t-km (O-D matrix)
	$TC_{o,b}$	Transportation cost of oil from crushing mill o to biorefinery b, $/t-km (O-D matrix)
	$TC_{b,d}$	Transportation cost of SAF from biorefinery b to airport d, $/t-km (O-D matrix)
	MP	Price of carinata meals, $413.3/t [103]
	PPr	Price of propane, $670.2/t [113]
	NP	Price of naphtha, $1030.7/t [114]
	D_d	Average quarterly demand of total jet fuel at the airport d, 879533 t/quarter [102]
Factors and Constraints	O'	The conversion factor from seeds to oil, 0.4329 [115]
	M	The conversion factor from seed to meal 0.56 [115]
	J	The conversion factor from oil to SAF, 0.7198 [116]
	Pr	The conversion factor from oil to Propane, 0.0882 [116]
	N	The conversion factor from oil to Naphtha, 0.062[116]
	SL	% of seed loss in the store for each quarter, 1% [103]
	SV, OV, BV	Capacity of each storage (1134 t of seeds /year), crushing mill (1037323 t of seeds/quarter), and biorefinery (110279 t of oil/quarter), respectively [111]
	D'	Share of total jet fuel demand, that must be met by SAF, 13%

The objective function of the MILP model is presented in Eq. 1-6. The seed cost was determined from the harvested area (AC), yield potentials (Y), seasonal production potentials (PP), and carinata contact price (P) at the farm gate (Eq. 2). Country-level farms' area and yield potential data were estimated by the DayCent model (Figure 3.3 (a & b)). The PP was dependent on the four seasonal quarters of a year. Carinata seeds were harvested in the first quarter of a year and for the rest of the year, the seeds were stocked in the storage units. The binary PP value set the seed

production in every first quarter of the year and maintained the nonproduction condition for the rest of the quarters.

The total capital costs were calculated from the number of facilities and fixed capital cost (Eq. 3). The initial capital costs of storage (SCAP), crushing mills (OCAP) and biorefineries (BCAP) were fixed at $125,000, $16,130,000 and $409,220,000, respectively [111]. The capital costs were determined as an investment in the base year. Therefore, adjustments with the inflation and discounted rates were not applied for the capital costs.

There are two categories of variable costs in the supply chain model – operational costs and transportation costs (Eq. 4 & Eq. 5). Both of these cost categories were dependent on the materials' production, flow, and stocks in the storage units (FS, SO, SS, OB, and BA). The first two cost items in Eq. 4 referred to the seed handling cost of loading and unloading (LU) in the storage units. Other cost items were unit operational cost involved for stocking seeds at the storages (SS), producing oil for biorefineries (OB), and producing SAF for the airport (BA). Unit transportation costs (TC) for carrying per metric ton of materials were imported from previous O-D matrices determined by network analysis (Eq. 5).

The cost returns from coproducts were determined from the conversion factors and unit prices of each coproduct (Eq. 6). Carinata meals were produced at the crushing mill with a conversion factor of 56% of seeds [115]. Propane and naphtha were produced at the biorefinery with conversion factors of 8.82% and 6.2% of oil [116].

The constraints for the above objective function are expressed by Eq. 7-18, which can be sub-divided into supply constraints (Eq. 7-8), stock constraints (Eq. 9), mass balance constraints (Eq. 10-11), demand constraints (Eq. 12) and capacity constraints (Eq. 13-15).

$$\text{minCost} = Seedcost + CapitalCost + OperationCost + TransportCost - Coproduct \quad \ldots\ldots(1)$$

where,

$$Seedcost = \sum_{t,c,q} \Upsilon_{c,q} \times P \times \beta^{t-1},$$

$$\forall \text{ seed supply}, \Upsilon_{c,q} = AC_{c,q} \times Y_c \times PP_q \quad \ldots\ldots(2)$$

$$CapitalCost = \sum_{s} (S_s \times SCAP) + \sum_{o} (O_o \times OCAP) + \sum_{b} (B_b \times BCAP) \quad \ldots\ldots(3)$$

$$OperationCost = \sum_{t,c,s,q} \left(FS_{c,s,q} \times LU \times \beta^{t-1}\right) + \sum_{t,s,o,q} \left(SO_{s,o,q} \times LU \times \beta^{t-1}\right) + \sum_{t,s,q} \left(SS_{s,q} \times SOP \times \beta^{t-1}\right) + \sum_{t,o,b,q} \left(OB_{o,b,q} \times OOP \times \beta^{t-1}\right) + \sum_{t,b,d,q} \left(BA_{b,d,q} \times BOP \times \beta^{t-1}\right) \quad \ldots\ldots(4)$$

$$TransportCost = \sum_{t,c,s,q} \left(TC_{c,s} \times FS_{c,s,q} \times \beta^{t-1}\right) + \sum_{t,c,o,q} \left(TC_{c,o} \times FO_{c,o,q} \times \beta^{t-1}\right) + \sum_{t,s,o,q} \left(TC_{s,o} \times SO_{s,o,q} \times \beta^{t-1}\right) + \sum_{t,o,b,q} \left(TC_{o,b} \times OB_{o,b,q} \times \beta^{t-1}\right) + \sum_{t,b,d,q} \left(TC_{b,d} \times BA_{b,d,q} \times \beta^{t-1}\right) \quad \ldots\ldots(5)$$

$$Coproduct = \sum_{t,c,o,q} \left(FO_{c,o,q} \times M \times MP \times \beta^{t-1}\right) + \sum_{t,s,o,q} \left(SO_{c,o,q} \times M \times MP \times \beta^{t-1}\right) + \sum_{t,o,b,q} \left(OB_{o,b,q} \times Pr \times PPr \times \beta^{t-1}\right) + \sum_{t,b,d,q} \left(OB_{o,b,q} \times N \times NP \times \beta^{t-1}\right) \quad \ldots\ldots(6)$$

As carinata can be cultivated once in a three years row, Eq. 7 sets that constraint, which assumes that one-third of the available farm area could be used for a particular year. Equation 8 sets the parameters of maximum seed supplies that can flow from firms to the crushing mills and

the storage units. Equation 9 states stock function which is dependent on the incoming seeds from fields (FS), rate of seed decay per quarter (SL), and outgoing seeds to the crushing mills. The seeds were transported to the storage units from farms in the first quarter. In the subsequent quarters, the stock amounts were the outstanding seeds after the decay from the previous quarter and the amounts dispatched for the crushing mills.

$Supply\ contraints$:

$$AC_{c,t} \leq \frac{A_{c,t}}{3}, \forall\, c,t \quad \ldots\ldots (7)$$

$$\sum_{s} FS_{c,s,q} + \sum_{o} FO_{c,o,q} \leq \Upsilon_{c,q}, \forall\, c,q \quad \ldots\ldots (8)$$

$Stock\ constraints$:

$$SS_{s,q} = \begin{cases} \sum_c FS_{c,s,q} - \sum_o SO_{s,o,q}\,, & q = 1 \\ SS_{s,q-1} * (1 - SL) - \sum_o SO_{s,o,q}\,, & q > 1 \end{cases} \quad \ldots\ldots (9)$$

$Mass\ balance\ constraints$:

$$\sum_{b} OB_{o,b,q} = O' \times \left(\sum_{s} SO_{s,o,q} + \sum_{c} FO_{c,o,q} \right), \forall\, o,q \quad \ldots\ldots (10)$$

$$\sum_{d} BA_{b,d,q} = J \times \sum_{o} OB_{o,b,q}, \forall\, b,q \quad \ldots\ldots (11)$$

$Demand\ constraints$:

$$\sum_{b} BA_{b,d,q} \geq D_{d,q} \times D', \forall\, d,q \quad \ldots\ldots (12)$$

$Capacity\ constraints$:

$$\sum_{c} FS_{c,s,q} \leq S_s \times SV, \forall\, s,q \quad \ldots\ldots (13)$$

$$\sum_{s} SO_{s,o,q} + \sum_{c} FO_{c,o,q} \leq O_o \times OV, \quad \forall\, q \quad \ldots\ldots (14)$$

$$\sum_{o} OB_{o,b,q} \leq B_b \times BV, \quad \forall\, q \quad \ldots\ldots (15)$$

The mass balance constraints set in Eq. 10 & 11 reflect the conversion factors that were applied at the crushing mills and biorefineries. At the crushing mills, 43.3% of oilseeds coming

from firms and storage units were extracted as unrefined oil [115]. The unrefined oil was refined at a factor of 71.98% at the biorefineries to produce SAF [115].

The total demand for aviation fuel at the Atlanta airport per quarter was estimated at 879,533 t [20]. It was assumed that at least 13% of this demand would be fulfilled by the SAF produced in selected biorefineries (Eq. 12). The assumption of this demand threshold was determined from the possible SAF production with the available seed supplies and their respective conversion factors.

Constraints in Eq. 13-15 express that the seed stocks, oil production, and SAF production cannot exceed their respective capacities, where the total capacities are dependent on the decision variables, i.e., the number of facilities. The capacities of each storage, crushing mill, and biorefinery were 1134 t of seeds, 1,037,323 t of oil production, and 1,10,279 t of SAF production, respectively [111]. The minimum numbers of crushing mills and biorefineries were set at 1 and 2, respectively. These minimum numbers were required in the system according to their respective capacities to fulfill the minimum SAF demand

3.2.6. Life Cycle Assessment and abatement cost

The LCA GHG emission was estimated at each level of supply chain configuration along with the transportation network (Eq. 19). The emission was determined against final aviation fuel production (Eq. 20-22) and distribution at the airport (Eq. 23). Besides, the emission reduction due to soil organic carbon sequestration was included in the final assessment (Eq. 24). The GHG parameters used for the equations are given in Table 3.3. Other supply chain parameters have already been explained in Table 3.2.

Table 3.3: The parameters of GHG emissions at different stages of the supply chain [55]

Parameter	Description
seedGHG	Emissions related to the seed production, 0.419 t CO_2/t of seed
oemGHG	Emissions related to the operations in the crushing mills, 0.0755 t CO_2/t of oil
bioGHG	emissions related to the operations in the biorefineries, 0.537 t CO_2/t of SAF
$TG_{i,j}$	Accumulated GHG emissions through the transportation networks between the facilities for transporting each tonne of materials, data-driven from network analysis, where i ϵ c,s,o,b, and j ϵ s,o,b,d
SOC_c	DayCent driven county-wise soil organic carbon sequestration.

$$GHG = GHG_{seed} + GHG_{Storage} + GHG_{OEM} + GHG_{BIO} + GHG_{TRANS} - GHG_{SOC} \quad (19)$$

where,

$$GHG_{seed} = \sum_{c,q} \Upsilon_{c,q} \times seedGHG \times O' \times J \quad (20)$$

$$GHG_{OEM} = \sum_{o,b,q} OB_{o,b,q} \times oemGHG \times J \quad (21)$$

$$GHG_{BIO} = \sum_{b,d,q} BA_{b,d,q} \times bioGHG \quad (22)$$

$$GHG_{TRANS} = O' \times J \times \left\{ \sum_{c,s,q} TG_{c,s} \times FS_{c,o,q} + \sum_{c,o,q} TG_{c,o} \times FO_{c,o,q} + \sum_{s,o,q} TG_{s,o} \times SO_{s,o,q} \right\} + J \times \left\{ \sum_{o,b,q} TG_{o,b} \times OB_{o,b,q} \right\} + \sum_{b,d,q} TG_{b,d} \times BA_{b,d,q} \quad (23)$$

$$GHG_{SOC} = \sum_{c,q} (\Upsilon_{c,q} \times SOC_c \times O' \times J) \quad (24)$$

Similar to LCA, supply chain costs at different stages were calculated factored by the proportions of SAF production. All the costs and emissions were converted to unit per liter of SAF

production with a conversion factor of 0.00092 t L^{-1} [117]. Finally, the carbon abatement cost was estimated with the following equation [49].

$$GHG\ abatement\ cost = \frac{production\ cost\ of\ SAF\ per\ liter\ -\ wholesale\ price\ of\ petrolium\ jet\ fuel\ per\ liter\ in\ 2021}{carbon\ intensity\ of\ SAF\ per\ liter\ -\ carbon\ intensity\ of\ petrolium\ jet\ fuel\ per\ liter} \quad \ldots\ldots (25)$$

3.3. Results and Discussions

3.3.1. Supply chain configuration

A SAF supply chain was designed at a minimum cost to determine the harvested land area, seed supplies, number, and location of facilities from the candidate counties (Figure 3.5).

Seeds were supplied from farms only in the first quarter. The metric ton of seeds supplied from the counties followed almost similar higher to lower ranges of distribution to the area harvested from the candidate counties (Figure 3.5(a) & 3.5(b)). However, the counties in southeast Georgia did not supply a high amount of seeds due to lower yields (Figure 3.3(b) & Figure 3.5(b)).

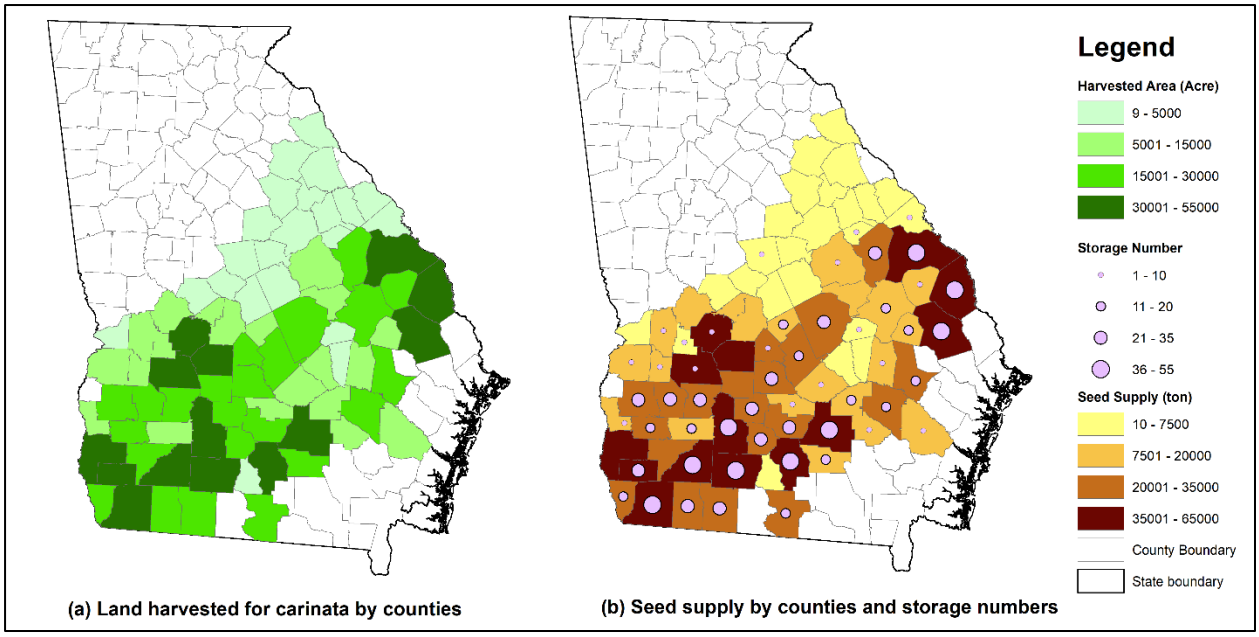

Figure 3.5: Distribution of land harvested for seed production and annual seed supply.

Storage facilities were selected in 52 counties out of 93 counties that supplied seeds (Figure 3.5(b)). The number of storage units under the selected counties was created generally according to the availability of seed supplies. For instance, the locations of the largest number of storage units, the Store D category, collected around 426.6 thousand t (91.4%) and 39.2 thousand t (8.5%) of seeds from the Farm D and Farm C, which were counties of a large number of seed supplies (Figure 3.6). Similarly, Store C collected 301.5 thousand t (99.95%) of seeds from the Farm C category. For Store B, 54% and 46% of seeds flowed from Farm C and Farm B, respectively. The seeds availability from Farm A was not sufficient to operationalize Store A. Therefore, 75%, 11%, 8%, and 6% of the seeds flowed into Storage A from Farm B, Farm C, Farm A, and Farm D, respectively.

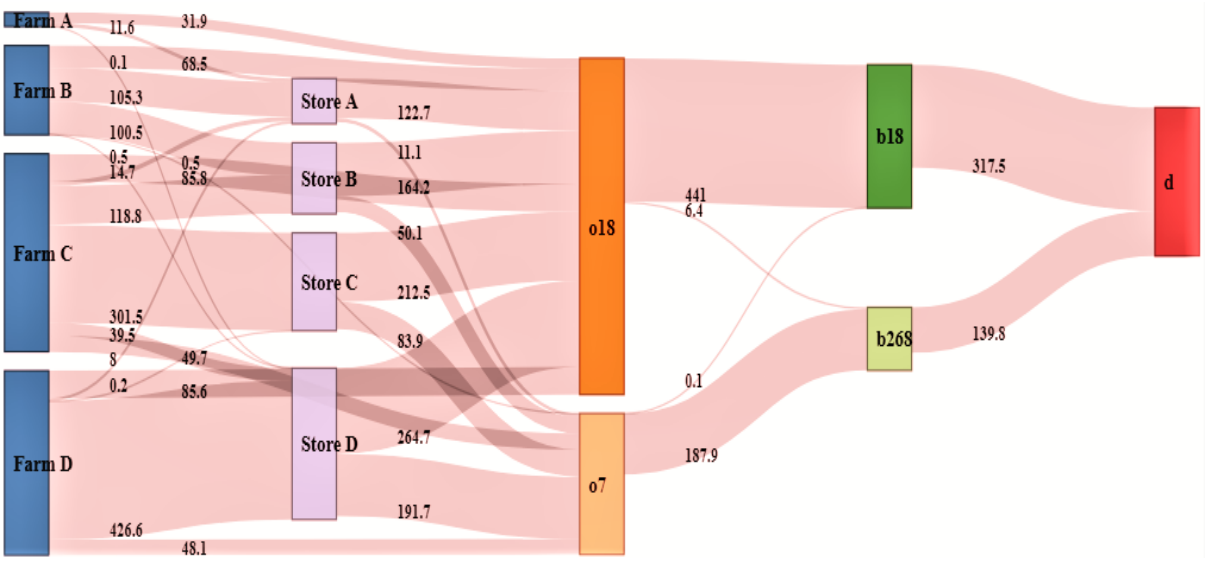

Figure 3.6: A Sankey diagram of annual material flows (in thousand t) along the farm and facilities. Farms and storages were classified into A, B, C, and D according to the ranges of seed supplies and storage unit numbers. A represents ranges of lowest values, and sequentially, D represents ranges of highest values. The ranges of seed supplies for a farm of A, B, C, and D are <=7.5, 7.5-20, 20-40, and >=40 thousand t, respectively. The ranges of storage units of A, B, C, and D are <=10, 10-20, 20-30 and >=30, respectively. The sets of o, b, d represent oil crushing mill, biorefineries and airport's locations.

Annually, 1127.3 thousand t of oilseed was collected from farms to storage units (Figure 3.6). However, no seeds went to the crushing mill from storage units in the first quarter because of loading and unloading costs. On average, 375.8 thousand t of seeds for each subsequent quarter was utilized to outflow 366.9 thousand t of seeds from storage units to crushing mills with an average rate of 1.06% seed losses [103]. The same amount of seeds flowed from farms to crushing mills in the first quarter to avoid transloading costs. In the fourth quarter, no seeds remained in the stock for any storage units, and allowed full seed stock for the next year. Seeds were not collected to the crushing mill from all the locations of storage units for every quarter. For instance, for the second, third, and fourth quarters, seeds were collected to a crushing mill from 23, 18, and 15 locations of storage units, respectively. Such variation occurred due to a trade-off with transportation costs in the supply chain system where seeds were collected from the best proximity of storage locations against the locations of crushing mills and farms.

Two crushing mills were selected in the Baker and Bibb counties to produce 447.4 thousand t and 188 thousand t of unrefined oil per year, respectively (Figure 3.6 & 3.7). Two biorefineries were selected at the Bibb and Twiggs counties to produce 317.5 thousand t and 139.8 thousand t of SAF per year, respectively. The feasibility of the supply chain could be validated by visualizing the configuration output (Figures 3.5 & 3.7). For instance, rail transportation was the cheaper option for seeds and unrefined oil transportation. Therefore, one crushing mill was located in Bibb County, which is at the center of Georgia, and connected to the other seed available counties through the rail networks. Baker county, which is located in the southwest part of Georgia, was selected for another crushing mill because of the higher amounts of seeds' availability in that region. In other words, the southwest of Georgia was the hotspot for the carinata feedstock supply (Figure 3.5(b)). Then, Baker county is well connected with Bibb and Twiggs, i.e., the locations of

biorefineries, through the rail network (Figure 3.7). Therefore, unrefined oil could be transported with the cheapest transportation routes. Even though one crushing mill was enough to produce the total volume of unrefined SAF, two crushing mills were created in the distributed supply chain model to minimize the overall cost.

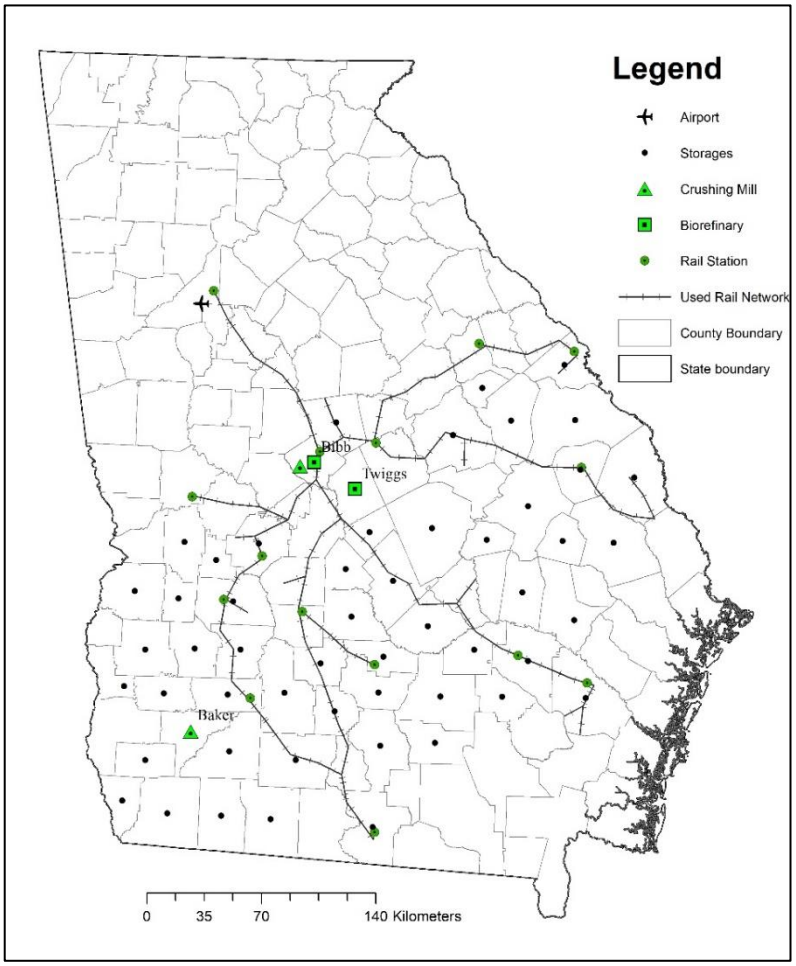

Figure 3.7: Locations of facilities along the supply chain configurations.

Two biorefineries were selected near the rail stations that directly connect to the Atlanta airport. However, the pipeline could not contribute to improving the efficiency of the supply chain model even though that was slightly cheaper than rail transportation (Table 3.1). This resulted for two possible reasons. First, transporting SAF from biorefineries could be cheaper compared to the

current suggested rail network, but in that case, there could have more costs involved in collecting seeds and unrefined oils from farms, storage units, and crushing mills. Second, Georgia has several pipeline connections. But there were not enough stations or multimodal facilities to avail pipelines to locate biorefineries in more suitable places. However, a greater regional level study, such as the supply chain for Alabama, Georgia, and Florida, could have utility for using both pipelines and rail networks. Nonetheless, supply chain modeling with different simulations periods should be also run to better understand the utilities of all sorts of transportations and location factors.

3.3.2. Supply chain cost and emissions

The total minimum supply chain cost for 20 years was around $11.3 billion. Without coproduct sale, the cost was $17.2 billion, of which seed cost, SAF production at the biorefineries, capital cost for establishing facilities, and transportation costs contributed 54%, 35%, 6%, and 2%, respectively. With all cost parameters and coproduct credits, the minimum price or net production cost of SAF for the 20 years was as low as $1.14 L^{-1} (see Figure 3.8 (a) for break-even production costs L^{-1}). This estimate was about $0.64 higher than the price of CAF [118]. Without coproduct credit, the minimum price could be as high as $1.73 L^{-1}. The techno-economic analysis paper showed that the carinata-based SAF price could range between $0.66 - $1.28 L^{-1} depending on the variation in variable costs, co-product credit, and other government credit [103]. However, our study did not consider such variabilities of cost parameters, which could be the reason for having a deviation of our estimated prices from that techno-economic study. Chu et al. [119] reported $0.75 L^{-1} of SAF from carinata, which is $39 L^{-1} lower than our cost estimation. For a similar oilseed crop, Camelina, the estimated cost of SAF was between $72 L^{-1} [120] and $0.78 L^{-1} [121].

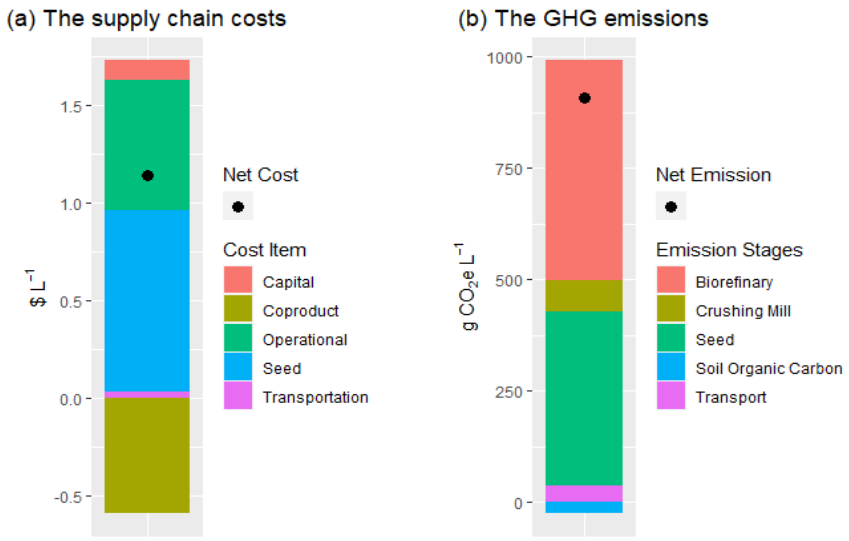

Figure 3.8: The supply chain costs and GHG emissions at various stages of supply chain productions and facilities for per liter of SAF production. The gross cost and net cost are estimated with coproduct credit and without coproduct credit, respectively. The gross emission and net emission are estimated with Soil Organic Carbon sequestration and without Soil Organic Carbon sequestration, respectively.

The annual carbon emission along the supply chain was 964.82 g CO_2e L^{-1} of carinata-based SAF, which was 63% relative carbon savings compared to the emission from CAF (2618 g CO_2e L^{-1}) [122]. Biorefineries were the biggest contributor to this emission (50%). Among others, seed production, oil crushing mill, and transportation contributed 39%, 7%, and 4% of emissions, respectively (see Figure 3.8(b) for break-even GHG emissions). In the techno-economic study, the relative carbon savings was also around 65%, with an emission rate of 918.67 g CO_2e L^{-1} of carinata-based SAF [38]. Our study validated that techno-economic research and extended it by configuring a supply chain. The assumption of transportation distances in the techno-economic research was based on the radius from farms and facilities, which is somewhat arbitrary. Multi-modal transportation facilities were not considered in that study. Therefore, a full LCA over spatially explicit supply chain configurations should be more accurate. In that sense, we accomplished that job by embedding the LCA model over our supply chain configurations. The

carbon abatement cost in consideration of our supply chain was found to be \$387.13 t^{-1} of GHG emissions. This result suggests that a minimum carbon tax of \$387.13 t^{-1} of GHG emissions (CO_2 equivalent) would be needed to equalize the energy equivalent cost of utilizing carinata-based SAF and CAF.

3.4. Conclusion

This paper developed a model for a carinata-based SAF supply chain to optimize the locations of farms and facilities in Georgia. The GIS-based network analysis model predetermined the location of farms and facilities and the least-cost transportation routes. Throughout these transportation routes, the final locations of farms, facilities, and flow of materials were optimized using the MILP model. The inclusion of seasonal seed supplies from the storage units can be a viable option to maintain stability in the feedstock market. Besides this temporal dimension, the estimation of carbon footprint captured the environmental feasibility of carinata-based SAF, which also made this study unique from other GIS-based integrated supply chain models.

The necessity of spatially explicit supply chain configuration became obvious from the results of this study. For instance, the seed supply was influenced by the distribution of seeds availability across the counties. The selection of locations and number of storages validated the requirement of the distributed supply chain for bioenergy-based aviation fuel, for which the feedstock is collected in varying amounts from different areas of a dispersed region. The selection of crushing mills and biorefineries' locations near the rail stations clearly shows how the use of geodatabase of actual transportation modes and networks can be a decisive factor for an optimization model. At the same time, the missing opportunity of the pipeline was immediately realized due to a trade-off between cost factors and the lack of terminal facilities. Besides cost

estimation, the LCA-based carbon footprints assessment along the supply chain networks appeared with more accuracy than the traditional supply chain and techno-economic analysis, which include the transportation mode and distances exogenously.

However, the supply chain of bioenergy crops, such as carinata, could be affected by the yield variations due to the impacts of weather and other factors, e.g., soil conditions. The model application over an extended geographical region may have a different optimization result for using greater connectivity among the transportation networks that allow transporting of materials from a dispersed region with cheaper transportation modes. Finally, the simulation of the model with different periods could have different tradeoff benefits between the transportation costs and locating farms and facilities. To maintain brevity, those issues were not considered in this paper. However, a key challenge of designing a supply chain is making a configuration in the first place based on all the major system processes, decision variables, parameters, and most pertinent constraints. That challenge has been addressed in this current study. Our future study will apply the stochasticity parameter of yields along with different demand constraints, over several simulation periods, for a greater regional level study. That study would fulfill the research gaps that were identified in this paper.

CHAPTER 4

DESIGNING CARINATA-BASED SUSTAINABLE AVIATION FUEL SUPPLY CHAIN IN GEORGIA UNDER UNCERTAINTY [4]

[4] Ullah, K.M. & Dwivedi, P. To be submitted to [Biofuel, Bioproducts & Biorefining]

Abstract

Carinata is a promising dedicated energy crop for producing sustainable aviation fuel (SAF) in the United States south. However, only a handful of studies have been done to configure the supply chain of carinata-based SAF, while none of the studies reflected the uncertainty in supply. Thus, this study aims to design a stochastic supply chain model for carinata-based SAF production by optimizing the location of farms and facilities (e.g., storage units, crushing mills, biorefineries) with a minimum transportation cost under four simulation periods with five years intervals each, along with three probability scenarios. The research extends a previous deterministic single-period simulation model, which applied an integrated Mixed Integer Linear Programming (MILP) model associated with the Geographical Information System (GIS) to design a spatially explicit supply chain configuration. This study shows that the unit cost of the overall supply chain could be as high as \$1.86 L^{-1} for a short-term simulation period (e.g., 5-years) and as low as \$1.15 L^{-1} for a long-term period (e.g., 20-years). With long-term planning, there is a 95% confidence that a carbon tax of \$255.92 t^{-1} of GHG emissions on conventional aviation fuel would be needed to promote carinata-based SAF in the region.

Keywords

Biomass Supply Chain, Carbon Abatement Cost, GHG, Oilseed, Stochastic Programming

4.1. Introduction

The United States government came up with a new 'Sustainable Aviation Fuel Grand Challenge' that targeted to produce at least 11.4 billion liters of sustainable aviation fuel (SAF) production per year to reduce greenhouse gas (GHG) emissions to 20% by 2030 and produce 132.5 billion liters of SAF per year in the long term to meet 100% of aviation fuel demand by 2050 [6]. The intention of emphasizing SAF use to achieve the target of net-zero GHG emissions is very clear. For the last 60 years, the United States has improved the energy efficiency of aircraft by improving engine technologies and air traffic operations, which reduced the energy intensity of air travel by 75% [4]. But, the commercial aviation industry is still using the same petroleum-based conventional aviation fuel (CAF) that contributes 12% of United States transportation emissions and accounts for 3% of total GHG produced from all the national economic sectors [3]. Therefore, using SAF is the best remaining option to combat GHG emissions from the aviation industry. However, sustainable sources of feedstocks for SAF production might be challenged by lack of adequate yield and supply, conflicts with food crops, lack of compatibility with current crop rotations to avoid deforestation, and potential direct and indirect impacts on land use changes [13].

Brassica carinata, sometimes called Ethiopian mustard, Abyssinian mustard, or simply carinata, is a promising annual oilseed crop for the commercial production of SAF [14,15]. The crop is rich in oil content (42%-52%) and could be produced with traditional crop rotation without competing with food crops and causing deforestation [14,16]. The carinata-based SAF could reduce up to 68% of greenhouse gas emissions relative to conventional aviation fuel [55]. In the Southeast (SE) United States, carinata can be grown with a potential yield of 0.55 t/ha [18]. In Alabama, Georgia, and Florida, carinata can be potentially cultivated on about 1.4 million ha of fallow agricultural land during the winter season without impacting existing land uses [19]. By using this

full potential of carinata feedstock production, CSAF could replace up to 2.3% of conventional aviation fuel consumption in the United States [19]. On the other hand, thirteen southern states of the United States consume about one-third of the nation's total aviation fuel consumption [20]. Therefore, the large supply of carinata feedstock can meet the immediate demand for SAF in the Southern United States.

Even though the vast potentiality of CSAF is already known in the context of the United States south [14,15,17–19], limited research has been done to understand its economic feasibility and potential reduction of carbon footprint [55]. Alam et al. [55] performed a techno-economic analysis to estimate the unit cost and unit GHG emission of CSAF. But, they did not embed their study with any supply chain configuration. To extend their study, we designed a supply chain for CSAF production in Georgia, United States, that was reported in the third chapter of this dissertation. We applied a spatially and temporally explicit distributed supply chain model for 20 years. By integrating Geographical Information System (GIS), MILP, and combining multimodal transportation systems (e.g., road, rail, and pipeline) as well as LCA, we determined the carbon abatement cost for producing per tonne of CSAF. While Chapter Three prepared a base configuration for a supply chain of CSAF in terms of framing the discrete steps of the biomass supply chain (BSC) and applying computational techniques, it did not address two important aspects of uncertainty in a typical BSC [26,28]. First, the uncertainty associated with risks, such as variability in biomass supply, properties (e.g., moisture content), prices, and costs is not considered. Second, uncertainty associated with simulation techniques and their respective parameters is not emphasized. Especially, the biomass supply can fluctuate to a large extent due to weather impacts [29] and farmers' attitudes towards adopting newly introduced bioenergy crops [21,23,56–58,123,124]. Additionally, the optimization scenarios of BSC can vary a great deal due to

simulation with multi-period models [16]. Because of the return from investments in capital costs, the scale of economies in a tradeoff between transportation and production costs can differ from short-term to long-term supply chain operation and scheduling decisions.

Several studies endeavored to capture the potential uncertainties in BSC [42,43]. Among that literature, the most prominent approach is the use of stochastic programming. We found that two-stage solution techniques are predominant in the recent literature on stochastic programming for biomass supply chain modelings (Table 4.1). The studies on two-stage stochastic programming primarily applied the expected values of features presumed uncertain in the first place, then undertake scenario analysis in the second stage. Quddus et al. [125] used a chance-constrained solution technique to determine the threshold of municipal waste that could be utilized in a supply deficit in agricultural and forest biomass. This probabilistic technique is useful for the cases, where much reliable data is not available [126]. In our study, therefore, we used a chance-constrained technique to capture the stochasticity in carinata yield as no reliable historical data was available to apply the most conventional two-stage stochastic programming technique.

However, none of the uncertainty modeling studies applied a GIS-based integrated supply chain model to optimize the transportation cost (Table 4.1). Aguilar et al. [46] used GIS to include the climatic and biophysical variables associated with uncertainty. However, their study did not apply any optimization technique to design a supply chain, rather, their work primarily focused on a suitability modeling for locating facilities, regardless of its cost-effectiveness in a supply chain system. Several GIS-based BSC approaches were applied to investigate the accurate and precise transportation networks and modes, which can be directly utilized in MILP models to optimize the number, capacities, and locations of feedstock's farms and facilities to satisfy a certain level of demand at a minimum cost [35,47]. However, none of those researches incorporated the uncertainty

in BSC design, and two major aspects were missing – 1) the planning decisions affected by simulation periods; 2) the carbon footprint generated by the proposed BSCs. To fulfill this research gap, this study extended the previous techno-economic analysis [55] and supply chain model (Ch3) of CSAF with a stochastic model by applying multi-period simulations under several uncertainty scenarios in carinata seed supply.

Table 4.1: Literature on stochastic programming for biomass supply chain

Reference	**Feedstock**	**Techniques**	**Simulation period**	**Features of uncertainty**
Memişoğlu & Üster [127]	Switchgrass	Two-stage	Multi-period	Yield/supply; Price
Bijay et al. [128]	Switchgrass	Two-stage	Single-period	Yield/supply
Lee et al. [129]	Palm tree	Two-stage	Multi-period	Demand; Price
Fattahi & Govindan [130]	Agricultural residues; Forest biomass	Multi-stage	Multi-period	Yield/supply; Natural disaster
Quddus et al. [125]	Corn stover; Forest residues; Municipal waste	Two-stage (chance-constrained)	Single-period	Seasonality
Shabani et al. [44]	Forest biomass	Two-stage	Multi-period	Profit
Li & Hu [131]	Corn stover	Two-stage	Single-period	Yield/supply; Technology; Price
Nur et al. [132]	Switchgrass; Corn stover	Two-stage	Multi-period	Weather/supply
Huang et al. [133]	Corn; Forest reidues	Two-stage	Single-period	Yield/supply

4.2. Method

4.2.1. The system, process, and overview of modeling

Our study modeled the CSAF by including five echelons - 1) farms, 2) storage units, 3) crushing mills, 4) biorefineries, 5) airport(s) (Figure 3.1 in Ch3). Carinata seeds were harvested

from farms in the 1st quarter of a year. Each year had four quarters. In the 1st quarter, a portion of seeds directly went to crushing mills to avoid loading-unloading costs. The rest of the seeds went to storage units to supply seeds to the crushing mills for the 2nd, 3rd, and 4th quarters. After the 4th quarter, there were no outstanding seeds for the next year from the previous year. At the crushing mills, crude oils and carinata meal as a coproduct were extracted from seeds. The crudes oils were transported to biorefineries to produce SAF. The Hydro-processed Easter and Fatty Acids (HEFA) technological pathway was utilized to produce SAF and other coproducts, such as propene and naphtha. The SAF was finally transported to store it in the airport depo, assumed to be located at the Atlanta airport.

To model this system process, we applied two techniques – 1) a GIS-based network analysis; 2) a MILP-based supply chain optimization (Figure 3.2 in Ch3). After selecting the candidate locations of farms and facilities (e.g., storage units, crushing mills, biorefineries), we calculated the least-cost routes among them (Origin-Destination matrices or O-D matrices) by using GIS-based network analysis. Table 3.1 (Ch3) shows the modes of transportation used and their associated costs and emissions for transporting materials. Then, by applying the MILP optimization technique, we built the supply chain models to select the final locations of farms and facilities by estimating the minimum costs. Along with these supply chain configurations, we calculated the LCA-based GHG emissions and finally determined the carbon abatement costs. The models were applied in the context of Georgia, United States. The details about these modeling techniques, including the study area, selecting the location of farms and facilities from the candidate counties, the application of network analysis and MILP technique as well as the use of LCA, were discussed in Ch3. The following section discusses the MILP-based stochastic technique that we applied to the extent of the previous model.

4.2.2. MILP-based Stochastic Programming

In chapter Ch3, we applied a deterministic model with fixed supply and demand. In this study, we assigned a chance-constrained stochastic model [134] with three probabilistic parameters for four different simulations periods (5,10,15, and 20 years) to address the uncertainty issue in seed supply. The definition of sets, variables, factors, and constraints used in this modeling study and associated unit and data sources are presented in Table 3.2 (Ch3).

The original seed supply constraint in chapter Ch3 is represented by Eq. 1. This study adopted the original seed supply constraint equation with a probabilistic stochastic function, where α was the probability of the supply constraint that was satisfied (Eq. 2-3). In the original deterministic model, only the mean seed supply was used. In the current model, the mean and standard deviation of seed supply was used to determine the probabilities of supply, assuming the level of uncertainty under three α-cuts (.01, .05, and .10). The three α-cuts represent the 99%, 95%, and 90% of confidence interval (CI), respectively. The corresponding normalized values (Z_α) of each α-cuts were calculated from the standard probability distribution (Eq. 4). Thus, after simplification, the final deterministic form of the stochastic function was achieved (Eq. 5).

$$\sum_s FS_{c,s,q} + \sum_o FO_{c,o,q} \leq \Upsilon_{c,q} \quad \ldots\ldots (1)$$

$$\left[\sum_s FS_{c,s,q} + \sum_o FO_{c,o,q} \leq \Upsilon_{c,q}\right] \geq \alpha \quad \ldots\ldots (2)$$

$$P\left[\frac{\left(\sum_s FS_{c,s,q} + \sum_o FO_{c,o,q}\right) - \overline{\Upsilon}_{c,q}}{\sigma_{\Upsilon_{c,q}}} \leq \frac{\Upsilon_{c,q} - \overline{\Upsilon}_{c,q}}{\sigma_{\Upsilon_{c,q}}}\right] \geq \alpha \quad \ldots\ldots (3)$$

$$P\left[\frac{\left(\sum_s FS_{c,s,q} + \sum_o FO_{c,o,q}\right) - \overline{\Upsilon}_{c,q}}{\sigma_{\Upsilon_{c,q}}} \leq Z_\alpha\right] \geq \alpha \quad \ldots\ldots (4)$$

$$\sum_s FS_{c,s,q} + \sum_o FO_{c,o,q} \leq \overline{\Upsilon}_{c,q} - Z_\alpha \sigma_{\Upsilon_{c,q}} \quad \ldots\ldots (5)$$

According to the above supply constraints, we precalculated the maximum demand threshold that could be achieved in the system. The calculation was done in consideration of seed loss at the storage units and conversion factors to produce crude oil in the crushing mills as well as producing SAF in the biorefineries. With this precalculated condition, we could avoid the infeasible models and sort out the maximum feasible ones. Table 4.2 shows the amount of seed supply and the maximum amount of SAF demand that was fulfilled with corresponding probability scenarios. These estimated supply and demand amounts worked as input parameters for the model simulations.

Table 4.2: Total seed supply, SAF demand, and demand ratio against the total demand for aviation fuel per quarter.

α-value	**Seed Supply (t)**	**SAF Demand (t)**	**Demand ratio (SAF/Total jet fuel demand*)**
0.01	1110633.64	84435.17	9.6 %
0.05	1243741.96	95432.23	10.8 %
0.10	1314701.51	100876.95	11.4 %

*Total jet fuel demand per quarter is set as 879533 t [102].

4.3. Results and Discussions

4.3.1. The supply chain configurations

The supply chains under the simulation periods and probability scenarios were configured according to the carinata seed supply, which was dependent on the land available for carinata production and carinata yield (Figures 4.1 & 4.2). The probabilistic stochastic functions were applied using the county-wise annual mean carinata yields and their respective standard deviations (Figure 4.2 & Eq. 5).

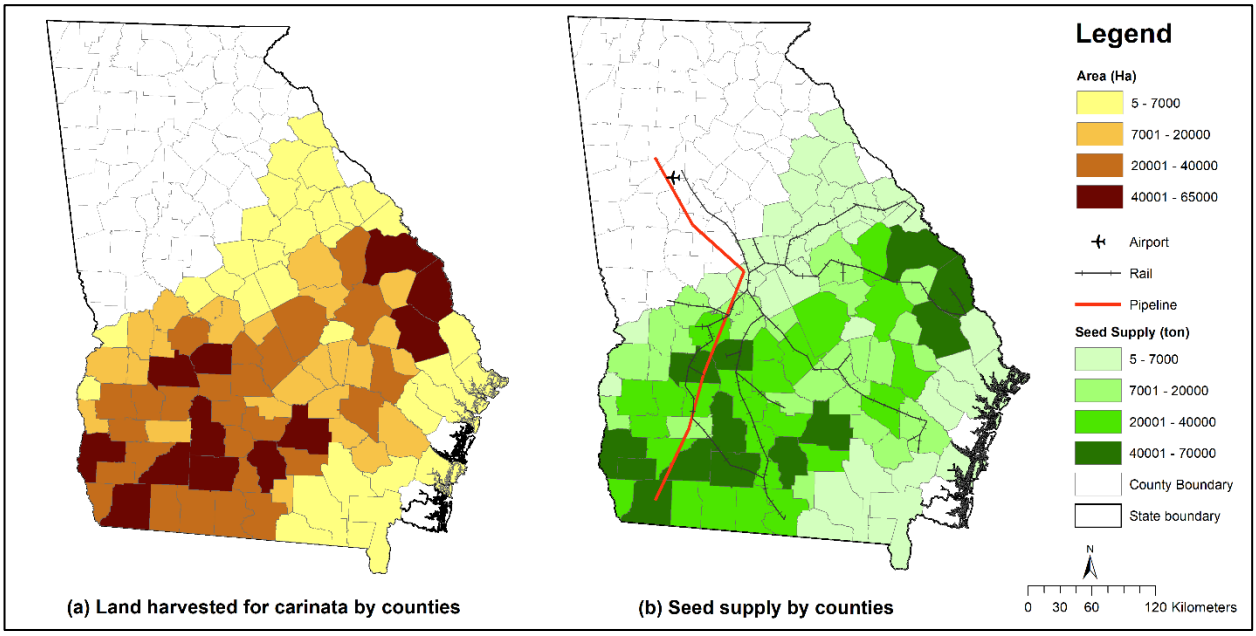

Figure 4.1: County-wise land available for carinata production and annual mean carinata seed supply in Georgia.

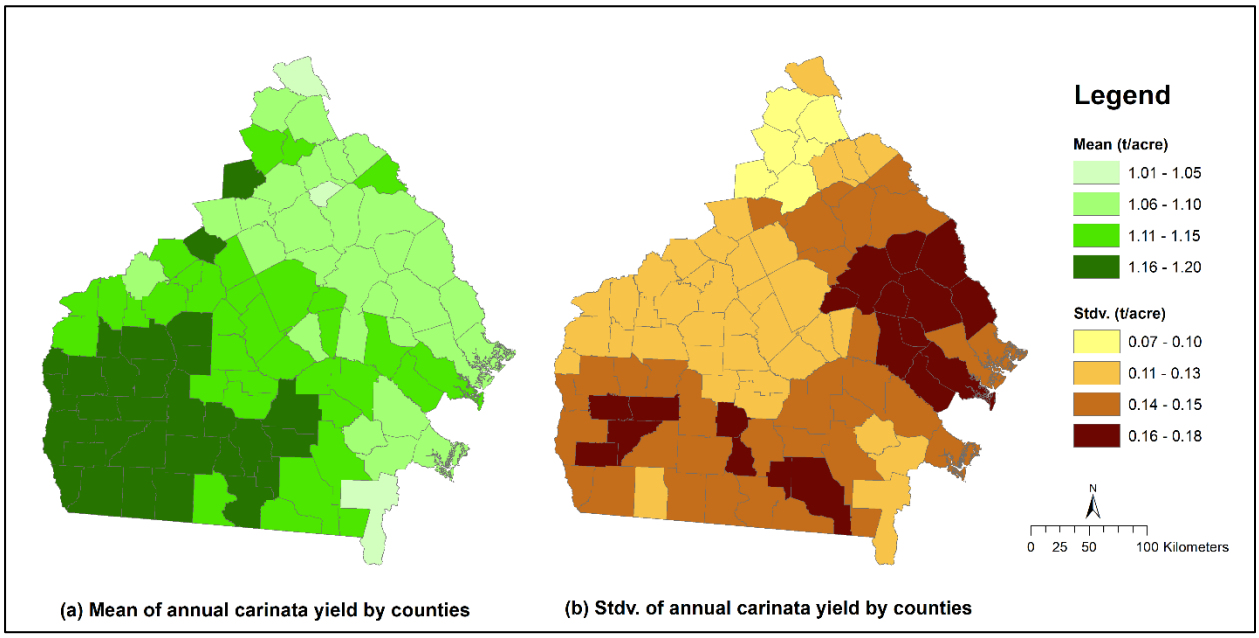

Figure 4.2: County-wise carinata yield distribution.

According to Figure 4.1(b), 95 counties had seed supplies, among which the annual mean supplies ranged between 5-10000, 10001-20000, 20001-40000, and 400001-70000 t for 41, 16, 25, and 13 counties, respectively. The counties with a low range to high range of seed supplies followed a similar low to a high rank of land availability (Figure 4.1). This finding suggests that total available land for carinata production across the counties could have more influence on supply chains than the county-wise yields. Figure 4.1(b) also shows that the dispersed counties are connected with an active rail network towards the airport, while the active pipeline primarily connects the remote southwest counties. The following discussions highlight how this connectivity along with the distribution of seed supplies, worked as determining factors for locating the facilities (storage units, crushing mills, and biorefineries).

Figure 4.3 shows the locations of storage units, crushing mills, and biorefineries within the supply and demand region (selected from the seed supplying counties, Figure 4.1) under four simulation periods with three probabilistic scenarios.

One simulation output is immediately obvious if we compare these figures with the land availability and distribution of seed supplies presented in Figure 4.1 – the larger storage units were located in the counties having a larger area of land availability and higher seed supply. For instance, out of 12 simulation scenarios, Colquitt, Mitchell, and Worth counties were selected for seven scenarios for the largest storage units (30-60). For other scenarios, at least one county among these three neighboring counties was selected as the same for four out of five scenarios. The only scenario (Figure 4.3(a)) did not select any storage unit with the largest value range. For all the 99% CI scenarios (Figure 4.9(a, d, g, & j)), a limited number of higher storage units were selected as the demand per quarter was lowest in those cases.

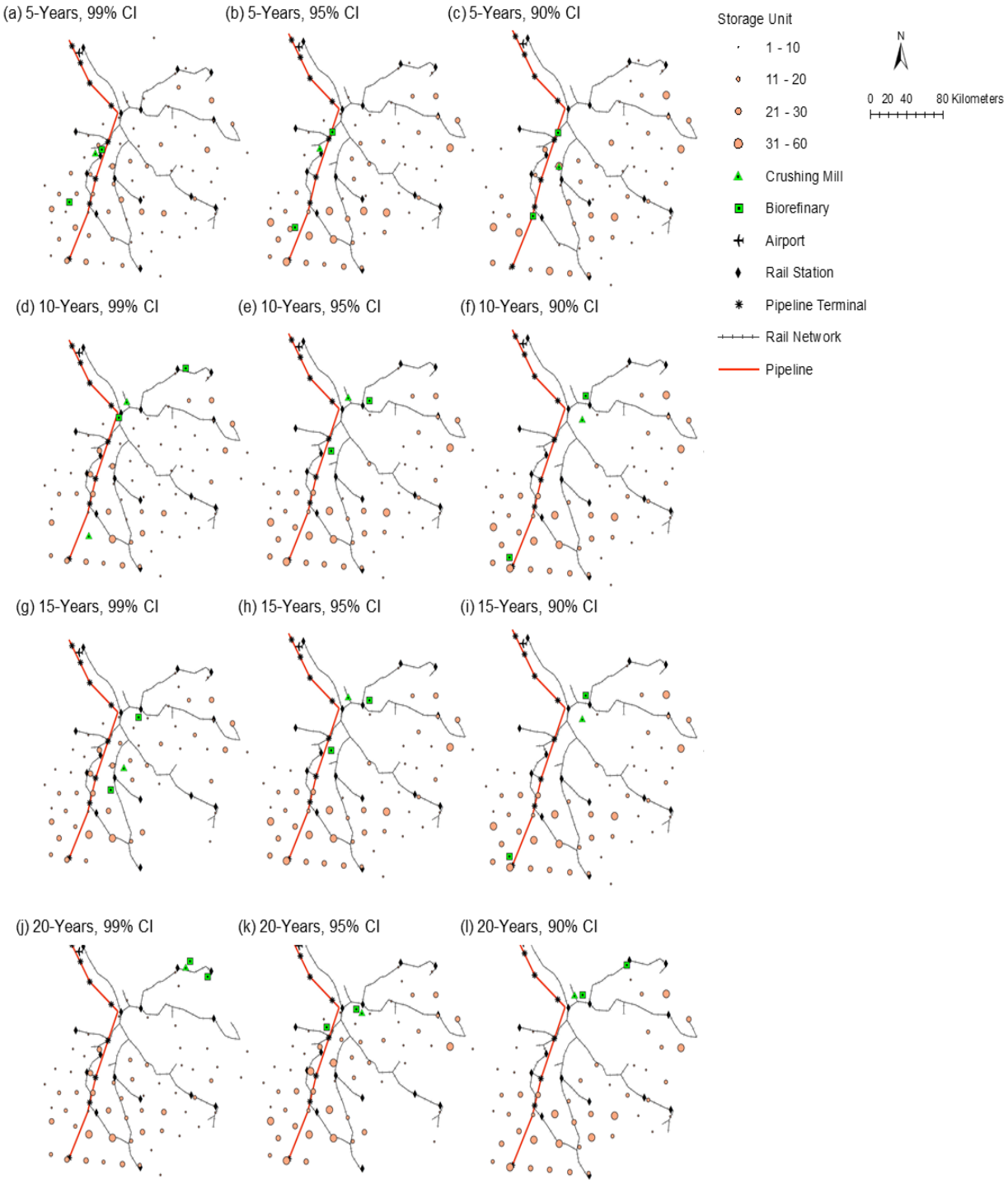

Figure 4.3: The location of facilities at different years of simulation period with three confidence interval (CI) scenarios.

The crushing mills were located primarily in the center of those counties, which were part of the demand-supply region except for the 20-year, 99% CI scenario (Figure 4.3). At least one biorefinery was located near the pipeline in nine out of 12 scenarios, as the pipeline is the cheapest transportation mode for transporting SAF. For other cases, biorefineries were selected near the rail network, which is cheaper than road transport. Two biorefineries were selected in every scenario. One biorefinery was selected close to the crushing mill for eight out of the 12 scenarios to avoid transportation costs for shifting crude oil. However, the suitability of these selected locations of facilities is approximate. The optimality gap could influence selection of more accurate locations, for which the researchers may not have any control. For instance, the locations of crushing mills and biorefineries in the 20-year, 99% CI scenario were selected in distant locations from higher seed supply counties (Figure 4.3(j)). The fact is, the optimality gap of this scenario was the highest among all the 12 scenarios (Table 4.3).

Table 4.3: Optimality gap under simulation periods with probability parameters

Simulation period	**Optimality gap**		
	$\alpha = 0.01$	$\alpha = 0.05$	$\alpha = 0.10$
5-year	1.12	1.23	1.20
10-year	3.77	3.99	3.35
15-year	3.95	3.64	3.72
20-year	4.58	4.45	4.02

4.3.2. The supply chain costs and emission

Figure 4.4 shows the supply chain costs for producing per liter SAF under three probability scenarios at four different simulation periods. The overall supply chain cost goes down with the increase in simulation periods. For instance, the cost per liter is $1.86 with the probability value,

α = 0.01, at the 5-years simulation period. Those costs with the same probability parameter are $1.5, $1.32, and $1.18 for the periods of 10-years, 15-years, and 20-years, respectively.

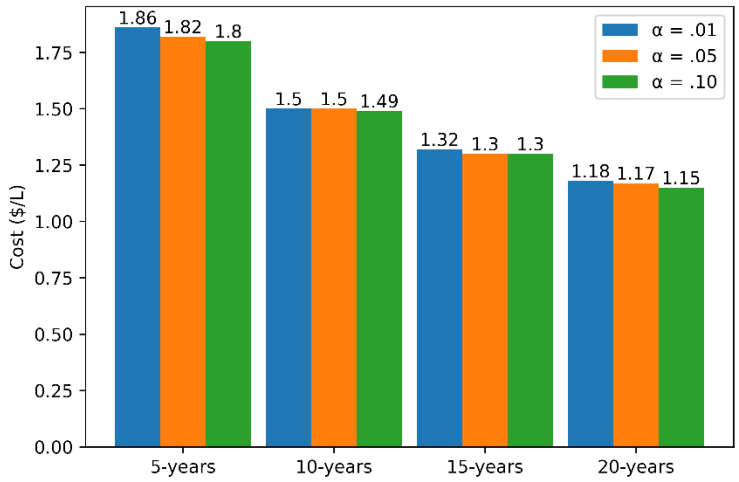

Figure 4.4: The costs of producing SAF at four simulation periods under three probabilities.

The unit cost generally gets slightly lower with higher α values for having some additional SAF demand in the system (Figure 4.5 & Table 4.3). However, for the 10-years simulation period, the costs are the same at $1.5 L^{-1} for α = 0.01 and 0.05. This situation occurred due to having optimality gaps in the models (Table 4.3). A similar situation was found in the case of a 15-years period with α = 0.05 and 0.10.

The reasons for the lower unit costs with higher simulation periods and the minor variations of costs across the probability scenarios within the same simulation period can be explained with the break-even costs (Figure 4.5). According to Figure 4.5(a), the break-even costs are lower at shorter simulation periods except for the unit cost of transportation. The unit costs of seeds, operations, and coproduct sales diminish proportionately with the increase in simulation periods. This happened because of multiplication with adjusted discounted values over time. There was no adjustment with discounted value for capital costs. The unit capital costs got lower due to higher

aggregated supply and demand from higher simulation periods. While, the total quantity of supply and demand had no effect on the unit costs of seeds, operations, and coproduct sales, as those items were proportionately variable as per their fixed unit costs. These findings could be further justified with the comparisons of the probability scenarios under the same simulation periods (Figure 4.5). For instance, the unit costs of seeds, operations, and coproduct sales are exactly the same at $ 0.93, $0.67, and -$0.59 with $\alpha = 0.01, 0.05$, and 0.10 under the 20-years simulation periods even though their total quantity supply and demand were different. While the capital costs vary within the same simulation periods due to variation of total supply and demand quantity with different α values. However, these variations could not always be accurately proportionate to the total supply and demand because of the integrality of the capital establishment, such as establishing an additional expensive facility with a small amount of increase in supply and demand quantity.

The contribution of transportation costs is the lowest in the systems, ranging between \$0.03-0.07 L^{-1} (Figure 4.5). The unit transportation cost was adjusted with the discounted values. However, the final supply chain configurations associated with their optimality gaps were the major deciding factor for this least-cost item. Therefore, there are no visible patterns in unit transportation costs across the simulation periods as well as the probability scenarios.

The transportation networks, which were optimized from the models, affected the proportion of the GHG reduction in the systems. Other factors, such as emissions in seed productions, crushing mills, and biorefineries contributed to GHG emissions proportionate to the SAF demand. Hence, their unit contribution to GHG reduction remained the same across the simulations periods as well as the probability scenarios. The emissions from seed, crushing mills, and biorefineries were 391.27, 69.54, and 494.21 g CO_2e L^{-1}, respectively. Besides, there was an 82.43 g CO_2e L^{-1} of soil organic carbon sequestration for carinata seed production. The annual

carbon emission along the supply chains ranged between 959.82 to 907.29 g CO_2e L^{-1} of carinata-based SAF, which was 63-65% relative carbon savings compared to the emission from CAF (2618 g CO_2e L^{-1}) [122].

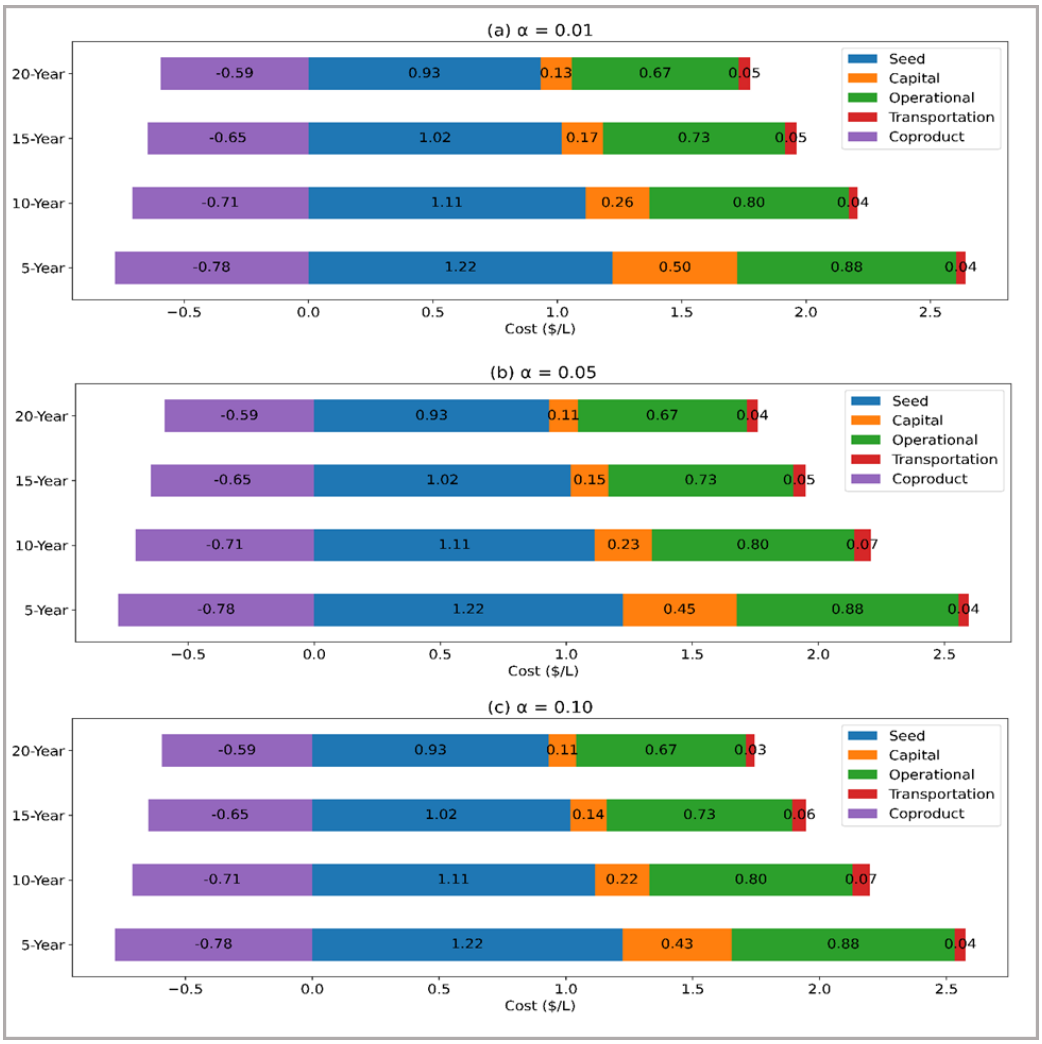

Figure 4.5: Break-even costs under four simulation periods with three probability scenarios.

However, the carbon abatement costs diminished considerably for higher simulation periods due to lower overall unit costs in the supply chain (Figures 4.4 & 4.6). For instance, the carbon abatement cost is highest at \$519 t^{-1} SAF production under a 5-years simulation with α = 0.01 probability. While that cost is lowest at \$248 t^{-1} for a 20-years simulation with α = 0.10. With

95% confidence (α = 0.05), the abatement cost is $256 with the same simulation period. Even though the relative carbon savings remained very close across the scenarios, the abatement costs vary due to the variation in overall unit costs in the supply chain systems.

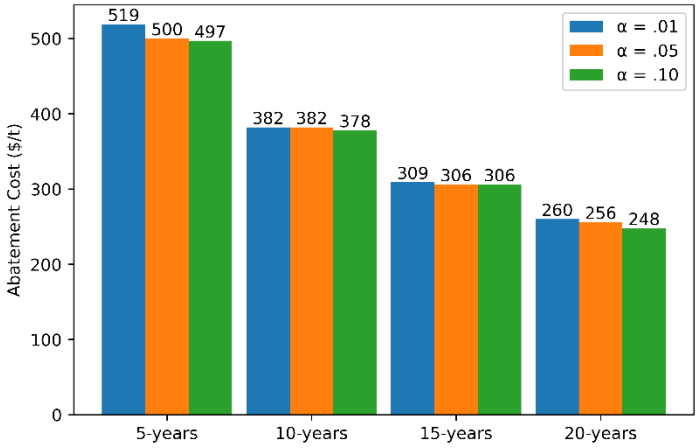

Figure 4.6: The carbon abatement costs of saving relative carbon emissions at four simulation periods under three probabilities.

4.4. Conclusions

In the previous deterministic study (Ch3), the sensitivity in seed supply was not addressed. Therefore, there was a lack of understanding of uncertainty in the newly introduced CSAF. This research fulfilled that important research gap. Besides, this study simulated the model for four different periods, which would help the bioenergy investors to set the durations of an operational plan. Long-term planning will be a more viable option for the investors to recover the investment in the capital costs with a lower unit price of CSAF, while the government will have to impose a lower tax burden on the CAF. However, the study does not necessarily suggest considering very long-run planning. Rather, it suggests the policymakers set a win-win situation, where a rational amount of tax burden should be imposed on CAF so that the bioenergy investors can recover their investment within a reasonable time with a fair price.

This study also validated the necessity of spatially explicit supply chain configuration, which already became obvious in the previous study (Ch3). However, both studies were conducted only in Georgia due to achieving small optimality gaps within a short time of a model run. Then, these studies did not consider several other uncertainties, such as farmers' adoption behavior and subsequent seed supplies, demand uncertainty, price and cost uncertainties, and geographical obstacles in selecting locations of facilities. We will address those limitations in our future research.

CHAPTER 5

CONCLUSIONS

The dissertation endeavored to understand the adoption challenges of carinata production as a newly introduced bioenergy crop, its cost-effectiveness, and the environmental feasibility to produce sustainable aviation fuel (SAF). The first study (Ch2) showed that a reasonable fixed contract price and initial adoption rate of farmers are the two most influential determining factors to build a positive attitude of the farmers toward carinata adoption. Therefore, it was suggested that subsidy, risk premium, and campaign programs could be useful policy measures to promote carinata cultivation in the Southern United States. The supply chain results (Ch3 & Ch4) estimated that the minimum price of carinata-based sustainable aviation fuel (CSAF) would be at least double the average price of conventional aviation fuel (CAF) regardless of the supply chain scheduling period as well as certainty and uncertainty in carinata seed supply. However, the potential greenhouse gas (GHG) reduction (63-65%) of CSAF is much more promising. Therefore, an appropriate carbon tax can equalize the energy equivalent cost of utilizing CSAF.

From a modeler's perspective, the dissertation applied three modeling techniques to understand the overall economics of CSAF at the landscape level – 1) a spatially explicit agent-based model, ABM (Ch2); 2) a deterministic supply chain model (Ch3); 3) a stochastic programming model (Ch4).

The fact about the existing literature on ABM is that they were not truly spatially explicit; could not jointly determine the profitability, neighborhood influences, and risk aversion of the farmers to understand their combined utility towards adopting bioenergy crops. By fulfilling these

research gaps, we prepared a novel ABM technique with a clear discussion about the modeling framework along with open access protocol for sharing computational codes. However, we had limitations in data availability and validation with primary survey results. Then, the model was performed within a small-scale watershed level to maintain brevity. In our future research, we would improve and validate the model with a primary survey, more available datasets, and extend the model at a regional scale.

Our supply chain models were spatially and temporally explicit. To the best of our knowledge, none of the existing supply chain literature integrated the spatial, temporal, and carbon footprint components with a single supply chain model. Our deterministic MILP-based supply chain model integrated with GIS and LCA eliminated this important research gap firsthand. Thereafter, we extended our deterministic model with a stochastic programming approach for multiperiod simulations with multilevel probabilistic scenarios. This study will be useful for short-term to long-term supply chain operations and scheduling decisions under various uncertainty in seed supply. However, further research would be necessary to simulate the model at a regional level (e.g., the states of Alabama, Georgia, and Florida) with more uncertain conditions, such as farmers' adoption behavior and subsequent seed supplies, demand uncertainty, price and cost uncertainties, and geographical obstacles in selecting locations of facilities. A joint ABM and supply chain study could be conducted in this regard, which we could not accomplish within the scope of this dissertation.

Our current supply chain model would lead to the extension of our current agent-based model to capture the potential market of bioenergy crops and associated land-use changes on the greater regional landscape. In our future work, we would incorporate a hydrological model (e.g., SWAT model [17]), a biogeochemical model (e.g., DayCent model [105]), and a spatially explicit LCA

model [135] over the proposed regional landscape model to understand the potential regulatory ecosystem services/disservices for introducing bioenergy crops and possible land-use changes. Consequently, we would like to design a multi-objective sustainable bioenergy landscape model by trading off the aquatic, terrestrial, and atmospheric regulatory ecosystem services/disservices with the production economics of bioenergy crops, constrained by behavioral, physical environmental, and market conditions.

REFERENCES

1. ICAO. ICAO Environmental Report 2016 [Internet]. 2016 [cited 2021 Feb 7]. p. 253. Available from: http://www.icao.int/environmental-protection/Pages/ENV2016.aspx%0Ahttp://www.icao.int/environmental-protection/Documents/ICAO Environmental Report 2016.pdf
2. Staples MD, Malina R, Suresh P, Hileman JI, Barrett SRH. Aviation CO2emissions reductions from the use of alternative jet fuels. Energy Policy. 2018;114(December 2017):342–54.
3. EPA. Regulations for Greenhouse Gas Emissions from Aircraft. 2017.
4. Overton J. Fact Sheet, The Growth in Greenhouse Gas Emissions from Commercial Aviation, Part 1 of a Series on Airlines and Climate Change. 2019.
5. IATA. Sustainable Aviation Fuels Sustainable Aviation Fuels Fact Sheet 5 SAF-SUSTAINABILITY CONSIDERATIONS [Internet]. 2018 [cited 2022 Jan 27]. Available from: https://www.iata.org/whatwedo/environment/Pages/sustainable-alternative-jet-fuels.aspx
6. U.S. Department of Energy EIA. Memorandum of Understanding: Sustainable Aviation Fuel Grand Challenge [Internet]. 2021 [cited 2021 Nov 11]. Available from: https://www.energy.gov/sites/default/files/2021-09/S1-Signed-SAF-MOU-9-08-21_0.pdf
7. Agusdinata DB, Zhao F, Ileleji K, Delaurentis D. Life cycle assessment of potential biojet fuel production in the United States. Environ Sci Technol. 2011;45(21):9133–43.
8. Han J, Elgowainy A, Cai H, Wang MQ. Life-cycle analysis of bio-based aviation fuels. Bioresour Technol. 2013;150:447–56.
9. De Jong S, Antonissen K, Hoefnagels R, Lonza L, Wang M, Faaij A, et al. Life-cycle analysis of greenhouse gas emissions from renewable jet fuel production. Biotechnol Biofuels. 2017;10(1):1–18.

10. Ganguly I, Pierobon F, Bowers TC, Huisenga M, Johnston G, Eastin IL. 'Woods-to-Wake' Life Cycle Assessment of residual woody biomass based jet-fuel using mild bisulfite pretreatment. Biomass and Bioenergy. 2018;108(October 2017):207–16.
11. Fortier MOP, Roberts GW, Stagg-Williams SM, Sturm BSM. Life cycle assessment of bio-jet fuel from hydrothermal liquefaction of microalgae. Appl Energy. 2014;122(July 2011):73–82.
12. Doliente SS, Narayan A, Tapia JFD, Samsatli NJ, Zhao Y, Samsatli S. Bio-aviation Fuel: A Comprehensive Review and Analysis of the Supply Chain Components. Front Energy Res. 2020;8(July):1–38.
13. Wei H, Liu W, Chen X, Yang Q, Li J, Chen H. Renewable bio-jet fuel production for aviation: A review. Vol. 254, Fuel. Elsevier Ltd; 2019. p. 115599.
14. Seepaul R, Bliss CM, Wright DL, Marois JJ, Leon R, Dufault N, et al. Carinata, the Jet Fuel Cover Crop 2015 Production Manual for the Southeastern United States. UF/IFAS Extension, Univ Florida. 2016;(SS-AGR-384):1–8.
15. Seepaul R, Kumar S, Iboyi JE, Bashyal M, Stansly TL, Bennett R, et al. Brassica carinata: Biology and agronomy as a biofuel crop. Vol. 13, GCB Bioenergy. Blackwell Publishing Ltd; 2021. p. 582–99.
16. Tiwari R, Reinhardt Piskáčková TA, Devkota P, Mulvaney MJ, Ferrell JA, Leon RG. Growing winter *Brassica carinata* as part of a diversified crop rotation for integrated weed management. GCB Bioenergy. 2021 Mar 9;13(3):425–35.
17. Hoghooghi N, Bosch DD, Bledsoe BP. Assessing hydrologic and water quality effects of land use conversion to Brassica carinata as a winter biofuel crop in the southeastern coastal plain of Georgia, USA using the SWAT model. GCB Bioenergy. 2021 Mar 1;13(3):473–92.
18. Seepaul R, Small IM, Mulvaney MJ, George S, Leon RG, Paula-Moraes S V, et al. Carinata, the Sustainable Crop for a Bio-based Economy: 2018-2019 Production Recommendations for the Southeastern United States 1. 2019.
19. Alam A, Dwivedi P. Modeling site suitability and production potential of carinata-based sustainable jet fuel in the southeastern United States. J Clean Prod. 2019 Dec 1;239:117817.
20. US Department of Transportation. Airline Fuel Cost and Consumption [Internet]. 2021

[cited 2021 Jul 3]. Available from: https://www.transtats.bts.gov/fuel.asp

21. Fewell JE, Bergtold JS, Williams JR. Farmers' willingness to contract switchgrass as a cellulosic bioenergy crop in Kansas. Energy Econ. 2016 Mar 1;55:292–302.
22. Miao R, Khanna M. Are Bioenergy Crops Riskier than Corn? Implications for Biomass Price. Choices Mag Food, Farm, Resour Issues. 2014;29(1):1–6.
23. Khanna M, Louviere J, Yang X. Motivations to grow energy crops: the role of crop and contract attributes. Agric Econ. 2017 May 1;48(3):263–77.
24. Huang S, Hu G, Chennault C, Su L, Brandes E, Heaton E, et al. Agent-based modeling of bioenergy crop adoption and farmer decision-making. Energy. 2016;115:1188–201.
25. Alexander P, Moran D, Rounsevell MDA, Smith P. Modelling the perennial energy crop market: the role of spatial diffusion. J R Soc Interface. 2013 Nov 6;10(88):20130656.
26. Sharma B, Ingalls RG, Jones CL, Khanchi A. Biomass supply chain design and analysis: Basis, overview, modeling, challenges, and future. Renew Sustain Energy Rev. 2013 Aug 1;24:608–27.
27. George S, Seepaul R, Geller D, Dwivedi P, DiLorenzo N, Altman R, et al. A regional inter-disciplinary partnership focusing on the development of a carinata-centered bioeconomy. GCB Bioenergy. 2021 Jul 1;13(7):1018–29.
28. Yue D, You F, Snyder SW. Biomass-to-bioenergy and biofuel supply chain optimization: Overview, key issues and challenges. Comput Chem Eng. 2014 Jul 4;66:36–56.
29. Tuck G, Glendining MJ, Smith P, House JI, Wattenbach M. The potential distribution of bioenergy crops in Europe under present and future climate. Biomass and Bioenergy. 2006 Mar 1;30(3):183–97.
30. Macal CM, North MJ. Tutorial on agent-based modelling and simulation. J Simul. 2010 Sep 19;4(3):151–62.
31. Berger T, Troost C. Agent-based Modelling of Climate Adaptation and Mitigation Options in Agriculture. J Agric Econ. 2014 Jun 1;65(2):323–48.
32. Schulze J, Gawel E, Nolzen H, Weise H, Frank K. The expansion of short rotation forestry: characterization of determinants with an agent-based land use model. GCB Bioenergy. 2017 Jun 1;9(6):1042–56.
33. Xie F, Huang Y. Sustainable Biofuel Supply Chain Planning and Management Under

Uncertainty. Transp Res Rec J Transp Res. 2013;2385:19–27.

34. de Jong S, Hoefnagels R, Wetterlund E, Pettersson K, Faaij A, Junginger M. Cost optimization of biofuel production – The impact of scale, integration, transport and supply chain configurations. Appl Energy. 2017;195:1055–70.
35. Jeong H, Sieverding HL, Stone JJ. Biodiesel Supply Chain Optimization Modeled with Geographical Information System (GIS) and Mixed-Integer Linear Programming (MILP) for the Northern Great Plains Region. Bioenergy Res. 2019;12(1):229–40.
36. Jeong H, Karim RA, Sieverding HL, Stone JJ. An Application of GIS-Linked Biofuel Supply Chain Optimization Model for Various Transportation Network Scenarios in Northern Great Plains (NGP), USA. BioEnergy Res. 2021;14.
37. Kang S, Heo S, Realff MJ, Lee JH. Three-stage design of high-resolution microalgae-based biofuel supply chain using geographic information system. 2020;
38. He-Lambert L, English BC, Lambert DM, Shylo O, Larson JA, Yu TE, et al. Determining a geographic high resolution supply chain network for a large scale biofuel industry. 2018;
39. Kim S, Kim S, Kiniry JR. Two-phase simulation-based location-allocation optimization of biomass storage distribution. Simul Model Pract Theory. 2018 Aug 1;86:155–68.
40. Ng RTL, Kurniawan D, Wang H, Mariska B, Wu W, Maravelias CT. Integrated framework for designing spatially explicit biofuel supply chains. 2018;
41. Zhang F, Wang J, Liu S, Zhang S, Sutherland JW. Integrating GIS with optimization method for a biofuel feedstock supply chain. Biomass and Bioenergy. 2017 Mar 1;98:194–205.
42. Awudu I, Zhang J. Uncertainties and sustainability concepts in biofuel supply chain management: A review. Vol. 16, Renewable and Sustainable Energy Reviews. 2012. p. 1359–68.
43. Shabani N, Akhtari S, Sowlati T. Value chain optimization of forest biomass for bioenergy production: A review. Renew Sustain Energy Rev. 2013 Jul 1;23:299–311.
44. Shabani N, Sowlati T, Ouhimmou M, Rönnqvist M. Tactical supply chain planning for a forest biomass power plant under supply uncertainty. Energy. 2014 Dec 15;78:346–55.
45. Castillo-Villar KK, Eksioglu S, Taherkhorsandi M. Integrating biomass quality variability in stochastic supply chain modeling and optimization for large-scale biofuel production. J Clean Prod. 2017 Apr 15;149:904–18.

46. Santibanez-Aguilar JE, Flores-Tlacuahuac A, Betancourt-Galvan F, Lozano-García DF, Lozano FJ. Facilities Location for Residual Biomass Production System Using Geographic Information System under Uncertainty. ACS Sustain Chem Eng. 2018 Mar 5;6(3):3331–48.
47. Zhang F, Wang J, Liu S, Zhang S, Sutherland JW. Integrating GIS with optimization method for a biofuel feedstock supply chain. Biomass and Bioenergy. 2017;98:194–205.
48. Martinez-Valencia L, Camenzind D, Wigmosta M, Garcia-Perez M, Wolcott M. Biomass supply chain equipment for renewable fuels production: A review. Vol. 148, Biomass and Bioenergy. Elsevier Ltd; 2021. p. 106054.
49. Dwivedi P, Wang W, Hudiburg T, Jaiswal D, Parton W, Long S, et al. Cost of Abating Greenhouse Gas Emissions with Cellulosic Ethanol. 2015;
50. ICAO. New ICAO Aircraft CO2 Standard One Step Closer To Final Adoption [Internet]. 2016 [cited 2021 Mar 25]. Available from: https://www.icao.int/Newsroom/Pages/New-ICAO-Aircraft-CO2-Standard-One-Step-Closer-To-Final-Adoption.aspx
51. Grewe V, Champougny T, Matthes S, Frömming C, Brinkop S, Søvde OA, et al. Reduction of the air traffic's contribution to climate change: A REACT4C case study. Atmos Environ. 2014 Sep 1;94:616–25.
52. Grewe V, Matthes S, Frömming C, Brinkop S, Jöckel P, Gierens K, et al. Feasibility of climate-optimized air traffic routing for trans-Atlantic flights. Environ Res Lett. 2017 Feb 27;12(3):034003.
53. Larsson J, Elofsson A, Sterner T, Åkerman J. International and national climate policies for aviation: a review. Clim Policy. 2019 Jul 3;19(6):787–99.
54. Ritchie BW, Kemperman A, Dolnicar S. Which types of product attributes lead to aviation voluntary carbon offsetting among air passengers? Tour Manag. 2021 Aug 1;85:104276.
55. Alam A, Masum MFH, Dwivedi P. Break-even price and carbon emissions of carinata-based sustainable aviation fuel production in the Southeastern United States. GCB Bioenergy. 2021 Sep 3;00:1–14.
56. Brown C, Bakam I, Smith P, Matthews R. An agent-based modelling approach to evaluate factors influencing bioenergy crop adoption in north-east Scotland. GCB Bioenergy. 2016 Jan 1;8(1):226–44.
57. Krah K, Petrolia DR, Williams A, Coble KH, Harri A, Rejesus RM. Producer Preferences

for Contracts on a Risky Bioenergy Crop. Appl Econ Perspect Policy. 2018 Jun 1;40(2):240–58.

58. Bergtold JS, Shanoyan A, Fewell JE, Williams JR. Annual bioenergy crops for biofuels production: Farmers' contractual preferences for producing sweet sorghum. Energy. 2017 Jan 15;119:724–31.
59. Kuehne G, Llewellyn R, Pannell DJ, Wilkinson R, Dolling P, Ouzman J, et al. Predicting farmer uptake of new agricultural practices: A tool for research, extension and policy. Agric Syst. 2017 Sep 1;156:115–25.
60. Ridier A, Roussy C, Chaib K. Adoption of crop diversification by specialized grain farmers in south-western France: evidence from a choice-modelling experiment. Rev Agric Food Environ Stud. 2021 Sep;102(3):265–83.
61. Fisher DK, Norvell J, Sonka S, Nelson MJ. Understanding technology adoption through system dynamics modeling: Implications for agribusiness management. Int Food Agribus Manag Rev. 2000;3(3):281–96.
62. Scandizzo PL, Savastano S. The adoption and diffusion of GM crops in United States: A real option approach. AgBioForum. 2010;13(2):142–57.
63. Nolan J, Parker D, van Kooten GC, Berger T. An Overview of Computational Modeling in Agricultural and Resource Economics. Can J Agric Econ Can d'agroeconomie. 2009 Dec 1;57(4):417–29.
64. Railsback SF, Grimm V. Agent-Based and Individual-Based Modeling: A Practical Introduction, Second Edition. Princeton University Press; 2019.
65. Ding D, Bennett D, Secchi S, Ding D, Bennett D, Secchi S. Investigating Impacts of Alternative Crop Market Scenarios on Land Use Change with an Agent-Based Model. Land. 2015 Nov 24;4(4):1110–37.
66. Guillem EE, Murray-Rust D, Robinson DT, Barnes A, Rounsevell MDA. Modelling farmer decision-making to anticipate tradeoffs between provisioning ecosystem services and biodiversity. Agric Syst. 2015;137:12–23.
67. Jin E, Mendis GP, Sutherland JW. Spatial agent-basagent ed modeling for dedicated energy crop adoption and cellulosic biofuel commercialization. Biofuels, Bioprod Biorefining. 2019;13(3):618–34.

68. Malawska A, Topping CJ. Applying a biocomplexity approach to modelling farmer decision-making and land use impacts on wildlife. Toit du J, editor. J Appl Ecol. 2018;55(3):1445–55.
69. Shu K, Kozak M, Fradj N Ben, Zylowski T, Rozakis S. Simulation of sorghum introduction and its impacts on land use change—A case study on Lubelski region of Eastern Poland. GCB Bioenergy. 2020 Apr 1;12(4):252–74.
70. Shastri Y, Rodríguez L, Hansen A, Ting KC. Agent-based analysis of biomass feedstock production dynamics. BioEnergy Res. 2011 Dec 3;4(4):258–75.
71. Malawska A, Topping CJ. Applying a biocomplexity approach to modelling farmer decision-making and land use impacts on wildlife. Toit J du, editor. J Appl Ecol. 2018 May 1;55(3):1445–55.
72. Alexander P, Moran D, Rounsevell MDA, Smith P. Modelling the perennial energy crop market: the role of spatial diffusion. J R Soc Interface. 2013 Sep 11;10(88):20130656–20130656.
73. Shastri Y, Rodríguez L, Hansen A, Ting KC. Agent-Based Analysis of Biomass Feedstock Production Dynamics. BioEnergy Res. 2011;4(4):258–75.
74. Rogers EM. Diffusion of Innovations. 5th ed. New York, NY: Free Press; 2003.
75. Keener VW, Feyereisen GW, Lall U, Jones JW, Bosch DD, Lowrance R. El-Niño/Southern Oscillation (ENSO) influences on monthly NO3 load and concentration, stream flow and precipitation in the Little River Watershed, Tifton, Georgia (GA). J Hydrol. 2010 Feb 15;381(3–4):352–63.
76. USDA National Agricultural Statistics Service Cropland Data Layer. Published crop-specific data layer [Online] [Internet]. USDA-NASS, Washington, DC; 2019 [cited 2020 Jul 5]. Available from: nassgeodata.gmu.edu/CropScape
77. USDA Economic Research Service. Comodity Costs and Returns [Internet]. 2020 [cited 2020 Jul 25]. Available from: https://www.ers.usda.gov/data-products/commodity-costs-and-returns/
78. Mulvaney MJ, Seepaul R, Small I, Wright D, Paula-moraes S, Cockson P, et al. Frost Damage of Carinata Grown in the Southeastern. 2018;(2016):2–5.
79. Perdue S, Hamer H. Georgia State and County Data, Volume 1, Geographic Area Series ,

Part 10. 2019.

80. Godsey LD. Economic Budgeting for Agroforestry Practices [Internet]. 2008 [cited 2021 Jul 28]. Available from: www.centerforagroforestry.org
81. Drake WL, Jordan DL, Johnson PD, Shew BB, Brandenburg RL, Corbett T. Peanut response to planting date, tillage, and cultivar in North Carolina. Agron J. 2014 Mar 1;106(2):486–90.
82. Alkemade F, Castaldi C. Strategies for the diffusion of innovations on social networks. Comput Econ. 2005 Feb;25(1–2):3–23.
83. Shang L, Heckelei T, Gerullis MK, Börner J, Rasch S. Adoption and diffusion of digital farming technologies - integrating farm-level evidence and system interaction. Agric Syst. 2021 May 1;190:103074.
84. Alexander P, Moran D. Impact of perennial energy crops income variability on the crop selection of risk averse farmers. Energy Policy. 2013 Jan 1;52:587–96.
85. Markowitz H. Portfolio Selection. J Finance. 1952 Mar;7(1):77.
86. Freund RJ. The Introduction of Risk into a Programming Model. Econometrica. 1956;24(3):253–63.
87. Markowitz H. Portfolio Selection: Efficient Diversification of Investments. New York, NY: John Wiley & Sons; 1959.
88. Kaiser HM, Messer KD. Mathematical Programming for Agriculture, Environmental and Resource Economics. New Jersey, NJ: John Wiley and Sons, Inc.; 2011. 347–400 p.
89. Bennett R. Introduction to PortfolioAnalytics [Internet]. 2018 [cited 2020 Aug 29]. Available from: https://cran.r-project.org/web/packages/PortfolioAnalytics/vignettes/portfolio_vignette.pdf
90. Upadhaya S, Dwivedi P. The role and potential of blueberry in increasing deforestation in southern Georgia, United States. Agric Syst. 2019 Jul 1;173:39–48.
91. Christ B, Bartels WL, Broughton D, Seepaul R, Geller D. In pursuit of a homegrown biofuel: Navigating systems of partnership, stakeholder knowledge, and adoption of Brassica carinata in the Southeast United States. Energy Res Soc Sci. 2020 Dec 1;70:101665.
92. The World Bank. Air transport, passengers carried [Internet]. 2021 [cited 2021 Jul 2].

Available from: https://data.worldbank.org/indicator/is.air.psgr

93. The White House. Fact Sheet: Biden Administration Advances the Future of Sustainable Fuels in American Aviation | The White House [Internet]. Statement and Releases . 2021 [cited 2022 Feb 18]. Available from: https://www.whitehouse.gov/briefing-room/statements-releases/2021/09/09/fact-sheet-biden-administration-advances-the-future-of-sustainable-fuels-in-american-aviation/
94. De Jong S, Hoefnagels R, Wetterlund E, Pettersson K, Faaij A, Junginger M. Cost optimization of biofuel production-The impact of scale, integration, transport and supply chain configurations.
95. Sharifzadeh M, Garcia MC, Shah N. Supply chain network design and operation: Systematic decision-making for centralized, distributed, and mobile biofuel production using mixed integer linear programming (MILP) under uncertainty. Biomass and Bioenergy. 2015 Oct 1;81:401–14.
96. Trejo-Pech CO, Larson JA, English BC, Edward Yu T. Cost and profitability analysis of a prospective pennycress to sustainable aviation fuel supply chain in southern USA. Energies. 2019 Aug 8;12(16):3055.
97. Perkis DF, Tyner WE. Developing a cellulosic aviation biofuel industry in Indiana: A market and logistics analysis. Energy. 2018;142:793–802.
98. U.S. Department of Energy EIA. Movements between PAD Districts. 2021.
99. Lewis KC, Baker G, Lin T, Smith S, Gillham O, Fine A, et al. Biofuel transportation analysis tool : description, methodology, and demonstration scenarios. (U.S.) JAVNTSC, editor.
100. Average Freight Revenue per Ton-Mile | Bureau of Transportation Statistics [Internet]. [cited 2021 Jun 16]. Available from: https://www.bts.gov/content/average-freight-revenue-ton-mile
101. Usery EL. Geographic Regions of Georgia: Overview [Internet]. New Georgia Encyclopedia. 2018 [cited 2021 Jun 28]. Available from: https://www.georgiaencyclopedia.org/articles/geography-environment/geographic-regions-georgia-overview
102. US Department of Transportation. Airline Fuel Cost and Consumption. 2019.

103. Alam A. Break-even price and carbon emissions of carinata-based sustainable aviation fuel production in the Southeastern United States. GCB Bioenergy. 2021;00:1–14.
104. Parton WJ, Hartman M, Ojima D, Schimel D. DAYCENT and its land surface submodel: description and testing. Glob Planet Change. 1998 Dec;19(1–4):35–48.
105. Field JL, Zhang Y, Dwivedi P, Seepaul R, Paustian K. Assessing the yield potential, biogenic emissions, and carbon sequestration value of winter carinata adoption in the Southeast. Front Energy Res. 2022;
106. Seepaul R, Small IM, Mulvaney MJ, George S, Leon RG, Geller D, et al. Carinata, the Jet Fuel Cover Crop: 2016 Production Recommendations for the Southeastern United States 1.
107. U.S. Census Bureau. TIGER/LINE shapefiles [Internet]. [cited 2021 Oct 1]. Available from: https://www.census.gov/geographies/mapping-files/time-series/geo/tiger-line-file.html
108. US Department of Transportation. Geospatial at BTS: Open Data Catalog [Internet]. [cited 2021 Oct 1]. Available from: https://data-usdot.opendata.arcgis.com/
109. Sims R, Schaeffer R, Creutzig F, Cruz-Núñez X, D'Agosto M, Dimitriu D, et al. Transport. In: Edenhofer O, Pichs-Madruga R, Sokona Y, Farahani E, Kadner S, Seyboth K., et al., editors. Climate Change 2014: Mitigation of Climate Change Contribution of Working Group III to the Fifth Assessment Report of the Intergovernmental Panel on Climate Change. Cambridge, United Kingdom and New York, NY, USA: Cambridge University Press; 2014.
110. Tarnoczi T. Life cycle energy and greenhouse gas emissions from transportation of Canadian oil sands to future markets. Energy Policy. 2013 Nov 1;62:107–17.
111. Chu PL, Vanderghem C, MacLean HL, Saville BA. Financial analysis and risk assessment of hydroprocessed renewable jet fuel production from camelina, carinata and used cooking oil. Appl Energy. 2017 Jul 15;198:401–9.
112. Zhang F, Johnson D, Johnson M, Watkins D, Froese R, Wang J. Decision support system integrating GIS with simulation and optimisation for a biofuel supply chain. Renew Energy. 2016;85:740–8.
113. Energy Information Administration (EIA). Propane Residential Price. Petroluem and Other Liquids (2021) [Internet]. [cited 2021 Jul 2]. Available from: https://www.eia.gov/dnav/pet/hist/LeafHandler.ashx?n=PET&s=M_EPLLPA_PRS_NUS_

DPG&f=M

114. Trading Economics. Naphtha. Markets (2021) [Internet]. [cited 2021 Jul 2]. Available from: https://tradingeconomics.com/commodity/naphtha

115. HL S, X Z, L W, JJ S. Life-Cycle Assessment of Oilseeds for Biojet Production Using Localized Cold-Press Extraction. J Environ Qual. 2016 May;45(3):967–76.

116. Agronne. GREET (The Greenhouse gases, Regulated Emissions, and Energy use in Technologies) Model. Computer Program developed by Argonne National Laboratory. (2020).

117. Teixeira da Silva de La Salles K, Meneghetti SMP, Ferreira de La Salles W, Meneghetti MR, dos Santos ICF, da Silva JPV, et al. Characterization of Syagrus coronata (Mart.) Becc. oil and properties of methyl esters for use as biodiesel. Ind Crops Prod. 2010 Nov 1;32(3):518–21.

118. IATA. Jet fuel price monitor [Internet]. 2021 [cited 2021 Oct 29]. Available from: https://www.iata.org/en/publications/economics/fuel-monitor/

119. Chu PL, Vanderghem C, MacLean HL, Saville BA. Financial analysis and risk assessment of hydroprocessed renewable jet fuel production from camelina, carinata and used cooking oil. Appl Energy. 2017 Jul 15;198:401–9.

120. Agusdinata DB, Zhao F, Ileleji K, Delaurentis D. Life cycle assessment of potential biojet fuel production in the United States. Environ Sci Technol. 2011;45(21):9133–43.

121. Natelson RH, Wang WC, Roberts WL, Zering KD. Technoeconomic analysis of jet fuel production from hydrolysis, decarboxylation, and reforming of camelina oil. Biomass and Bioenergy. 2015;75:23–34.

122. US EPA. Lifecycle Greenhouse Gas Results | Fuels Registration, Reporting, and Compliance Help | United States Environmental Protection Agency [Internet]. 2016. [cited 2021 Aug 6]. Available from: https://www.epa.gov/fuels-registration-reporting-and-compliance-help/lifecycle-greenhouse-gas-results

123. Huang S, Hu G, Chennault C, Su L, Brandes E, Heaton E, et al. Agent-based modeling of bioenergy crop adoption and farmer decision-making. Energy. 2016 Nov 15;115:1188–201.

124. Ullah KM, Dwivedi P. Modelling adoption and supply chain of carinata as a potential crop for sustainable aviation fuel production in the Southern United States (Ch1). University of

Georgia; 2022.

125. Quddus MA, Chowdhury S, Marufuzzaman M, Yu F, Bian L. A two-stage chance-constrained stochastic programming model for a bio-fuel supply chain network. Int J Prod Econ. 2018;195(October):27–44.
126. Li C, Grossmann IE. A Review of Stochastic Programming Methods for Optimization of Process Systems Under Uncertainty. Front Chem Eng. 2021 Jan 28;0:34.
127. Okhan G, Memis¸o M, Uster H€. Design of a biofuel supply network under stochastic and price-dependent biomass availability Gökhan Memişoğlu & Halit Üster Design of a biofuel supply network under stochastic and price-dependent biomass availability. 2021;
128. Sharma BP, Edward Yu T, English BC, Boyer CN, Larson JA. Stochastic optimization of cellulosic biofuel supply chain incorporating feedstock yield uncertainty. Energy Procedia. 2019 Feb 1;158:1009–14.
129. Lee C-Y, Sun W-C, Li Y-H. Biodiesel Economic Evaluation and Biomass Planting Allocation Optimization in Global Supply Chain. IEEE Trans Eng Manag. 2019 Mar 18;69(3):602–15.
130. Fattahi M, Govindan K. A multi-stage stochastic program for the sustainable design of biofuel supply chain networks under biomass supply uncertainty and disruption risk: A real-life case study. Transp Res Part E Logist Transp Rev. 2018;118(September):534–67.
131. Li Q, Hu G. Supply chain design under uncertainty for advanced biofuel production based on bio-oil gasification. 2014;
132. Nur F, Aboytes-Ojeda M, Castillo-Villar KK, Marufuzzaman M. A two-stage stochastic programming model for biofuel supply chain network design with biomass quality implications. IISE Trans. 2021;53(8):845–68.
133. Huang Y, Fan Y, Chen CW. An Integrated Biofuel Supply Chain to Cope with Feedstock Seasonality and Uncertainty. https://doi.org/101287/trsc20130498. 2014 Mar 6;48(4):540–54.
134. Olson DL, Wu D. Enterprise risk management models. 3rd ed. Enterprise Risk Management Models. Berlin, Germany: Springer-Verlag; 2020. 1–211 p.
135. Chaplin-Kramer R, Sim S, Hamel P, Bryant B, Noe R, Mueller C, et al. Life cycle assessment needs predictive spatial modelling for biodiversity and ecosystem services. Nat

Commun 2017 81. 2017 Apr 21;8(1):1–8.

136. Lark TJ, Mueller RM, Johnson DM, Gibbs HK. Measuring land-use and land-cover change using the U.S. Department of agriculture's cropland data layer: Cautions and recommendations. Int J Appl Earth Obs Geoinf. 2017 Oct 1;62:224–35.
137. SPARC. Carinata Facts. 2019. (Volume 1, Issue 1).
138. Waldhoff G, Lussem U, Bareth G. Multi-Data Approach for remote sensing-based regional crop rotation mapping: A case study for the Rur catchment, Germany. Int J Appl Earth Obs Geoinf. 2017 Sep 1;61:55–69.
139. University of Georgia Extension. UGA Peanut Production: 2020 Quick Reference Guide [Internet]. 2020 [cited 2020 May 12]. Available from: https://peanuts.caes.uga.edu/content/dam/caes-subsite/peanuts/docs/2020/UGA-Peanut-Quick-Reference-Guide-2020.pdf

APPENDIX 1

EVALUATION OF PHYSICAL ENVIRONMENTAL CONDITIONS

A1.1. Estimating land resources

Between 2015 and 2017, we used a remote sensing-based Crop Data Layer for determining the total potential land available for carinata cultivation in the study area. But, direct pixel counting of CDL within parcel boundary has at least three limitations. First, as parcel boundaries are not aligned with the pixels, there can be sub-pixel area biased. Second, the annual edge effect of 30-meter resolution data can falsely suggest incremental changes along the field boundary. Finally, a single crop field can be represented by two crops due to the occurrence of 'within-field spackle' [136]. To avoid these limitations as best as possible, we resampled the major row crop land covers using the *Nearest Neighborhood* method in ArcGIS 10.7.1 and converted the 30-meter resolution raster to a 90-meter resolution for locating 3 by 3 cells in the input space. The nearest neighborhood method is found to be the best option for reclassifying discrete cropland covers as this method does not change the values of the cells (ArcGIS Pro Tool Reference). Then, we used the *Spatial Analyst: Tabulate Area* tool in ArcGIS 10.7.1 to capture the land under major row crops within each parcel boundary. Finally, we selected the parcels whose total row crop areas were equal to or higher than 10 acres for every year starting from 2009

A1.2. The rotation plan for carinata

Carinata can be rotated with corn, cotton, peanuts, and soybeans in the Southern United States [137]. However, carinata should not be cultivated every year in the same field. Once every

three years was suggested to reduce the potential disease impacts. Therefore, it is vital to make a rotation plan before cultivating carinata. In this regard, at first, we identified the most preferred and profitable rotations for the study area by following the steps per Waldhoff et al. (2017). First, we reclassified the CDL raster data to major crop classes. Second, we converted raster to polygon. Thrid, we generalized polygons by eliminating any polygon whose area was less than or equal to 2.47 acres (a hectare). Fourth, we overlapped multiple time-series crop maps between 2009 and 2018 for preparing crop sequence dataset (Table S1). We used ArcGIS 10.7.1 for all the geoprocessing work.

According to Table S1, cotton and peanuts are the most popular crops. Cotton-cotton-cotton rotation is the most popular rotation in two out of three sequences of years. Considering the yield, price, and production costs, peanuts are more profitable than cotton. However, cultivating peanuts without any year gap is not feasible due to at least 40% of yield losses [139]. Due to this agronomic condition, two cotton and one peanut in a three-year row should be the most preferred and profitable option for the study area, which can be included to plan for rotation with carinata. Carinata should not be cultivated just after peanuts for having potential herbicide effects [18]. Therefore, we selected cotton-carinata-peanut-cotton in our model as three years rotational plan to adopt carinata.

A.1.3. Weather impact potential

The susceptibility of frost damage for carinata depends on the duration of temperature below a certain degree of a threshold and crop growth stage. Participating scientists under the SPARC program suggested including the probability of frost events based on the historical data [19]. Alam & Dwivedi [19] defined the frost event as when the temperature is less than 20^0F for 20 or

more hours between October to March. In this study, we offered a novel methodology to include potential seasonal weather impacts on crop yield based on that frost event definition. We defined Weather Impact Potential (WIP) as the reduced percentage of crop yield due to the probability of weather vulnerability and severity under the given number of seasonal events (Equation 1). The weather vulnerability (*H*) is estimated from the probability of events' occurrences at least once a year from the given period (e.g., ten years). The severity (*L*) is the subjective or estimated proportion of crop damages (e.g., 80% yield loss) due to exposure to weather vulnerability. The number of events' occurrences (*d*) (e.g., 1,2, or 3 events in a season) helps for scenario analysis, as in some situations, more than one event can occur in the same season and have a greater degree of impacts. For vulnerability (*H*) estimation, we considered the 'At Least One' occurrence in the observed years to avoid the duplicity with the number of events' occurrences (*d*).

$$WIP = (1 - H * L)^{d} * 100\ \% \ldots\ldots\ldots\ldots\ldots\ldots\ldots\ldots (1)$$

where,

H = probability of one or more frost event frequencies in a year

L = proportion of crop damage potential due to event exposures

d = number of events^' occurrences under the given season.

But there is no record of temperature below 20^0F for selected stations for 20 hours or more. Therefore, there is no effect of weather impact potential on carinata in the study area, and there is no potential yield reduction. In other words, the *WIP* value for our model simulation is 1.

Table A1.1: The cultivated Area and their cumulative percentages of three years crop rotations between 2009 and 2018. Crop code: 1 = corn, 2 = cotton, 3 = Soybean, 4 = peanuts, 5 = fallow land. Rotation 222 = cotton-cotton-cotton and so on. Data Source: USDA National Agricultural Statistics Service Cropland Data Layer (2019).

2009-2011			**2012-2014**			**2015-2017**		
Rotation	*Area (acre)*	*Cumulative (%)*	*Rotation*	*Area (acre)*	*Cumulative (%)*	*Rotation*	*Area (acre)*	*Cumulative (%)*
222	2331	31.4	242	1828	27.9	222	1884	24.9
242	1286	48.7	222	1630	52.8	242	1199	40.7
224	738	58.7	422	843	65.7	422	1010	54.1
424	623	67.1	224	641	75.5	244	903	66.0
422	359	71.9	142	256	79.4	224	595	73.9
212	327	76.3	244	207	82.5	424	241	77.1
442	303	80.4	122	187	85.4	412	232	80.1
241	301	84.4	412	164	87.9	144	155	82.2
141	164	86.6	241	110	89.6	252	145	84.1
264	144	88.6	424	108	91.2	254	131	85.8
122	120	90.2	246	71	92.3	142	128	87.5
464	106	91.6	442	69	93.4	212	125	89.2
262	93	92.9	214	53	94.2	462	89	90.4
244	73	93.9	144	53	95.0	452	88	91.5
114	59	94.7	126	46	95.7	211	88	92.7
246	55	95.4	124	44	96.3	442	67	93.6
441	54	96.1	121	43	97.0	664	55	94.3
414	53	96.8	212	43	97.6	214	49	94.9
666	41	97.4	141	37	98.2	662	44	95.5
221	37	97.9	444	29	98.7	122	41	96.1
444	30	98.3	221	29	99.1	221	37	96.5
266	30	98.7	622	23	99.4	414	31	97.0

412	26	99.0	112	21	99.8	464	30	97.3
214	23	99.4	146	8	99.9	342	29	97.7
211	20	99.6	522	8	100.0	164	28	98.1
466	16	99.8				241	25	98.4
112	12	100.0				641	22	98.7
						622	21	99.0
						454	16	99.2
						262	15	99.4
						444	11	99.5
						141	11	99.7
						421	10	99.8
						232	9	99.9
						621	5	100.0

APPENDIX 2

CODE TO ESTIMATE AGENTS' ADOPTION RATE ON *NETLOGO 6.2.0.* PLATFORM

```
globals [ProfC1 ProfC2 ProfC3 ProfC4 carinataProfit AR t d]
; ProfC1 = profit from corn, C2 = Cotton, C3 = Soybeans, C4 = Peanuts, AR = adoption ratio, t = time, d = degree of
weather impact

patches-own [Id ProfitT ProfitB
  X15C1 X15C2 X15C3 X15C4 X16C1 X16C2 X16C3 X16C4 X17C1 X17C2 X17C3 X17C4 Tot15 Tot16 Tot17
   UtilityDifference AT a? RA]
; ProfitT = profit from tradional crop rotation without carinata
; ProfitB = profit from crop rotation with carinata
; X15C1 = Land allocation for cultivating crop C1 in year 2015
; AT = adoption threshold
; a? = If farmer adopted carinata
; RA = Risk Avrsion Param

to setup
  clear-all
  file-open "LandResource.txt" ;Input land resource file.
  while [not file-at-end?]
  [
    let next-X file-read
    let next-Y file-read
    let X-15C1 file-read
    let X-15C2 file-read
    let X-15C3 file-read
    let X-15C4 file-read
    let X-16C1 file-read
    let X-16C2 file-read
    let X-16C3 file-read
    let X-16C4 file-read
    let X-17C1 file-read
    let X-17C2 file-read
    let X-17C3 file-read
    let X-17C4 file-read
    let X-Tot15 file-read
    let X-Tot16 file-read
    let X-Tot17 file-read

    ask patch next-X next-Y [set X15C1 X-15C1]
    ask patch next-X next-Y [set X15C2 X-15C2]
    ask patch next-X next-Y [set X15C3 X-15C3]
    ask patch next-X next-Y [set X15C4 X-15C4]
```

```
    ask patch next-X next-Y [set X16C1 X-16C1]
    ask patch next-X next-Y [set X16C2 X-16C2]
    ask patch next-X next-Y [set X16C3 X-16C3]
    ask patch next-X next-Y [set X16C4 X-16C4]
    ask patch next-X next-Y [set X17C1 X-17C1]
    ask patch next-X next-Y [set X17C2 X-17C2]
    ask patch next-X next-Y [set X17C3 X-17C3]
    ask patch next-X next-Y [set X17C4 X-17C4]
    ask patch next-X next-Y [set Tot15 X-Tot15]
    ask patch next-X next-Y [set Tot16 X-Tot16]
    ask patch next-X next-Y [set Tot17 X-Tot17]
  ]
  file-close
  set t 0
  (foreach (sort patches) (range count patches) [ [p n] ->
    ask p [ set id n ]
  ])
  ask patches [
    set AT random-normal 0.2 AdoptThreshold ; sd = 0.102 -> 2.5% innovator category; sd = 0.1920 -> 15%
innovator category; sd = 0.2965 -> 25% innovator category
    set pcolor (ifelse-value
      AT <= 0 [green - 2] ; Innovator
      AT > 0 and AT <= 0.3[green]
            [green + 2]
     )
    ;set plabel precision AT 2

    set plabel id
    set RA random-float 1 + 0.5
    set plabel precision RA 3
      ]
 set AR 0
 ;set d 1
 reset-ticks
end

to go
  profit
  cultivate
  ARatio
  if ticks = 11 [stop]
  plot-farmer
  tick
 end

to profit
  let YC1 random-normal 154 17.5
  let PC1 random-poisson 4.82
  let CC1 random-poisson 372.43
  set ProfC1 (YC1 *  PC1 - CC1)

  let YC2a random-normal 840.9 98.4
  let PC2a random-normal  0.745 0.1
  let YC2b random-normal 1360.2 159
```

```
  let PC2b random-normal 0.08 0.02
  let CC2 random-normal 559.6 44.6
  set ProfC2 (YC2a * PC2a + YC2b * PC2b - CC2)

  let YC3 random-normal 35.8 3.7
  let PC3 random-normal 10.96 1.8
  let CC3 random-normal 184.86 22.9
  set ProfC3 (YC3 *  PC3 - CC3)

  let YC4 random-normal 4212.5 383.3
  let PC4 random-normal 0.21 0.03
  let CC4 random-normal 489.85 36.6
  set ProfC4 (YC4 *  PC4 - CC4)

 ; Carinata cost and return
 let carinataYeild 50
 let carinataCost 275
 set carinataProfit (CarinataPrice * carinataYeild * ((1 - FrostEventFrequency *  Severity) ^ d) - carinataCost)
end

to cultivate
   let NP (1 / 1.06)
   ask patches [
   set ProfitT NP ^ (3 * t + 1) * (X15C1 * ProfC1 + X15C2 * ProfC2 + X15C3 * ProfC3 + X15C4 * ProfC4) +
            NP ^ (3 * t + 2) * (X16C1 * ProfC1 + X16C2 * ProfC2 + X16C3 * ProfC3 + X16C4 * ProfC4) +
            NP ^ (3 * t + 3) * (X17C1 * ProfC1 + X17C2 * ProfC2 + X17C3 * ProfC3 + X17C4 * ProfC4)
   set ProfitB NP ^ (3 * t) * ProfC2 * (X15C1 + X15C2 + X15C3 + X15C4) +
            NP ^ (3 * t + 1) * ProfC2 * (X16C1 + X16C2 + X16C3 + X16C4) +
            NP ^ (3 * t + 2) * carinataProfit * (X16C1 + X16C2 + X16C3 + X16C4) +
            NP ^ (3 * t + 3) * 0.9 * ProfC4 * (X17C1 + X17C2 + X17C3 + X17C4)

   set UtilityDifference (precision  (ProfitB  - ProfitT) 0)
   set pcolor (ifelse-value
     UtilityDifference > 0  and AT <= AR [green - 2]
                                [green])
   set a? (ifelse-value
   UtilityDifference > 0  and AT <= AR [TRUE]
                              [FALSE])      ;; ultimately exclude the farmer who has negetive experiences in the previous
time step.
                                        ;;we do not assume farmers having negetive experience will never adopt energy
crop.
   ;set plabel precision UtilityDifference 0
   set plabel a?
      ]
end

to ARatio
  let positive count patches with [UtilityDifference > 0 and AT <= AR]
  let negetive count patches with [UtilityDifference < 0 and AT <= AR]
  set AR  (positive - negetive) / count patches
  set t t + 1
end
to plot-farmer
  set-current-plot "Biofuel Farmer"
```

```
 set-current-plot-pen "patches"
end
```